OCT 26 1936

VOLUME 84 NUMBER 3

THE ASTROPHYSICAL JOURNAL

AN INTERNATIONAL REVIEW OF SPECTROSCOPY AND ASTRONOMICAL PHYSICS

Founded in 1895 by GEORGE E. HALE *and* JAMES E. KEELER

Edited by

HENRY G. GALE
Ryerson Physical Laboratory of the University of Chicago

FREDERICK H. SEARES
Mount Wilson Observatory of the Carnegie Institution of Washington

OTTO STRUVE
Yerkes Observatory of the University of Chicago

OCTOBER 1936

PHOTOGRAPHIC PHOTOMETRY - - - - - - - - - - - - - *Frank E. Ross* 241

THE LUMINOSITY FUNCTION OF NEBULAE. II. THE LUMINOSITY FUNCTION AS INDICATED BY RESIDUALS IN VELOCITY-MAGNITUDE RELATIONS *Edwin Hubble* 270

VARIATIONS IN THE SPECTRUM OF P CYGNI - - - - - - - O. C. Wilson 296

LOW-DISPERSION SPECTRA OF RED STARS - - - - - - - - - *Rupert Wildt* 303

THE MOTIONS OF PROMINENCES OF THE ERUPTIVE AND SUN-SPOT TYPES *Edison Pettit* 319

THE CHANGE OF THE SOLAR VELOCITY WITH INCREASING DISTANCES OF THE STARS FROM THE GALACTIC PLANE - - - - - *Emma T. R. Williams* 346

FRAUNHOFER'S SPECTRUM IN THE INTERVAL FROM 77,000 TO 110,000 A. *Arthur Adel and V. M. Slipher* 354

NOTES

CONFIRMATION OF THE DUPLICITY OF CAPELLA H - - - - - - - G. P. Kuiper 359

NOTES ON VISUAL BINARIES OF LARGE PARALLAX - - - - - - - G. P. Kuiper 359

REVIEWS

Molekülspektren, H. Sponer (David M. Dennison), 362; *Consider the Heavens*, F. R. Moulton (Philip Fox), 363; *Stars and Telescopes*, James Stokley (O. C. Collins), 366; *L'origine des mondes*, Paul Labérenne (Otto Struve), 367.

THE UNIVERSITY OF CHICAGO PRESS
CHICAGO, ILLINOIS, U.S.A.

October 1936 Vol. 84, No. 3

THE ASTROPHYSICAL JOURNAL

AN INTERNATIONAL REVIEW OF SPECTROSCOPY AND ASTRONOMICAL PHYSICS

Edited by

HENRY G. GALE
Ryerson Physical Laboratory of the University of Chicago

FREDERICK H. SEARES
Mount Wilson Observatory of the Carnegie Institution of Washington

OTTO STRUVE
Yerkes Observatory of the University of Chicago

WITH THE COLLABORATION OF

WALTER S. ADAMS, Mount Wilson Observatory
JOSEPH S. AMES, Johns Hopkins University
WILLIAM W. CAMPBELL, Lick Observatory
HENRY CREW, Northwestern University
CHARLES FABRY, Université de Paris
ALFRED FOWLER, Imperial College, London
EDWIN HUBBLE, Mount Wilson Observatory
HEINRICH KAYSER, Universität Bonn
ROBERT A. MILLIKAN, Institute of Technology, Pasadena
HUGH F. NEWALL, Cambridge University
FRIEDRICH PASCHEN, Reichsanstalt, Charlottenburg
HENRY N. RUSSELL, Princeton University
FRANK SCHLESINGER, Yale Observatory
HARLOW SHAPLEY, Harvard College Observatory

Former Editors:

GEORGE E. HALE JAMES E. KEELER EDWIN B. FROST

The Astrophysical Journal is published by the University of Chicago at the University of Chicago Press, 5750 Ellis Avenue, Chicago, Illinois, during each month except February and August. ¶The subscription price is $6.00 a year; the price of single copies is 75 cents. Orders for service of less than a half-year will be charged at the single-copy rate. ¶Postage is prepaid by the publishers on all orders from the United States, Mexico, Cuba, Porto Rico, Panama Canal Zone, Republic of Panama, Dominican Republic, Canary Islands, El Salvador, Argentina, Bolivia, Brazil, Colombia, Chile, Costa Rica, Ecuador, Guatemala, Honduras, Nicaragua, Peru, Hayti, Uruguay, Paraguay, Hawaiian Islands, Philippine Islands, Guam, Samoan Islands, Balearic Islands, Spain, and Venezuela. ¶Postage is charged extra as follows: for Canada and Newfoundland, 30 cents on annual subscriptions (total $6.30); on single copies, 3 cents (total 78 cents); for all other countries in the Postal Union, 80 cents on annual subscriptions (total $6.80), on single copies, 8 cents (total 83 cents). ¶Patrons are requested to make all remittances payable to The University of Chicago Press, in postal or express money orders or bank drafts.

The following are authorized agents:

For the British Empire, except North America, India, and Australasia: The Cambridge University Press, Fetter Lane, London, E.C. 4. Prices of yearly subscriptions and of single copies may be had on application.

For Japan: The Maruzen Company, Ltd., Tokyo.

For China: The Commercial Press, Ltd., 211 Honan Road, Shanghai. Yearly subscriptions, $6.00; single copies, 75 cents, or their equivalents in Chinese money. Postage extra, on yearly subscriptions 80 cents, on single copies 8 cents.

Claims for missing numbers should be made within the month following the regular month of publication. The publishers expect to supply missing numbers free only when losses have been sustained in transit, and when the reserve stock will permit.

Business correspondence should be addressed to The University of Chicago Press, Chicago, Illinois.

Communications for the editors and manuscripts should be addressed to: Otto Struve, Editor of THE ASTROPHYSICAL JOURNAL, Yerkes Observatory, Williams Bay, Wisconsin.

The cable address is "Observatory, Williamsbay, Wisconsin."

The articles in this journal are indexed in the *International Index to Periodicals*, New York, N.Y.

Applications for permission to quote from this journal should be addressed to The University of Chicago Press, and will be freely granted.

Entered as second-class matter, January 17, 1895, at the Post-Office, Chicago, Ill., under the act of March 3, 1879.
Acceptance for mailing at special rate of postage provided for in Section 1103, Act of October 3, 1917, authorized on July 15, 1918.

PRINTED IN THE U.S.A.

THE ASTROPHYSICAL JOURNAL

AN INTERNATIONAL REVIEW OF SPECTROSCOPY AND ASTRONOMICAL PHYSICS

VOLUME 84 OCTOBER 1936 NUMBER 3

PHOTOGRAPHIC PHOTOMETRY

FRANK E. ROSS

ABSTRACT

A thermoelectric photometer is described, and the theory of photometric measurement is developed. The influence of variable fog on the photographic plate, including the Eberhard effect, is investigated. It is shown that, in general, the ratio of the galvanometer deflection for the star to that for the fog in the immediate neighborhood is a measure of stellar magnitude. Experimental evidence is adduced. Since the standards of magnitude (the Polar Sequence) are located at the pole, the effects on photometry of the unavoidable errors of adjustment of the polar axis of the instrument, especially serious in long exposures, are pointed out and steps which should be taken for their reduction are suggested. The difficulties always met in the photometric measurement of plates taken with wide-angle lenses—in particular, distance errors—are discussed. The background effect, due to unresolved clusters and to dark and bright nebulae, is shown to be inappreciable. Experiments were made to determine the best method of development. It was found, unexpectedly, that development without rocking or agitation of any kind gave superior results.

A catalogue of the magnitudes and approximate positions of all stars as bright as 12.0 photovisual magnitude in the BD zones 88° and 89° is given, with a chart for identification. Comparison is made with Seares's values for normal distribution and mean color indices.

In 1931 a grant was secured from the Rumford Fund of the National Academy of Sciences to construct a thermoelectric photometer. The well-known and widely used Schilt type was considered to be the best basic model. For reasons of expense, and for other reasons, many changes were found desirable and have been incorporated in the instrument to be described here. The photometer was made in the shops of the Yerkes Observatory by Charles Ridell, to whom I am indebted for many details of design, in particular the mechanism for moving the plate carriage in its two coordinates, which is exceedingly satisfactory.

1. DESCRIPTION OF THE INSTRUMENT

The instrument, in its operative setup, is shown in Plate X. The observer is at the left, where he can conveniently operate the knobs h_1 and h_2 and make the necessary settings through the viewing telescope, *t*. The galvanometer (high sensitivity), *g;* the scale, *s*, with rack and pinion, *r;* and the illuminating unit, *i*, containing lamp, condenser, and fiducial wire, are all from Leeds and Northrop. The resistance of the galvanometer is balanced against that of the thermoelement, so that its operation is deadbeat.

In planning a simplification of the viewing system, it was found necessary to increase the focal length of the pair of micro-objectives which are mounted on each side of the plate being measured, in order to allow sufficient space for the simple illuminating system back of the plate and for the telescopic viewing system in front. Accordingly, 32-mm Bausch and Lomb objectives have been used.

The telescopic viewing system, *t*, moves in and out in accurately constructed ways, through a lever system connected with the operating handle, h_3. The wedge, *w*, is connected with h_3. Its function is to raise or lower the plate-illuminating unit, *f*, synchronously with the motion of the viewing telescope. In designing the illuminating system it was the aim to secure as large a field as possible. The illuminating unit, *f*, consists of a low-voltage lamp, preferably of the solid-bulb type, mounted in front of a reflector and behind a ground glass disk 2 cm in diameter. This gives a uniform illumination of the plate over the large field desired.

The viewing telescope.—A reflecting prism having a square base of 2 cm is mounted at the right end of *t*. Halfway between the prism and the eyepiece, *e*, is a lens of focal length 9 cm, giving unit magnification of the field. The ocular is a 15-mm Ramsden, by Bausch and Lomb, with a field lens 17 mm in diameter—which is approximately the diameter of the field seen on the plate in good illumination. A field of this extent is a great convenience in making the settings upon a star and in passing from one star to another, without having to follow the dotted line, as is necessary with some instruments. Cross-threads are at *x*, fine adjustment of which is made by means of the capstan screws shown.

Motion of the plate carriage.—In designing the details of these motions, it was considered desirable to get away from connecting

PLATE X

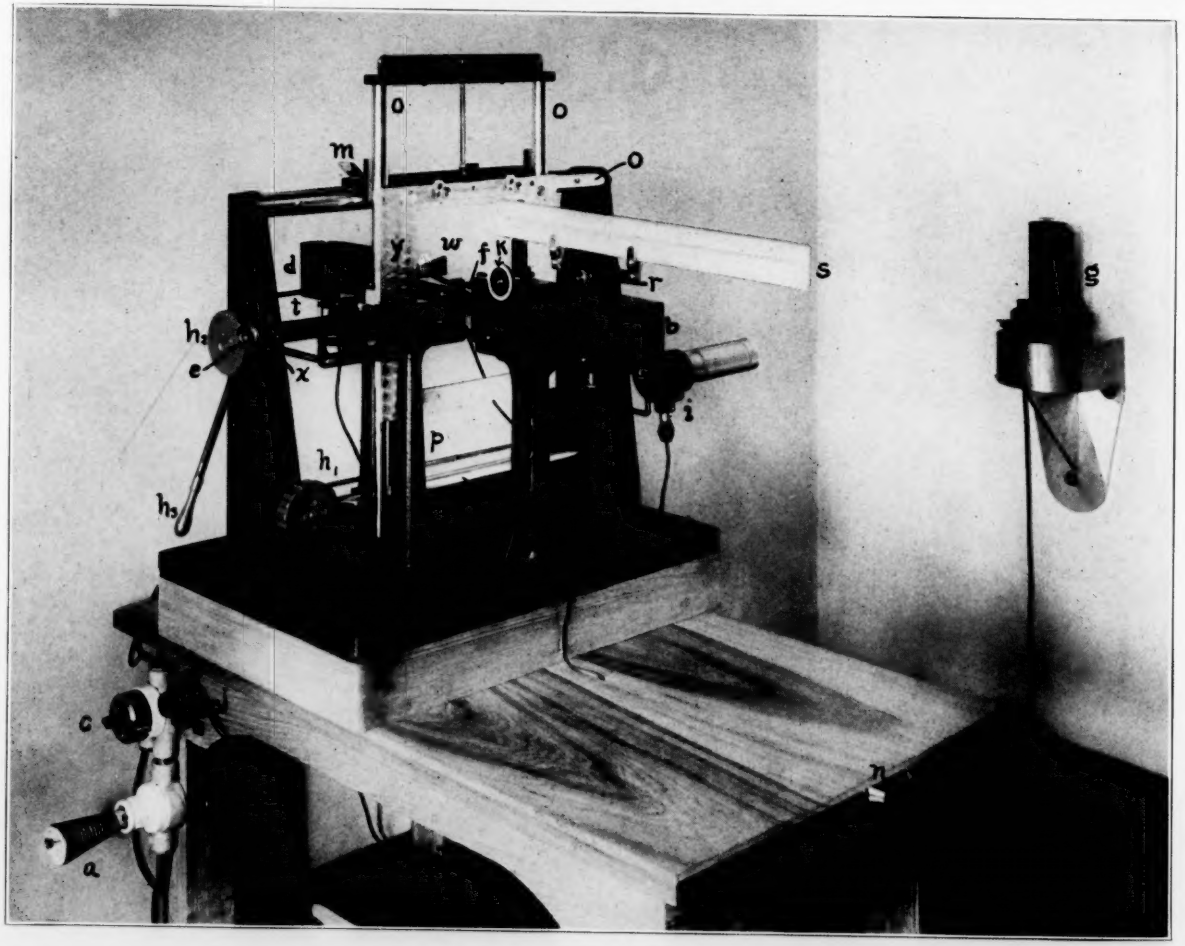

THERMOELECTRIC PHOTOMETER OF THE YERKES OBSERVATORY

UNIV. OF WICH.

gears. I am indebted to Mr. Ridell for the design and attainment of a very satisfactory smooth motion with a minimum of lost motion. For the horizontal motion, the carriage, *y*, carrying the plate is attached to an endless chain connected with a strong spring, *p*. The chain meshes into four sprocket wheels at the four corners, one of which is visible in the photograph. The lower left sprocket is connected directly with the knob h_1. The horizontal and vertical pairs of bearing rods, *o*, are of chromium-plated stainless steel and are hollow. For the horizontal motion there are two V-bearings resting on the upper rod *o*, the lower serving for guiding only. For the vertical motion there are four rolling V-bearings of the spool type, one at each corner of the plate carriage, *y*. The vertical motion is by rack and pinion, operated by the knob h_2. The pinion, of $\frac{1}{2}$-inch diameter, not visible in the photograph, necessarily extends the entire width of the instrument, 26 inches. It engages with two racks fastened to the back of *y*, one on each side, 8 inches apart. In order to keep the pinion from flexing, it was found necessary to run it through a pair of closely fitting bearings, set as close to the racks as possible. In operation, both horizontal and vertical motions, each secured by a different method, are very satisfactory. A star image can be centered on the cross-threads in a few seconds with an error of a very few microns. The weight of the carriage is carried by lead counterpoises within the vertical tubes *o*.

The photometer lamp.—Since it is essential to be able to project on the plate a disk of light which will be uniform in intensity, a great deal of attention was given to the selection of a suitable lamp. Many commercial types were tried and found unsatisfactory. I am indebted to Dr. W. E. Forsythe, of the Nela Park Research Laboratory, for the type finally selected. The filament is straight, 2 mm in length, and of exceedingly close coil, the outside diameter of which is about 0.75 mm. Its voltage is 6.5, drawing 2.4 amperes. The lamp is not seen in the photograph, being behind the shield, *d*. The shield is hinged, making lamp, condenser, and diaphragm easily accessible. The lamp is set with the filament horizontal, at an angle of 45° to the line of collimation. The result is a very uniform disk of light of high specific intensity. A reflector of suitable radius is set in the rear.

The lamp is provided with adjustment in three co-ordinates, for

the accurate collimation necessary to secure a uniformly illuminated image of the diaphragm. Having been set, it need not be disturbed. The leads must be soldered to the lamp. Uniformity of illumination is frequently tested by inserting the largest diaphragm and viewing its image in the telescope. The tube containing the condenser lens and the projection lens, seen only in part in the photograph, is movable by rack and pinion for accurate focusing of the diaphragm on the plate. The optical reduction factor is 6.5. The smallest diaphragm used has a diameter of 1 mm, giving an illuminated disk of 0.15-mm diameter. This is used for very small images.

The image of the above-described diaphragm image, in the center of which the star image has been placed by operating the handles h_1 and h_3, is projected on the receiving disk of the thermoelement by means of a Bausch and Lomb micro-objective of 32 mm focal length, at a magnification of about 1.5. The receiver is a Zernike thermopile of eight elements, of bismuth alloys. The junctions are covered with a copper receiver 2 μ thick and 2 mm in diameter. It is made by Kipp and Sons, of Holland.

Centering the star image.—The inner position of the viewing telescope, which is used for finding and setting, is accurately controlled by a stop. In this position, the cross-wires should coincide accurately with the center of the illuminated disk. In its normal operation this cannot be tested, since the field illumination unit, *f*, obstructs. Accordingly a wedge is provided, which the observer slips under the rod holding *f*, thus raising it and allowing the diaphragm to be viewed and centered. For this adjustment the intensity must be cut down, for comfortable vision. The centering should be frequently checked, this taking but a moment.

A new feature of the instrument is the device for keeping the region of the plate being measured at a constant distance from the projection lenses. This, however, is not as essential with the long-focus lenses used in this instrument as it is with earlier types. On account of the large size of the plates ordinarily measured on this instrument (8×10 inches), there is apt to be considerable bending of the plate, up to 1 mm in amount. This bending is usually convex on the glass side of the plate. The plates are therefore measured glass side out. The divided head, *k*, operates a polished round-headed plunger, not visible in the photograph, which is set close to

the line of collimation and parallel with it. When a plate is inserted for measurement, the plunger is set by means of the divided head, *k*, until it is seen to bear against the plate at each of its four corners. The plunger will then be in contact with a convex or plane plate in all positions, insuring constancy of distance.

Silver-plated scales, divided to millimeters, are provided for reading the co-ordinates. They are so placed as to be easily read by the observer without changing his position. For reading the horizontal scale a mirror, *m*, is provided.

The galvanometer scale.—This is made of heavy ground glass, with millimeter and centimeter divisions, the length being 50 cm. It is placed with its zero at the right, which is the "dark" reading. Directly preceding each reading, whether on the plate fog or on the image, the dark reading is set accurately at zero, which is done by moving the scale itself with the screw *r*. Unless the temperature in the room is changing rapidly, the drift is very slight. This zero setting is a very great convenience, as it avoids a zero reading and its recording and subsequent subtraction for each setting. For the convenient reading of the zero and for its setting, a mirror, not shown in the photograph, is provided. Its base slips into the bracket *n*. Thus the observer does not have to change position.

After the correct diaphragm suitable for the work in hand has been chosen, the intensity of the lamp is adjusted by means of the resistance coil which is in circuit, so that a deflection of about 45 cm is obtained for the fog. This insures the highest sensitivity in the measurement. For very small diaphragms, if the fog is abnormally large, this cannot always be done. The scale is not read closer than 1 mm, which corresponds roughly to 0.01 mag.

At present the instrument is mounted in an office room and is consequently subject to great changes in temperature, especially in winter. This causes a steady drift of the zero. When this becomes too large, work must be discontinued; but this happens very infrequently. The effect of high wind, so troublesome with some types of receiver, is hardly sensible. The galvanometer is mounted on an inside wall of the observatory, and, to our surprise, is perfectly stable. It is planned to operate the instrument in a basement room, where temperature conditions are more uniform.

The current for the photometer lamp is obtained from a single

storage battery of the common type used in automobiles. When not in use, it can be charged through *a*. The four-cycle switch is shown at *c*. The rheostat in this circuit is behind the base and cannot be seen. The rheostat, *j*, controls the field lamp. Field and galvanometer lamps are operated from another storage battery, both batteries being on a lower shelf, as shown, and can be recharged as a unit.

With regard to the important matter of constancy of the current passing through the photometer lamp, it is all that can be desired; tests show its variation to be less than one-half of 1 per cent in a two-hour run. When first set up, trouble was encountered with the bayonet socket, giving erratic fluctuations. This was overcome by soldering the leads to the lamp. No trouble seems to be caused by the switch or the resistance coil. After recharging, it is best to run the lamp for about ten minutes before taking readings.

Speed of measurement.—Assuming that the co-ordinates or scale readings of the stars to be measured have been previously recorded, so that no time is lost in locating the stars, about 90 magnitudes can be measured and recorded in one hour. This includes one fog reading. For the highest accuracy, it is better to take two fog readings on opposite sides of the star being measured.

2. THE THEORY OF MEASUREMENT

Let it be assumed that readings of galvanometer deflections are made on a series of star images of varying magnitude, on the same plate, with a thermoelectric photometer of the type here described, the illuminated spot, of area A, being larger than the largest image.

Let μ be the average mass of silver per unit area in the image of a star of magnitude m, the exposure time being t. Neglecting the Schwarzschild exponent, which is immaterial here, we have

$$\mu = F(m, t) , \tag{1}$$

where F is a functional form, not necessary to specify.

Let ν be the mass of silver per unit area, due to fog; and let κ be the photographic constant, i.e., the mass of silver necessary to produce a photographic deposit of unit density.

Let us assume for the moment that the fog overlies the image itself in unreduced amount. Then the density of the image is

$$D_i = \kappa(\mu + \nu) \; ; \tag{2}$$

and its transmission,

$$T_i = 10^{-D_i} \; . \tag{2a}$$

Passing to the photometer, let I_0 be the intensity of the light energy per unit area incident on the plate. If A_i is the area of the image, we have

$$A_i = A\phi(m) \tag{3}$$

ϕ being a functional form, not necessary to specify.

The amount of energy transmitted by the image is then

$$I_i = I_o A \phi 10^{-\kappa(\mu+\nu)} \; ; \tag{4}$$

and that by the remaining, or fog area, is

$$I_f = I_o A (1 - \phi) 10^{-\kappa\nu} \; . \tag{5}$$

Addition gives the total energy passing through A.

Similarly for the fog, of area $A' = A$, adjacent to the image,

$$I' = I_o A 10^{-\kappa\nu} \; . \tag{6}$$

Passing now to the galvanometer, theoretically its deflections, G, are proportional to the impinging energy, or,

$$G = \sigma I \; . \tag{7}$$

Combining (4), (5), and (7), we have

$$G_A = \sigma I_o A [\phi 10^{-\kappa(\mu+\nu)} + (1 - \phi) 10^{-\kappa\nu}] \; , \tag{8}$$

which is the galvanometer deflection for the image. The deflection for the fog area A' is, from (6) and (7),

$$G_{A'} = \sigma I_o A 10^{-\kappa\nu} \; . \tag{9}$$

Putting

$$Q=\frac{G_A}{G_{A'}}, \tag{10}$$

we have, after reduction,

$$Q=1+\phi(10^{-\kappa\mu}-1). \tag{11}$$

Noting that ϕ and μ are functions of m (equations 1 and 3), and that t is a constant, we conclude that Q is a function of m alone. The equation can be inverted, giving

$$m=\psi(Q), \tag{12}$$

thus validating the choice of Q as a measure of the magnitude or brightness of a star.

It is seen from (8) that the galvanometer deflection for the image, G_A, even if the light source is kept constant, cannot be taken as a measure of magnitude, for ν, the fog density, enters into the equation, and this varies irregularly over the plate (see p. 254). For a similar reason the difference of the deflections, fog *minus* image, cannot be correctly used.

Strictly, the image is not of uniform density, as assumed above. Let us attempt to take account of a ring of reduced density at the border of the image. It is immaterial whether its density μ_1 be taken as a constant or as a function of the stellar magnitude. The area a_1 of this ring is obviously a function of the magnitude, and we can put, as in (3), $a_1=A\phi_1(m)$. The fog area is reduced by this amount, and is now

$$A_f=A(1-\phi-\phi_1). \tag{13}$$

Equation (8) becomes:

$$G_A=\sigma I_o A[\phi 10^{-\kappa(\mu+\nu)}+\phi_1 10^{-\kappa(\mu_1+\nu)}+(1-\phi-\phi_1)10^{-\kappa\nu}]. \tag{14}$$

Dividing by (9), we get an equation similar to (11), from which (12) follows. Thus Q is again validated. Obviously the proof is valid for any number of rings.

It has thus been proved that Q is a valid measure of stellar magnitude, even if the fog is variable over the plate, provided the fog

overlies the image in amount equal to its density in the immediate neighborhood of the image.

The Eberhard effect.—No matter what the law of the Eberhard effect may be, it does not invalidate Q, provided the fog remains constant over the plate. This is easy to show. With the Eberhard effect acting, the fog overlying the image is no longer equal to its value in the immediate neighborhood, but it becomes a function of the density of the image and of its size, the effect extending into the fog region itself. We conclude that, since the Eberhard effect is always present to a greater or less extent, and since the fog over the plate is likewise variable, Q is strictly not a valid measure of stellar magnitude in general. It is, however, the best measure attainable and leads only to errors purely accidental and small in amount. (See section 7.)

3. EFFECT OF MALADJUSTMENT OF THE POLAR AXIS

It is an undoubted convenience in many respects to have the standard sequence of stars located at the pole. But, where comparisons are made involving long, or even moderate, exposures, errors arise which may be troublesome, owing to the maladjustment of the polar axis and changes in refraction. Assuming non-coincidence of the instrumental pole with the apparent pole of the sky, and assuming for the moment that the clock rate is correct, it is not difficult to show that the images on a plate exposed to the polar field are, for all stars, nearly straight-line elements, parallel and of equal length, l, given by the equation,

$$l = 0.0044\, at\,,$$

where a is the distance in millimeters, measured on the plate, between the two poles, and t is the exposure-time in minutes.[1] Thus, since all images are elongated equally, no serious error in photometry should result were it not for the optical field-errors of the objective or mirror. For example, the radially elongated pattern produced by the coma in the mirror, combined with the above parallel elongations, produces an effect varying over the four quadrants,

[1] R. M. Fry, "The Adjustment of a Polar Axis by Star Trails Near the Pole," *J.B.A.A.*, **45**, 234, 1935.

which would be exceedingly difficult to handle as corrections. In the case of refractors with well-corrected field, the effect may not be so serious.

The difficulty may be overcome by guiding with a double-slide plateholder, as is customary in exposures with reflecting telescopes. This assumes that the clock rate is correct, which is not difficult to realize. For very long exposures, two guide stars are essential. In cases where the double-slide plateholder is not available, as with nearly all refracting telescopes, where guiding must be done in right ascension and declination with slow-motion screws which move the telescope itself, it is not possible to make the correction. In this case, with exposures of some duration being made at the pole, it would be well to have a guiding telescope set at an angle of at least 10° to the line of collimation. This would take care of the clock rate, and thus insure parallel images of equal length.

4. WIDE-ANGLE PHOTOMETRY

It may not be unprofitable to call attention to the many difficulties involved in photographic photometry over wide areas of the plate, corresponding to a large angular field. The special difficulties encountered at the pole, where the precise photometric standards are located, perhaps unfortunately, have been already considered (p. 249). Mirrors and lenses present problems peculiar to themselves. In the case of mirrors, on account of the complete achromatization, difficulties due to color are not present, while coma presents a serious problem. I am inclined to believe that photometric problems are best handled in the Schmidt mirror system, especially if it should be found practicable to bend the plate or film to the proper field curvature. In lens systems, coma is usually well corrected. Outstanding, however, are serious color errors (secondary spectrum), combined with astigmatism, field curvature, and possible errors of centering in the complicated system of lenses. We will consider in what way these errors introduce difficulties in photographic photometry.

It can be affirmed that in general these difficulties are due to nonsymmetrical distribution and concentration of light in the image formed on the photographic plate. To see the truth of this, one

has but to examine the image produced by any well-rated lens, through a microscope of moderate power, at a distance of several degrees from the axis. It is obvious that the light in the strongly concentrated portions of the image loses its efficiency in photographic recording after the earlier stages of the period of exposure. In the later periods it registers only by spreading, in accordance with the turbidity action of the emulsion. In general, it can be stated that the image pattern depends only on the distance from the axis of the telescope, so that errors can be tabulated as a function of the distance and thus allowed for (distance correction). However, theoretically this distance pattern depends upon the secondary color-curve of the objective, combined with the spectral sensitivity-curve of the plate and the atmospheric extinction. From this it would seem that the distance correction should depend upon spectral class. This is found to be true in the case of some types of objectives but not in others. A treacherous source of error is a lack of collimation, which may be in the lens itself or in the camera. This alters the relative light pattern in the four quadrants, leading to a distance correction which is a function of position angle.

I wish here to call attention to a close connection between distance correction and the photometry of the extra-galactic nebulae. The light pattern in each is very similar, consisting of condensations surrounded centrally or otherwise by areas of weak intensity. The difficulties encountered with distance correction however are mild compared with those encountered in the photographic photometry of these nebulae, owing to their great variety in form and structure.

A serious source of error is due to changes in focal length and in seeing conditions, combined with inequalities in guiding. The light pattern thus varies from night to night, leading to corresponding changes in distance correction. These difficulties are especially troublesome in the case of large reflectors, on account of their large scale combined with their uncorrected coma and their changes of astigmatism from one night to another.

It is of interest to trace the origin and mechanism of the photographic color equation. This divides into two groups: (1) color equation in photographic magnitudes; (2) color equation in photovisual magnitudes. Each may be divided into two subgroups, de-

pending upon the type of instrument: reflector or refractor. For the latter there are two subclasses, depending upon whether the lens is corrected photographically or visually.

Because of the perfect achromatization of the reflector, it is probably justifiable to accept a system of magnitudes determined with it as a zero or standard system, both for photographic and photovisual magnitudes. Even with it, troublesome secondary effects are present to such an extent as to make necessary the choice of a definitely determined system as a standard to which it is necessary to reduce all other determinations. This has been done in the International System of magnitudes. Owing to the introduction of aluminum-coated mirrors, whose spectral reflectivity-curve differs markedly from that of silvered mirrors, it is possible that a new system of photographic magnitudes will replace the present International System. Such a change would have the advantage of increasing color index. It would, however, be more sensitive to sky conditions and to changes in the spectral sensitivity-curve of photographic emulsions in the far violet, concerning which little is known at present.

In spite of their obvious advantages, comparatively little photometry has been carried on with reflecting telescopes. The bulk of the work has been done with refractors, perhaps on account of the large field available. Too little attention has been paid to the reduction to the standard system by workers with refractors. A part of this reduction or correction is known as the color equation. It is most tricky, for it depends on many factors. It is not correct to speak of the color equation of any given telescope, for it varies greatly with exposure time, plate, developer, seeing, focus, guiding, etc. Careful workers must take these into account. If care is taken to keep all of these factors as constant as possible in any given series, it will be found that the color equation is a function of two variables: the color of the star, and its magnitude. This latter has been too often neglected.

I should like, at this point, to correct an impression that color equation depends primarily on spectral transmission-curves. This is, of course, a factor. The greater part of the equation is due to the form of the secondary color-curve of the lens, combined with its

spherical aberration characteristics. There is a similar misconception with regard to distance correction, it being often conceived as a loss of light energy with distance from the center. Again this is a factor, but the preponderant effect is the change of light pattern with distance. To this is due the large dependence of distance correction on magnitude.

5. VARIABLE FOG

Before the introduction of the physical photometer (exception being made of the photometry of out-of-focus images) photographically determined magnitudes were based on measures of diameter of image and on comparisons with sequences of images on a scale plate. In these methods the intensity of the fog background does not enter directly, although it may enter indirectly or unconsciously. Physical photometers, on the other hand, are strongly sensitive to the fog background and to its variations over the plate. In section 2 a theoretical treatment of the problem has been presented. It is of importance, however, to strengthen by experimental evidence the conclusions there reached. In general the variation of fog over the plate is so small that any evidence obtained would be inconclusive. Fortunately for this investigation the series of plates secured at the Lowell Observatory, from which the photovisual magnitudes of section 8 were obtained, show, on each plate, a wide range in fog intensity, the variations appearing in bands easily visible to the eye. The material is therefore excellent for this investigation. Only one of these plates was measured. The measures were made in such a way that two methods of reduction could be used: (*a*) taking into account the fog readings in the neighborhood of the image, thus forming Q in the usual way; (*b*) taking no account of the variation in fog. In (*b*), correction must be made for variation in the intensity of the lamp. This was easily accomplished by making readings at short intervals on a definite spot on the plate. The range in intensity thus found was surprisingly small, being less than one-half of 1 per cent over a time interval of two hours. For the reduction, it is necessary to have accurate magnitudes of the stars measured. Dr. Seares kindly furnished me, in advance of publication, the magnitudes of the BD stars in the 88° and the 89° zones, some two hundred

in number. It was known that both the distance correction and color equation in this series are small, so that no corrections were necessary. The results of both sets of calculations, tabulated as a function of the fog readings and corrected for variations in the lamp, are contained in Table I.

The result is conclusive in showing that it is not correct to reduce the observations on a basis of uniform fog, and it substantiates the theoretical treatment in section 2. The slight progression of the errors in the third column may be significant and may point toward

TABLE I

ERRORS AS A FUNCTION OF FOG

Fog Reading	Relative Fog Density	Mean of Errors (*a*)	Average Error	Mean of Errors (*b*)	No. of Stars
491–500	0.000	+0^{M}037	±0.077	+0^{M}317	8
481–490	.006	+ .017	.067	+ .182	15
471–480	.012	+ .016	.053	+ .119	21
461–470	.018	− .002	.063	+ .015	25
451–460	.024	− .008	.075	− .074	54
441–450	0.031	−0.010	±0.068	−0.164	31

a small second-order correction for fog. I am inclined to think, however, that it is a residual effect of a small neglected distance correction. The weight of the large value (*a*) in the first line is seen to be very small.

6. BACKGROUND EFFECT

By "background effect" is meant an effect due to general or local veiling. Factors in its production are: (*a*) general field illumination, which is of importance only when the calibrating and field stars are taken on different plates; and (*b*) local illumination, or its lack, caused by bright or dark nebulae or by concentrated groups of faint stars. The following treatment applies to all of these cases, the effect on Q of the veiling exposure being computed. The calculation is applicable to either focal or extra-focal images. For focal images

the assumption will be made that the veiling light, or its deficiency, produces no change in the diameter of the image, but in its density only, the diameter change being considered a second-order effect. For the calculation, the "characteristic," or Hürter and Driffield

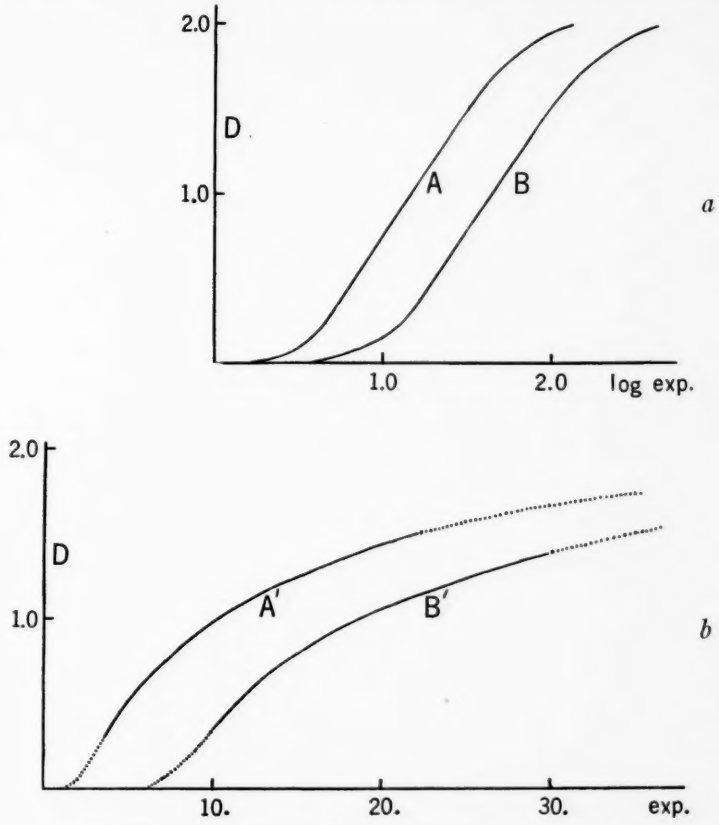

FIG. 1.—(*a*) Density plotted against log exposure. (*b*) Density plotted against exposure.

curve, of the emulsion will be needed. In Figure 1 two such curves are given, of different types, *A* and *B*, having respectively a short "toe," or underexposure region, and a pronounced toe. The latter type is characteristic of color-sensitive emulsions. These characteristics, neglected by the plate-manufacturer in giving the speed of their emulsions, are of the greatest importance in astronomy. Astronomers are more concerned with curves of the kind *A'* and *B'*,

obtained from A and B by replotting with exposure as abscissa. The intercept on the axis of the lower, approximately straight-line portion of A' or B' is a truer measure of speed than the intercepts obtained from the curves A and B, used by some manufacturers and interpreted as speed values.

Let A be the area of the image of density D_i, and C the area of illuminated or photometric "spot." Let D_0 be the fog density. Q then obviously takes the form[2]

$$Q=\frac{A \text{ rec } \log^{-1} D_i+(C-A) \text{ rec } \log^{-1} D_0}{C \text{ rec } \log^{-1} D_0}.$$

We will now examine the effect on Q of a veiling exposure, or an exposure of equal amount applied to the image and to the background in its immediate vicinity. The corresponding increments of density, ΔD_i and ΔD_0, are obviously not the same; nor can they be calculated with any accuracy. The general order of their relative magnitude can, however, be obtained from curve A' or B'. In general, it is seen from the curves that ΔD_0 is from five to ten times greater than ΔD_i. The relative values for the beginning and end of the straight-line portions of the A and B curves, which lines are indicated in the transformed or primed curves by a strengthening of the curve, are 11 and 5 for types A and B, respectively. The change in Q is thus seen to depend on the type of emulsion and upon the actual density of image and fog. I have carried through the calculation with various assumptions as to the density and the ratio of C to A. The greatest change in Q is found to be of the order of 0.002, with a corresponding change in the magnitude Δm of the order of 0.01. The least effect is where the stars are faint, for then ΔD_0 is more nearly equal to ΔD_i. The greatest effect is for the brighter stars, where the inequality in ΔD is more pronounced and where A nearly equals C. It thus appears that the background effect is small and much less than the errors of the kind considered in the following section.

7. DEVELOPMENT IRREGULARITIES

There is considerable uncertainty in placing the true cause of the comparatively large dispersion in the density of a photographic

[2] rec = reciprocal.

deposit, with its resultant effect on photographic magnitudes and on intensity determinations of one sort or another. A large amount of research has been devoted to this subject, which it is not my object to analyze at this time. For an excellent summary see a paper by J. Crabtree.[3] The onus for the objectionable dispersion has at various times been placed on the emulsion and alternatively on the development technique. The following is concerned with the problem of possible development irregularities, in so far as they can be separated from irregularities due to the emulsion itself. On account of the scantiness of the material collected, no attempt is made to generalize. It cannot be too strongly emphasized that each investigator must study the problem with reference to his own particular needs. Differences in the action of developers are so marked that general conclusions are unsafe. With one exception, all of the plates in the present investigation were developed in an Elon developer, of the following composition:

Elon	0.5 oz.	Potassium bromide	60 grains
Sodium sulphite	2.75 oz.	Water	80 oz.
Potassium carbonate	2.0 oz.		

This developer was chosen primarily on account of its high reduction potential. It has been exclusively used by the writer for many years in all work where the highest contrast is not desired. The development time is 3 minutes at 65° F.

It was decided to limit the investigation to three different development techniques, as follows:

a) Development without rocking or agitation of any kind.

b) Tray rocked continuously and irregularly. Size of tray, 14×17 inches; of plate, 4×5 inches.

c) Development with a multiple pseudo-squeegee device, due to Crabtree[4] and kindly loaned by him to the writer for these tests. Briefly described, this consists of twelve hard-rubber strips, 1 inch wide, set $\frac{3}{4}$ inch apart, with their lower edges coplanar and their upper edges rigidly connected, a handle being provided for convenient operation. Passing this back and forth across the plate at a

[3] *Uniformity in Photographic Development*, Tech. Pub., Bell Telephone System, B-907 (1935).

[4] *Ibid.*, p. 8.

moderate speed produces an efficient stirring and changing of the developer in contact with the plate. The plate is contained in a suitable recess in a hard-rubber plate, so that the squeegee is not in contact with it, the free space being of the order of 1 mm. This device has been found by Crabtree to be the most efficient in obtaining uniform development of the many methods which have been proposed, with the possible exception of the spray method, which is generally impracticable.

For the tests, plates were flashed to a density of nearly unity. Great care was devoted to securing a light source which would give constant illumination over the plate, of size 4×5 inches. In front of the light source (a 6-V auto headlight bulb) were placed two widely spaced flashed-opal glasses, the outer one being covered with a 2-inch diaphragm. After exposure and development, with careful drying, each plate was divided into a series of ninety squares, 1 cm on a side. A density reading at the center of each square was made with the thermoelectric photometer, described in section 1. By making the measures differential with respect to the central square, a high degree of accuracy was possible. The illuminated spot was chosen so large (0.7 mm) that a deflection of about 450 mm was obtained for the central square. This gives an accuracy of 0.001 in density for 1-mm change in deflection. For obtaining the density of the central square with respect to the fog, a smaller diaphragm must be used.

It would be of interest to give the detailed results of the measures. This being impracticable, it must suffice to give the extreme range of the observed densities in each case. Conversion into magnitude differences can be made by the formula

$$\Delta m = \frac{2 \cdot 5}{\gamma} \Delta D = \Delta DF ,$$

where γ is the contrast, measured in specular density. (On the average, specular density is 50 per cent greater than diffuse density.) The conversion factor F is given in Table II*a*, in which the results are summarized.

Columns (1) to (3) require explanation. In (1) the range in density over the entire ninety squares is given, so that readings at

1 cm from the edge of the plate are included. Under (2) the outer squares are omitted; under (3) the two outer rows and columns are omitted. Under (*b*) and (*c*) in nearly all cases the density in the center of the outer squares is notably high compared with the center, the differences being nearly equal to the extreme ranges shown in

TABLE II*a*

Plate	ΔD			D_c	F
	(1)	(2)	(3)		
	a) No Rocking				
E 40	0.066	0.043	0.025	0.87	2.1
E 40	.038	.036	.033	.97	2.1
Imp. Ecl.	0.030	0.021	0.012	0.81	1.8
	b) Plate Rocked				
E 40	0.187	0.136	0.104	0.89	1.9
E 40	.192	.117	.073	1.07	1.9
Imp. Ecl.	.164	.107	.069	0.98	1.6
Imp. Ecl.	0.100	0.060	0.034	0.48	3.2*
	c) With Crabtree Device				
E 40	0.104	0.042	0.025	1.28	1.4
E 40	.090	.057	.054	1.27	1.4
Imp. Ecl.	0.110	0.082	0.063	1.15	1.2

* Fine-grain development.

column (1), which would tend to cast suspicion on the plates themselves were it not for the very small differences under (*a*). The largest difference, 0.192, becomes, in magnitudes, 0.36 mag. The results shown in the table are indeed surprising. The superiority of (*a*) over (*c*), after taking into account the factor F, is not so marked except in the case of the Imperial Eclipse plates; but that it should be overwhelmingly superior to (*b*) was not to have been anticipated. No explanation is forthcoming. In view of the higher density secured with the Crabtree device, and taking into consideration the Eber-

hard effect, I would recommend its use in all cases where best results are desired.

On account of the progression in density outward from the center of the plate, shown in these results, it is seen that in photographic photometry a spurious distance correction is introduced, adding to the difficulties of photometric investigations. If standard squares are impressed on the plates near the edge, they will give a value of the contrast or scale factor which is too high.

TABLE II*b*

Plate	ΔD (1)	ΔD (2)	ΔD (3)	D_c	F
	a) No Rocking				
E 40	0.043	0.034	0.011	0.69	2.1
E 40	0.029	0.029	0.011	0.62	2.1
	b) Plate Rocked				
E 40	0.050	0.043	0.028	0.53*	1.9
E 40	0.079	0.057	0.043	0.89	1.9

* Plate had less exposure.

In the foregoing experiments, plates 4×5 inches were used. It would be of interest to repeat with larger and with smaller sizes of plates. I have done so with plates of size 4.0×1.6 inches, which are ordinarily used for spectrograms. The Crabtree device was not used in this case. The results are contained in Table II*b*. In (*a*) (no rocking) the variations of density along the length of the plate are exceedingly small, being no larger than 0.01. There is a decided gradient inward from the long edges, with highest density on the long medial line. It should be mentioned that for these small plates the division was into forty-eight rectangles of 10×5 mm. In the case of the rocked plates, the variation of density in both directions

TABLE III

CATALOGUE OF MAGNITUDES*

STAR		CO-ORDINATES (mm)		MAGNITUDE		COLOR INDEX
		X	*Y*	PV	PG	
		X: 0–10				
		7.4	64.0	11.61	11.96	0.35
	88° 92	7.9	66.1	9.95	10.20	0.25
		6.9	70.1	11.45	11.81	0.36
	88 98	3.7	78.2	11.66	12.05	0.39
		6.7	78.9	10.66	10.87	0.21
		8.2	81.7	11.93	12.67	0.74
		8.0	83.4	11.01	11.39	0.38
		6.1	85.3	11.22	11.67	0.45
		9.1	86.0	11.97	12.82	0.85
	88 100	7.5	87.0	9.06	9.46	0.40
		6.2	93.5	11.06	11.48	0.42
		7.7	93.6	11.03	11.32	0.29
		7.9	93.6	12.03	13.00	0.97
	88 103	8.2	97.8	8.20†	8.40†	0.20
	88 103	2.9	98.1	10.28	11.54	1.26
		2.0	99.7	10.96	11.40	0.44
		2.8	99.9	11.81	12.26	0.45
		5.9	103.0	11.82	12.30	0.48
		7.5	109.8	11.40	11.81	0.41
		9.1	111.9	10.93	11.37	0.44
	88 109	6.5	113.4	9.52	10.64	1.12
Dbl.	88 111	7.9	116.1	9.37	9.57	0.20
		8.9	120.2	11.77	12.28	0.51
	87 183	9.9	124.2	9.83	10.76	0.93
		10–20				
		14.1	56.7	11.98	13.25	1.27
		16.6	58.9	11.03	11.28	0.25
		13.6	60.2	11.30	11.71	0.41
		12.7	63.1	10.97	11.96	0.99
	88 91	18.8	63.6	10.27	10.50	0.23
	88 93	10.3	69.1	10.43	10.88	0.45
		19.9	72.0	11.59	12.88	1.29
		14.9	72.3	11.03	12.01	0.98
		15.4	73.1	12.13	13.50	1.37
		19.9	73.5	11.93	12.88	0.95
	88 94	17.1	76.5	9.14	10.66	1.52
		16.9	76.6	11.80	12.38	0.58
	88 95	16.9	77.0	10.70	11.23	0.53
	88 97	10.3	79.0	10.73	11.09	0.36
		14.5	80.2	11.15	11.68	0.53
	88 96	18.0	80.6	9.79	10.09	0.30
	88 99	11.8	83.0	10.17	10.64	0.47
		11.9	84.6	11.38	11.75	0.37
		14.9	86.8	11.54	11.96	0.42
		15.9	88.5	11.54	12.02	0.48
		16.9	90.5	11.44	12.30	0.86
		17.9	95.7	12.01	12.54	0.53
	88 102	18.0	96.3	9.46	9.87	0.41
		14.9	101.5	11.93	12.40	0.47
		13.4	104.8	11.89	12.86	0.97
	88 108	19.8	104.8	10.27	10.66	0.39
		14.5	106.0	11.82	12.99	1.17
		15.8	106.4	12.08	13.13	1.05
		12.8	106.5	10.99	11.51	0.52
		18.1	106.7	11.53	12.06	0.53
		15.7	112.4	11.60	12.72	1.12
		11.2	116.1	11.90	12.53	0.63
		18.7	116.8	11.61	12.22	0.61
		18.9	116.8	11.74	12.21	0.47
		16.4	118.6	11.93	12.34	0.41
		16.9	119.5	11.64	12.05	0.41
		10.9	124.3	11.56	12.95	1.39
	88°118	18.9	131.7	9.55	10.03	0.48
	87 191	19.3	138.1	10.08	11.08	1.00
		20–30				
	88 80	28.9	42.3	9.05	9.14	0.09
		25.9	45.3	11.65	12.63	0.98
	87 138	20.5	45.6	10.15	10.59	0.44
		22.9	47.7	11.91	12.24	0.33
Dbl.	88 86	24.4	47.9	8.88	.....	.....
		24.4	51.0	11.71	12.44	0.73
		29.9	51.1	11.21	12.29	1.08
		25.9	51.7	11.75	12.02	0.27
		28.9	55.7	11.20	11.71	0.51
		29.9	56.6	11.77	12.21	0.44
	88 89	22.0	60.4	10.44	11.61	1.17
		22.9	66.2	11.57	12.22	0.65
	88 90	25.9	66.9	9.05	9.81	0.76
		23.4	68.8	11.40	11.83	0.43
		22.9	72.6	11.71	12.69	0.98
		28.3	85.8	11.48	11.94	0.46
		20.1	88.0	11.40	12.49	1.09
		25.9	88.8	12.30	12.88	0.58
		21.8	89.8	11.66	12.53	0.87
		21.9	93.3	11.59	12.41	0.82
	88 101	21.1	94.9	9.24	9.55	0.31
		25.0	95.1	11.19	11.69	0.50
		22.5	97.8	12.03	13.28	1.25
	88 105	22.6	98.2	8.39†	9.04†	0.65
		21.0	99.1	10.92	12.09	1.17
	88 106	27.0	100.0	10.24	10.55	0.31
	88 107	29.6	100.5	9.85	11.48	1.63
		20.1	105.2	11.80	12.36	0.56
		20.4	107.8	11.41	12.28	0.87
	88 110	20.5	108.1	9.04	9.22	0.18
		22.8	109.6	10.70	11.32	0.62
		25.2	110.1	11.75	12.99	1.24
		26.8	112.9	11.74	12.15	0.41
		23.2	113.1	11.39	12.55	1.16
		20.8	115.1	10.62	11.88	1.26
	88 113	26.0	115.7	10.35	11.79	1.44
		21.2	116.3	11.18	11.63	0.45
4r	88 114	24.8	116.7	8.27‡	9.18‡	0.91
Var.	88 117	29.7	117.0	.....	.....	.....

* For stars marked "double" the total magnitude is given.

† Magnitudes taken from the *Mimeograph Catalogue* of Seares, Ross, and Joyner, 1935 (included for completeness).

‡ Magnitudes are "International" values.

TABLE III—*Continued*

Star	Co-ordinates X	Co-ordinates Y	Magnitude PV	Magnitude PG	Color Index
20–30—Continued					
	20.9	118.6	11.64	12.81	1.17
88°115	22.8	119.8	9.12	9.16	0.04
	26.8	119.9	10.81	12.48	1.67
	25.0	122.1	11.13	11.71	0.58
	23.9	122.8	11.70	12.10	0.40
	23.7	123.1	11.20	12.22	1.02
	21.9	123.5	12.27	13.30	1.03
	21.0	124.7	11.38	12.13	0.75
	27.7	125.6	11.79	12.36	0.57
88 119	25.3	126.9	10.50	10.84	0.34
	26.6	127.0	12.21	12.77	0.56
88 122	28.3	128.9	10.01	11.59	1.58
88 121	27.7	129.4	10.60	12.23	1.63
88 120	25.4	129.7	11.14	12.12	0.98
	29.7	130.6	11.05	11.41	0.36
88 124	27.9	134.2	9.58	10.91	1.33
88 123	25.1	135.1	10.38	10.61	0.23
88 128	27.8	139.5	10.42	10.72	0.30
30–40					
	37.0	43.1	11.90	12.48	0.58
	32.9	45.1	11.81	12.37	0.56
	31.9	45.6	11.45	12.35	0.90
88 77	38.9	46.6	8.54	8.79†	0.25
	38.5	46.7	11.49	12.26	0.77
	36.9	50.8	12.09	13.00	0.91
	38.6	51.0	11.12	12.09	0.97
88 81	32.9	52.8	10.95	11.24	0.29
	39.9	53.2	11.67	12.60	0.93
	35.9	54.1	11.07	11.34	0.27
88 83	32.9	55.5	10.38	10.77	0.39
88 85	33.7	58.4	9.38	10.36	0.98
88 82	36.5	58.7	10.45	11.00	0.55
88 84	34.9	59.7	10.58	11.09	0.51
88 87	33.2	61.0	10.95	11.31	0.36
88 88	35.5	66.6	10.81	11.26	0.45
	37.1	67.1	11.66	12.16	0.50
	35.7	68.4	11.76	12.81	1.05
	35.8	73.1	11.08	11.47	0.39
	36.4	73.3	11.96	12.43	0.47
89 27	36.5	77.0	10.45	10.99	0.54
	31.8	83.2	10.83	11.13	0.30
	32.9	83.1	11.88	12.95	1.07
	32.1	83.6	11.59	12.13	0.54
	32.0	83.7	11.70	12.03	0.33
	37.0	86.7	11.74	12.83	1.09
	39.0	87.9	11.54	12.10	0.56
89 28	39.7	89.1	8.68	10.11	1.43
	33.7	95.0	11.10	11.84	0.74
	36.8	95.2	12.41	13.00	0.59
	38.0	96.8	11.97	13.33	1.36
89 30	35.6	97.1	10.27	10.59	0.32
	37.0	101.9	11.95	13.06	1.11
89 32	38.8	102.1	10.45	10.85	0.40
	32.9	102.5	10.95	12.03	1.08
	30.8	106.6	10.63	12.02	1.39
88 112	32.0	110.0	6.32‡	7.93‡	1.61
	35.7	111.9	12.10	12.96	0.86
88 116	30.9	114.6	10.15	10.49	0.34
	34.9	118.8	11.92	12.54	0.62

Star	Co-ordinates X	Co-ordinates Y	Magnitude PV	Magnitude PG	Color Index
30–40—Continued					
	32.8	122.1	11.50	12.31	0.81
88°127	34.3	127.1	10.67	11.22	0.55
	39.7	127.8	11.75	12.41	0.66
	30.8	129.5	11.25	12.50	1.25
	32.3	130.3	11.70	12.19	0.49
88 125	32.2	130.7	10.55	11.54	0.99
	38.9	131.5	11.84	12.46	0.62
	39.2	136.2	11.21	12.53	1.32
	33.9	138.8	11.87	12.52	0.65
88 130	35.3	140.8	9.23	9.49	0.26
	37.3	141.2	11.70	12.75	1.05
	37.2	148.1	10.61	12.08	1.47
40–50					
	44.5	34.7	11.69	12.70	1.01
88 74	49.8	37.1	9.71	10.88	1.17
	42.9	45.2	12.01	12.81	0.80
	42.3	45.6	11.71	12.22	0.51
88 76	45.0	48.0	7.53†	8.87†	1.34
	48.4	54.4	11.34	11.74	0.40
	46.9	58.5	11.70	12.12	0.42
	48.5	59.1	11.33	11.67	0.34
	41.8	60.1	11.83	12.53	0.70
88 79	44.3	61.0	10.72	12.11	0.39
88 78	44.9	61.9	9.74	10.57	0.83
	47.6	63.0	11.45	12.03	0.58
	46.8	63.1	12.16	12.60	0.44
	47.9	63.6	11.93	12.40	0.47
	47.8	65.1	11.17	11.94	0.77
	49.9	65.1	11.60	12.21	0.61
	44.4	66.7	11.23	12.28	1.05
	46.8	67.8	11.93	12.37	0.44
	49.7	69.9	12.01	12.51	0.50
	47.8	70.6	11.48	11.92	0.44
	44.6	71.6	11.37	11.75	0.38
	47.7	72.8	11.98	12.48	0.50
	48.4	76.8	11.89	12.75	0.86
89 24	47.0	80.1	11.19	12.17	0.98
	47.9	82.0	11.65	12.10	0.45
	49.4	83.3	11.74	12.24	0.50
	48.5	84.1	12.16	13.25	1.09
	45.8	84.3	11.32	12.69	1.37
	46.6	89.6	10.80	11.84	1.04
	45.2	91.6	11.94	12.43	0.49
	46.2	92.3	11.30	12.73	1.43
89 31	49.9	96.6	10.42	11.41	0.99
	43.8	98.7	11.81	12.95	1.14
89 33	45.7	99.6	10.34	10.61	0.27
	46.9	99.8	11.16	12.65	1.49
	41.5	101.0	11.88	12.82	0.94
	47.8	102.7	11.00	11.45	0.45
89 34	40.8	103.2	9.90	10.62	0.63
	49.8	105.6	11.83	12.41	0.58
	48.6	108.7	11.64	12.89	1.25
	48.9	109.2	11.33	12.75	1.42
	45.9	112.6	11.31	12.58	1.27
	42.8	113.7	12.08	12.75	0.67
	47.6	114.7	12.22	13.12	0.90
88 126	41.9	117.6	11.03	11.45	0.42
88 129	40.9	125.9	10.61	10.95	0.34

TABLE III—*Continued*

Star		Co-ordinates		Magnitude		Color Index
		X	*Y*	PV	PG	
		40–50—*Continued*				
	88°131	45.9	127.0	8.88	8.97	0.09
		41.9	128.1	12.16	13.14	0.98
		40.6	129.4	11.91	13.38	1.47
		47.6	132.4	12.16	13.53	1.37
	88 134	49.9	133.1	9.28	10.29	1.01
	88 133	45.7	134.4	9.89	9.98	0.09
		46.3	134.6	12.18	13.45	1.27
	88 132	42.2	140.6	10.67	11.16	0.49
		44.6	146.8	11.53	12.70	1.17
		50–60				
		59.4	40.2	11.42	11.79	0.37
		50.3	42.5	10.56	11.89	1.33
2s	88 71	57.0	48.0	6.30‡	6.47‡	0.17
	88 72	56.9	50.7	9.64	9.95	0.31
		57.5	51.2	11.41	12.44	1.03
	88 73	55.9	53.1	10.26	10.61	0.35
		54.7	56.1	11.91	13.17	1.26
	88 75	51.4	57.0	9.09	9.39	0.30
		50.5	62.5	11.77	12.02	0.25
		55.0	63.9	11.87	12.34	0.47
5r	89 22	52.8	68.1	8.58	10.05	1.47
		57.3	71.4	12.05	12.61	0.56
		59.6	72.7	11.95	12.54	0.59
		50.8	74.0	11.65	12.17	0.52
	89 20	59.8	75.8	10.72	11.64	0.92
Dbl.	89 21	55.9	77.3	8.99	9.31	0.32
		59.5	79.2	11.95	13.05	1.10
	89 23	54.9	79.8	10.46	11.31	0.85
		54.6	80.2	12.06	12.61	0.55
		56.7	81.1	11.26	11.80	0.54
ps 12	89 25	52.8	86.2	9.73	10.18	0.45
9r		51.5	90.6	10.90	11.93	1.03
6s	89 26	57.8	91.0	10.65	11.35	0.70
10r		57.4	91.6	12.07	12.67	0.60
ps 13	89 29	51.9	92.7	10.31	10.58	0.27
7r	89 35	53.9	96.2	9.83	10.94	1.11
11r		57.7	97.5	11.98	13.26	1.28
5s+7s	89 37	57.3	97.7	.....	.....	.....
ps 19		55.9	99.3	12.21	12.69	0.48
ps 17		50.2	99.8	11.27	11.88	0.61
ps 20		57.9	100.9	12.28	13.02	0.74
ps 18		51.9	101.3	11.81	12.40	0.59
Too	close	54.6	102.3	.....	.....	.....
		54.7	102.6	10.81	10.98	0.17
	89 36	50.5	102.7	10.36	10.73	0.37
ps 16		53.9	105.5	11.17	11.62	0.45
		52.0	105.8	11.04	11.50	0.46
		56.6	106.1	11.94	13.14	1.20
		50.8	107.0	10.67	11.14	0.47
	89 38	55.1	121.1	9.71	9.88	0.17
	88 135	52.2	125.0	10.86	12.49	1.63
	88 141	58.2	129.8	10.06	10.51	0.45
		58.0	130.4	11.87	12.71	0.84
		54.8	131.6	11.90	12.62	0.72
	88 142	58.7	132.6	9.47	10.43	0.96
		55.7	133.6	11.60	12.21	0.61
	88 136	55.5	138.1	10.45	10.71	0.26
	88 137	55.4	139.8	9.91	10.25	0.34
	88 138	56.0	139.7	10.04	11.86	1.82

Star		Co-ordinates		Magnitude		Color Index
		X	*Y*	PV	PG	
		50–60—*Continued*				
	88°143	59.6	142.3	10.46	11.42	0.96
		56.8	142.5	11.54	12.01	0.47
		56.9	142.6	11.37	12.44	1.07
		51.6	143.1	11.28	12.52	1.24
	88 140	56.9	146.3	10.56	11.64	1.08
		56.8	149.7	11.06	11.36	0.30
	88 139	56.2	150.1	9.39	9.83	0.44
		53.5	150.8	10.91	12.01	1.10
		59.9	151.5	12.16	13.15	0.99
		60–70				
		62.2	38.8	11.57	11.92	0.35
		62.0	41.4	11.71	12.19	0.48
	88 67	67.0	48.4	10.27	10.66	0.39
		68.6	49.1	11.38	11.96	0.58
	88 68	64.9	51.0	10.38	11.03	0.65
	88 70	62.2	52.5	10.73	11.76	1.03
	86 65	68.3	54.2	10.00	10.29	0.29
		68.9	56.5	11.80	12.34	0.54
		61.7	60.5	11.40	11.86	0.46
	88 69	62.9	62.1	9.80	10.76	0.96
		66.0	66.1	11.92	12.99	1.07
		68.0	72.0	12.15	12.69	0.54
	89 19	62.7	79.6	10.89	11.43	0.54
	89 17	65.4	79.8	9.42	9.88	0.46
		67.0	83.0	11.48	11.95	0.47
ps 11	89 18	61.6	84.7	9.54	9.75	0.21
	89 16	67.0	85.3	10.73	12.17	1.44
		67.8	90.6	10.98	11.57	0.59
		66.4	96.0	12.12	13.60	1.48
ps 15		66.4	96.7	10.90	11.30	0.40
		69.6	101.1	11.01	11.38	0.37
ps 14	89 1	60.6	104.1	10.52	10.94	0.42
ps 10	89 3	66.9	105.8	9.02	9.10	0.08
		68.0	106.2	11.40	12.02	0.62
	89 4	68.4	108.3	10.48	10.88	0.40
		60.7	109.0	11.49	12.57	1.08
		63.9	113.6	11.36	12.46	1.10
		67.0	113.9	12.08	12.66	0.58
	89 2	69.8	120.1	9.21	10.71	1.50
		62.9	123.6	11.05	11.53	0.48
		62.5	125.8	11.60	12.17	0.57
	88 1	60.8	126.0	10.44	11.00	0.56
		65.8	128.5	11.88	12.68	0.80
		67.8	130.5	11.50	12.17	0.67
		68.7	131.7	11.17	12.71	1.54
	88 2	62.2	132.0	8.16†	8.88†	0.72
		65.7	132.9	11.80	12.36	0.56
	88 3	65.7	135.7	10.35	11.50	1.15
		64.2	136.2	11.51	12.05	0.54
		64.7	145.6	11.54	12.09	0.55
		60.5	151.6	12.14	12.60	0.46
		70–80				
	88 66	70.6	38.7	10.90	11.31	0.41
		71.9	42.5	11.48	11.82	0.34
	88 64	73.0	48.0	7.55†	7.35†	−0.20

TABLE III—*Continued*

Star		Co-ordinates		Magnitude		Color Index
		X	*Y*	PV	PG	
		70–80—*Continued*				
		70.5	51.4	11.59	12.04	0.45
		73.5	55.8	11.28	11.71	0.43
	88° 63	72.2	59.5	10.35	10.76	0.41
		78.2	59.9	11.79	12.94	1.15
	88 59	79.7	62.2	10.62	11.12	0.50
	88 62	73.3	64.1	10.68	11.85	1.17
		79.6	69.1	11.58	12.15	0.57
		77.7	71.1	11.61	12.09	0.48
		71.0	72.0	12.18	12.64	0.46
		75.0	75.5	11.80	12.94	1.14
		73.8	77.7	12.31	13.07	0.76
		74.7	77.7	11.89	12.72	0.83
		75.0	77.9	12.17	12.80	0.63
		77.2	78.6	11.56	12.96	1.40
		76.0	80.0	11.79	12.57	0.78
4s	89 12	70.8	91.5	9.81	10.32	0.51
		72.4	95.3	12.27	12.70	0.43
6r	89 9	75.4	97.2	9.23	10.45	1.22
		74.4	98.2	11.82	12.49	0.67
		78.8	99.1	11.77	12.98	1.21
		77.7	100.1	11.08	12.23	1.15
		78.6	103.0	10.97	11.48	0.51
		70.7	104.1	12.06	13.39	1.33
		72.9	106.7	11.79	12.42	0.63
		79.9	107.6	11.70	12.80	1.10
		78.4	109.2	11.52	12.02	0.50
		71.0	112.1	11.39	11.86	0.47
	89 5	70.8	112.6	10.43	11.56	1.13
	89 6	76.4	116.6	10.29	10.70	0.41
		75.0	118.7	11.36	11.89	0.53
	88 10	76.0	120.9	9.34	10.29	0.95
		72.7	121.6	10.94	12.05	1.11
		73.0	123.2	12.04	12.76	0.72
		78.3	123.5	11.95	13.00	1.05
		72.0	124.0	11.42	12.05	0.63
		76.0	126.4	11.95	12.77	0.82
		76.9	127.0	11.77	12.23	0.46
		79.5	130.9	11.06	12.63	1.57
Polaris	88 7–8	72.0	133.8	.....	.....	.....
		72.8	136.6	10.57	11.77	1.20
	88 6	73.8	139.7	9.78	10 10	0.32
		70.4	140.9	10.72	11.30	0.58
ps 5	88 4	70.8	143.0	6.45‡	6.46‡	0.01
	88 5	71.6	144.0	8.93	9.62	0.69
		70.3	145.9	11.63	12.67	1.04
		76.5	146.0	11.98	12.56	0.58
		79.9	149.6	10.55	11.70	1.15
		80–90				
		86.3	40.9	10.35	10.82	0.47
		85.8	50.9	11.75	12.64	0.89
	88 61	80.4	56.6	8.78	9.05	0.27
	88 60	86.1	58.1	11.48	12.02	0.54
		87.8	62.1	10.46	11.00	0.54
	88 57	83.0	62.8	10.41	10.99	0.58
	88 58	83.0	65.5	12.00	12.36	0.36
		81.3	66.6	11.78	13.56	1.78
	88 52	88.3	70.3	10.60	11.07	0.47
	88 54	83.8	71.4	10.07	10.48	0.41
		85.4	74.0	12.31	13.01	0.70

Star		Co-ordinates		Magnitude		Color Index
		X	*Y*	PV	PG	
		80–90—*Continued*				
		86.9	77.6	11.83	13.01	1.18
	89° 15	86.5	81.6	9.61	10.34	0.73
	89 14	87.4	83.0	10.68	11.09	0.41
ps 6	89 13	87.3	84.3	7.06‡	7.12‡	0.06
		86.5	86.6	11.36	11.99	0.63
		82.0	91.5	12.22	13.76	1.54
	89 11	87.7	92.6	10.74	11.18	0.44
		87.0	92.9	11.74	12.89	1.15
	89 10	86.4	94.1	10.33	10.74	0.41
		88.2	95.4	11.60	12.55	0.95
		86.4	97.1	11.33	12.49	1.16
		88.7	98.9	11.58	12.65	1.07
		83.2	100.1	12.00	12.60	0.60
		80.8	107.4	11.66	12.61	0.95
	89 8	85.0	107.6	10.70	11.62	0.92
		86.9	109.1	11.14	11.69	0.55
		83.5	109.6	11.71	12.21	0.50
	89 7	80.3	110.7	9.99	10.30	0.31
		87.5	110.7	11.88	12.53	0.65
	88 20	86.3	111.3	9.44	10.54	1.10
		83.9	114.1	11.80	12.34	0.54
		88.9	114.1	11.48	11.87	0.39
		87.9	114.8	11.87	12.82	0.95
		86.6	118.1	11.19	12.17	0.98
		80.2	121.8	11.94	12.60	0.66
	88 15	84.2	122.1	10.44	11.51	1.07
		88.4	123.4	11.04	12.21	1.17
		84.5	131.6	10.98	12.65	1.67
ps 8	88 9	81.0	132.0	8.13‡	8.32‡	0.19
ps 9	88 13	87.2	132.0	8.81	8.97	0.16
	88 12	89.3	136.8	9.21	10.69	1.48
	88 11	88.8	142.5	8.63	8.92†	0.29
		83.4	142.5	11.75	13.01	1.26
		80.9	144.7	11.23	11.84	0.61
		90–100				
	88 56	93.9	56.4	10.52	11.66	1.14
		92.1	57.7	11.83	12.38	0.55
	88 55	92.8	58.6	10.04	10.32	0.28
		93.2	60.6	11.53	12.06	0.53
		96.9	61.8	11.98	12.46	0.48
		98.7	62.8	11.73	12.27	0.54
		92.8	63.4	11.90	12.88	0.98
	88 50	99.4	64.1	10.96	11.91	0.95
	88 51	96.3	65.1	11.03	11.65	0.62
		92.5	67.6	11.81	12.29	0.48
Dbl.		94.3	72.2	11.73	12.39	0.66
	88 47	91.8	75.8	10.14	10 61	0.47
	88 43	92.9	79.3	9.59	9 99	0.40
	88 42	91.9	80.2	10.93	12.15	1.22
	88 41	94.9	81.5	9.95	10.28	0.33
	88 38	94.0	86.9	11.00	11.44	0.44
	88 36	93.8	93.8	10.09	11.22	1.13
		99.9	95.8	11.72	13.19	1.47
		92.9	96.6	10.58	11.90	1.32
		92.8	97.3	11.15	11.63	0.48
		97.0	97.4	11.96	13.14	1.18
		98.7	97.3	11.49	12.16	0.67
	88 32	91.0	97.9	9.88	11.47	1.59
		91.9	99.6	11.81	13.25	1.44

TABLE III—*Continued*

Star		Co-ordinates		Magnitude		Color Index
		X	*Y*	PV	PG	
		90–100—*Continued*				
	88° 29	97.2	102.1	9.27	10.06	0.79
		98.3	104.6	11.05	11.61	0.56
		97.9	105.9	11.71	12.29	0.58
	88 22	90.2	110.5	10.47	10.93	0.46
		94.6	114.7	11.00	11.69	0.69
		93.9	116.1	11.61	12.08	0.47
		98.9	116.3	11.02	11.56	0.54
		96.6	117.4	11.91	13.01	1.10
	88 19	95.7	118.7	9.71	11.08	1.37
		98.9	123.3	12.04	12.66	0.62
	88 16	93.4	131.0	9.69	10.14	0.45
	88 17	96.8	132.4	9.86	11.41	1.55
		93.0	132.7	10.93	11.98	1.05
	88 14	91.4	135.3	9.59	10.75	1.16
		94.7	135.2	11.45	12.06	0.61
		93.9	135.6	11.16	11.43	0.27
		96.5	136.8	11.00	11.52	0.52
		91.9	139.4	12.07	12.72	0.65
		100–110				
	88 53	105.3	56.1	10.51	10.95	0.44
		105.6	59.6	11.08	11.72	0.64
	88 49	102.5	63.5	10.59	10.96	0.37
		100.8	67.3	11.84	12.47	0.63
		100.4	69.3	11.98	12.58	0.60
	88 45	106.4	69.7	10.96	11.58	0.62
Dbl.	88 46	103.9	70.5	9.98	11.19	1.21
		101.8	81.7	11.84	12.52	0.68
		103.8	83.2	11.88	12.44	0.56
		104.3	87.4	12.12	12.48	0.36
		107.2	89.2	11.84	12.91	1.07
		109.8	90.6	11.78	12.87	1.09
		103.3	95.4	11.83	12.58	0.75
	88 34	100.5	95.7	10.29	11.11	0.82
	88 35	109.0	96.2	9.30	9.77	0.47
		104.9	97.7	11.30	12.08	0.78

Star		Co-ordinates		Magnitude		Color Index
		X	*Y*	PV	PG	
		100–110—*Continued*				
		109.9	98.2	11.68	12.88	1.20
	88° 33	101.3	98.3	10.05	10.42	0.37
		105.0	98.8	11.50	12.49	0.99
	88 31	106.3	102.0	9.51	10.98	1.47
		109.8	102.0	12.01	12.56	0.55
	88 30	107.9	104.2	10.49	10.91	0.42
	88 26	101.4	109.0	10.53	11.06	0.53
		102.6	110.9	11.77	12.11	0.34
		102.9	117.0	11.41	12.10	0.69
		100.9	122.7	12.16	12.76	0.60
	88 18	100.2	125.0	10.63	11.34	0.71
	88 21	108.6	125.5	10.78	11.07	0.29
		110–120				
	88 48	110.4	63.6	10.16	11.08	0.92
	88 44	113.9	69.0	9.91	11.09	1.18
		115.1	72.8	11.42	11.87	0.45
	88 40	111.3	78.9	10.36	11.22	0.86
		115.1	78.9	11.76	12.26	0.50
		118.4	79.4	11.52	12.61	1.09
		115.9	79.8	12.03	12.53	0.50
	88 39	117.5	80.1	9.16	9.31	0.15
		114.8	83.2	11.22	11.82	0.60
		116.9	85.7	11.80	12.41	0.61
	88 37	115.0	88.6	10.45	11.62	1.17
	87 48	118.9	88.9	9.59	11.20	1.61
		119.7	94.7	10.67	11.02	0.35
		115.0	99.1	11.04	12.18	1.14
		118.9	99.2	11.84	12.91	1.07
	88 28	115.7	107.2	10.64	11.15	0.51
		115.1	109.5	11.10	11.86	0.76
		115.2	110.1	11.98	12.61	0.63
	88 27	111.8	112.2	10.43	10.81	0.38
	88 25	114.8	114.9	10.62	11.26	0.64
	88 24	111 8	117.5	10.63	10.99	0.36
	88 23	111.6	118.1	10.92	11.25	0.33

is very marked and is of a progressive, not an accidental, nature. Here, as in the case of the larger plates, superiority of (*a*) over (*b*) is indicated.

8. PHOTOVISUAL AND PHOTOGRAPHIC MAGNITUDES OF STARS WITHIN 2° OF THE POLE (1855)

The privilege was accorded the writer, by Dr. V. M. Slipher, of securing plates with the 13-inch refractor of the Lowell Observatory for photometric measurement. The photovisual plates were taken by the writer in 1932 and 1934; and the photographic plates, by F. V. Edmonson in 1935. Cramer Isochromatic and Eastman 40

plates were used, respectively. The photovisual plates were slightly extra-focal; the photographic, focal.

Photovisual magnitudes.—Eight plates, each with an exposure time of 10 minutes, were measured with the photometer described

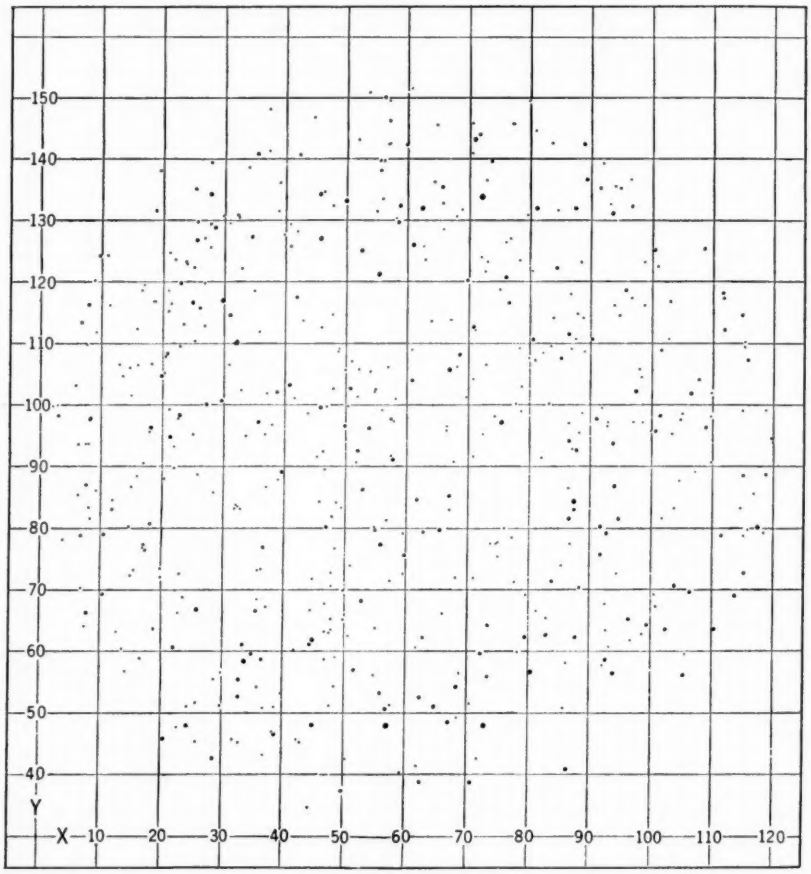

FIG. 2

in section 1. The limiting photovisual magnitude of these plates is 12.5. For additional material on the faint stars, two plates having an exposure time of 30 minutes and one of 60 minutes were used. All of the stars easily seen on one of the plates of 10 minutes' exposure were selected for measurement. It is accordingly to be pre-

sumed that the catalogue is fairly complete to 12.0 photovisual magnitude for the 88° and 89° BD zones (see Table IV). The plates were exposed in pairs, with the telescope direct and reversed, in order to eliminate asymmetry in the field. In addition, the centers were scattered over the field, with a wide range in the sidereal time of exposure; so it is to be presumed that field errors are well eliminated. A discussion of the material showed complete absence of color correction and only a small distance correction. The plates showed considerable fog, with irregularities, lying in broad bands. However, this has been shown (sec. 5) to have little or no effect on the measured magnitudes. The range in magnitude is about 3.5, which was easily handled with a single diaphragm in the photometer. The one used gave an illuminated disk of 0.22 mm in diameter on the plate. The internal probable error of a magnitude in the catalogue is ±0.02, each magnitude depending on eight plates, on the average.

Photographic magnitudes.—The photographic magnitudes in the catalogue depend upon four plates, all centered on the pole of 1935. They were taken in pairs, direct and reversed, and at sidereal times differing by 6 hours, thus reducing any effect of field asymmetry. Discussion of the material shows that the distance correction is large, compared with the photovisual. It was determined in two ways: (*a*) from a comparison with the polar catalogue of Seares, Ross, and Joyner (1935), and (*b*) from a series of equal polar exposures, with shifts in declination.

The positions of the stars in Table II are plotted in Figure 2. The co-ordinates in the figure are correlated with the co-ordinates in the table, making identification easy. For conversion into angle, 1 mm equals 122″.

The frequency distribution of the photovisual magnitudes, shown in Table IV up to the twelfth magnitude, agrees very well with Seares's Table XVII[5] after multiplying his values by the factor 0.76. The difference is a longitude or a local obscuration effect. No significance should be attached to the distribution of photographic

[5] *Ap. J.*, **62**, 362, 1925. The argument of Table XVII must be corrected according to the precept given on page 365.

magnitudes beyond 12.74, since the material has been selected on a basis of photovisual magnitude.

The drop in the number of photovisual magnitudes in compartment 12.00 to 12.24 to about one-third of the number normally to be expected, is of interest. It is not a question of errors in measurement; nor is it a question of the limiting magnitude of the plate on which the selection was made. Two observers participated in the selection,

TABLE IV

FREQUENCY DISTRIBUTION: MEAN COLOR INDICES

Magnitude Limits	No. of Stars		Mean Color Index	
	PV	PG	PV	PG
9.00– 9.24	15	.....	$0^{M}60$	.....
9.25– 9.49	11	5	.70	0.29
9.50– 9.74	16	3	.83	0.40
9.75– 9.99	17	10	.78	0.37
10.00–10.24	15	9	.68	0.66
10.25–10.49	40	15	.58	0.60
10.50–10.74	42	25	.75	0.59
10.75–10.99	30	26	.77	0.60
11.00–11.24	50	30	.69	0.67
11.25–11.49	50	35	.72	0.59
11.50–11.74	67	38	.73	0.71
11.75–11.99	92	40	.79	0.72
12.00–12.24	40	69	0.79	0.69
12.25–12.49	7	54	.....	0.70
12.50–12.74	.....	60	.....	0.85
12.75–12.99	.....	39	.....	1.02
13.00–13.24	.....	20	.....	1.04
13.25–13.49	.....	10	.....	1.28
13.50–13.74	.....	5	.....	.....

with close agreement. In order to determine the dispersion which might be expected from one plate to another in the limiting magnitude, all of the plates were re-examined with this in view, the polar sequence furnishing the criterion. Nos. 20, 21, and 12*r* of the polar sequence, all of magnitude 12.5, were visible on all of the plates, the variation in visibility being small. No. 19, of magnitude 12.24, was well seen, so that stars of this magnitude should not have been missed. Perhaps the reason for so many misses is to be found in the fact that the plate background was unusually bad, with graininess and streaky fog. To a greater or less extent, the phenomenon is a

normal, though puzzling, one. The point is brought up only to call attention to the dangers lying in statistical investigations depending on counts of faint images near the threshold of the plate.

Color indices.—Comparison of the mean color indices given in Table IV with Seares's values[6] has been made from a plot of the individual mean values. In the mean they are less than Seares's values by about 0.10 mag. The small value, 0.58, for mean $m = 10.37$, may have astrophysical significance. When comparison is made on the basis of photographic selection (last column of Table IV), better agreement is found; in fact, the two graphs are identical up to magnitude 12.37. Beyond this point the effect of the selection of the material enters.

YERKES OBSERVATORY
June 22, 1936

[6] *Ibid.*, **61**, 114, 1925.

THE LUMINOSITY FUNCTION OF NEBULAE*

EDWIN HUBBLE

II. THE LUMINOSITY FUNCTION AS INDICATED BY RESIDUALS IN VELOCITY-MAGNITUDE RELATIONS

ABSTRACT

Velocity-magnitude relations (log $v=0.2m+c$) are derived from apparent magnitudes of (*a*) brightest stars in resolved field nebulae, (*b*) field nebulae of all types, and (*c*) fifth brightest nebulae in clusters. Since the absolute magnitude of brightest stars, $\overline{M}_s$, is known, $\overline{M}_n$ and $\overline{M}_{c5}$ are indicated by the values of c in the three relations. Residuals in the relation for field nebulae of all types indicate the form of the luminosity function as distorted by peculiar motions. The effects of the distortion are reduced in velocity-distance relations ($v=kd$) derived from (*a*) brightest stars and (*b*) field nebulae. The coefficient k is about 526 km/sec per million parsecs, and the dispersion of peculiar motions is about 200 km/sec.

The luminosity function derived from the residuals agrees closely with that determined in Part I (*Mt. Wilson Contr.*, No. 548; *Ap. J.* **84**, 158) from brightest stars in resolved nebulae alone. The various types of nebulae are comparable, with the exception of the irregulars, which average about half as bright as the others.

The distance of the Virgo cluster is found to be of the order of 2.3×10^6 parsecs ($m-M=26.8$).

The velocity-distance relation is not only a phenomenon of great cosmological significance but also a powerful instrument of nebular research. It furnishes individual distances of unresolved field nebulae, and percentage errors actually diminish as distances increase. Residuals from the relation determine the forms of the luminosity functions of the more remote field nebulae of any or of all types. Since the relation is presumably unique, its formulation by means of different criteria of distance indicates the relative, intrinsic luminosities of the criteria, and, when the absolute magnitude of one criterion is known, the magnitudes of the others are readily calculated. These particular applications among the many that are possible will be made in the present investigation.

Observations furnish velocity-magnitude relations in which the observed quantities are red shifts,[1] expressed on the convenient scale

* *Contributions from the Mount Wilson Observatory, Carnegie Institution of Washington*, No. 549.

[1] Red shifts are combinations of actual motions (solar motion and peculiar motions) and distance effects. The interpretation of distance effects—whether or not they are

of velocities, and apparent magnitudes of nebulae or components of their stellar contents. The velocity-distance relation may be derived from the observed relations when the absolute magnitudes of the distance criteria are known.

CORRECTIONS TO RED SHIFTS

Red shifts are measured with relatively high accuracy, depending only on the scale of the spectrograms and not on the distances or faintness of the nebulae. The measured shifts must first be corrected for solar motion. The solar motion is a combination of the motion of the sun with respect to the center of the galactic system and the motion of the galactic system with respect to the nebulae. The former, which is essentially the motion known as "galactic rotation," has been determined independently. It is practically indistinguishable from the solar motion with respect to the nebulae (as indicated by the data now available), and, consequently, the motion of the galactic system as a whole is presumably small.

A re-examination of the data raises a question of considerable interest. Measured red shifts for nebulae which are members of the local group are almost entirely accounted for as reflections of galactic rotation. The mean residual, representing a combination of distance effects (necessarily positive) and the motion of the galactic system within the group, is a very small negative quantity. This result may be interpreted in two ways: either the distance effect does not operate within the group, or the galactic system, which lies near one end, is approaching the center of the group with a velocity that compensates the mean distance effect of the other members.

The significance of the question has led to investigations of the motion of the galactic system with respect to the nearer field nebulae (excluding members of the local group). However, the resolved nebulae with measured red shifts, which alone can be used for the purpose, are not well distributed, and the results are indeterminate. These nebulae tend to lie in a rather narrow belt, perpendicular to

---

Doppler effects—is immaterial in the present investigation. They behave as velocity shifts behave and may be expressed on the same scale in order to avoid confusion in separating out the actual motions. The term "velocity" in connection with distance effects will be understood to mean apparent velocity.

the galactic plane, and are divided into two groups by the heavy obscuration in the zone of avoidance. When the galactic rotation and the distance effects (corresponding to distances indicated by brightest stars) are removed from the red shifts, the residuals are almost negligible except for two small groups having opposite signs and situated about 90° apart in the sky. These groups completely dominate the distribution of residuals, and the calculated motion of the galactic system varies according to the method of weighting the data. About the only conclusions that can be drawn at present are: (*a*) the motion of the galactic system is small and (*b*) the motion is probably not in the direction of the center of the local group. The evidence, therefore, at the moment suggests that the velocity-distance relation does not operate within the local group. Current observing programs include the assembling of data necessary for further investigation—namely, red shifts for resolved nebulae in unobserved regions of the sky. Meanwhile the galactic rotation alone may be used for the solar motion with respect to the field nebulae, with no great sacrifice of accuracy. This motion is adopted as 275 km/sec toward an apex at galactic longitude 65°, latitude 0°.

Red shifts, when corrected for solar motion, are combinations of distance effects and peculiar motions of the nebulae. The latter appear to be distributed symmetrically about the zero value with a dispersion, suggested by observational data, of the order of 200 km/sec for nebulae in the general field and possibly treble that value for members of the great clusters.[2] When red shifts are plotted against distances, the residuals due to peculiar motions are symmetrically distributed about the correlation-curve and, in the mean, they cancel. On the other hand, when logarithms of red shifts are plotted against apparent magnitudes (which are linear functions of logarithms of distances), the residuals due to peculiar motions are unsymmetrically distributed. The displacements of mean residuals should always fall below the velocity-magnitude relation and may seriously distort the curve in the regions where distance effects are small. The amounts of the displacements can be estimated but are difficult to determine analytically.

[2] Smith, *Mt. W. Contr.*, No. 532; *Ap. J.*, **83**, 23, 1936.

CORRECTIONS TO APPARENT MAGNITUDES

The apparent magnitudes used in the present investigation are photographic magnitudes on the international system of brightest stars, of field nebulae, and of the fifth brightest nebulae in clusters. The derivation of magnitudes of stars and field nebulae has been discussed in Part I. The magnitudes of cluster members are probably more reliable than the others. They represent careful measures by various observers, and the consistency is very satisfactory.

Apparent magnitudes require corrections for local obscuration. The fringes of partial obscuration along the borders of the zone of avoidance are regions of uncertainty, and, in general, nebulae situated there are omitted from the discussion. Beyond the fringes the corrections may be represented by the cosecant law established in a survey of the distribution of nebulae over the sky to a definite limiting magnitude.[3] The corrections

$$\Delta m_\beta = 0.25\ (\operatorname{cosec}\beta - 1)\ ,$$

where β is the galactic latitude, account for the obscuration due to the substratum of diffuse material known as the "absorbing layer." In the higher latitudes the formula is believed to be trustworthy. In the very low latitudes it apparently introduces a small longitude effect; corrections in the direction of the galactic center are probably too small, while those in the opposite direction are too large. These second-order effects would cancel for large numbers of objects uniformly distributed in longitude, although the dispersion of residuals would be increased. Actually, the nebulae now considered are not so distributed, and both the mean magnitude and the dispersion may be influenced.

In addition to the correction for local obscuration, magnitudes of very distant nebulae must be corrected for effects of red shifts on apparent luminosity. The precise evaluation of these effects involves assumptions as to the cause of red shifts, the curvature of space, and the distribution of intensities in the ultra-violet spectra of nebulae. Nevertheless, the general order of the effects over the observed range in red shifts is much the same on any reasonable in-

[3] *Mt. W. Contr.*, No. 485; *Ap. J.*, **79**, 8, 1934.

terpretation of the data. The provisional correction to be subtracted from the observed magnitude,

$$\Delta m_\lambda = 3\,\frac{d\lambda}{\lambda}\,,$$

probably introduces no errors as large as 0.1 mag. in the data discussed in the following sections. The derivation of the formula will be presented in a later contribution.[4] It will be noticed that the corrections in magnitudes are merely the apparent velocities, in km/sec, divided by 100,000. Thus, for $v = 5{,}000$, $\Delta m_\lambda = 0.05$, and for $v = 25{,}000$, $\Delta m_\lambda = 0.25$.

The corrected magnitudes indicate distances, subject to the dispersion of the absolute magnitudes of the particular objects considered. The relation is

$$\log d = 0.2m + (1 - 0.2\overline{M})\,,$$

where the distance, d, is expressed in parsecs and $\overline{M}$ is the mean absolute magnitude for objects of the same apparent magnitude. Since the luminosity functions of nebulae and (presumably) of brightest stars approximate normal error-curves, the errors in $\log d$ for a given apparent magnitude will be symmetrically distributed, but the errors in d will be distributed asymmetrically. In the latter case the displacement of the mean distance, $\overline{d}$, with respect to the distance corresponding to the mean absolute magnitude is simply expressed by the relation[5]

$$\log \overline{d} = \overline{\log d} + 1.152\sigma^2_{\log d}\,,$$

where the dispersion, $\sigma_{\log d}$, is evidently a fifth of the dispersion of M in the luminosity function. For the dispersions adopted in Part I[6] of the present investigation the values are

	σ_M	$\sigma_{\log d}$	$1.152\sigma^2_{\log d}$
Brightest stars	0.41	0.08	0.0077
Resolved nebulae	0.85	0.17	0.0333

[4] A discussion of the principles involved is given by Hubble and Tolman, *Mt. W. Contr.*, No. 527; *Ap. J.*, **82**, 302, 1935. The formula above is similar to that derived by de Sitter, *B.A.N.*, **7**, 205, 1934, although the interpretation is somewhat different.

[5] The writer is indebted to Dr. Richard Tolman, of the California Institute of Technology, for this very useful general relation.

[6] *Mt. W. Contr.*, No. 548; *Ap. J.*, **84**, 158, 1936.

Therefore, statistical distances derived from brightest stars are systematically too small by about 1.8 per cent, and distances from nebular magnitudes are too small by about 8 per cent. The dispersion among the fifth brightest nebulae in clusters appears to be negligible.

From these considerations it is evident that the velocity-distance relation among resolved nebulae can be most advantageously studied in the form $v=kd$. Only among the remote, unresolved nebulae, where peculiar motions are small compared to distance effects, can the form $\log v=bm+c$ be investigated with precision. Nevertheless, by making reasonable allowance for the skew distribution of peculiar motions, approximate solutions for the latter form of the relation can be derived for all three classes of objects considered—namely, resolved nebulae, field nebulae, and clusters. This procedure is followed below, and later the form $v=kd$ is discussed.

THE VELOCITY-MAGNITUDE RELATION FOR CLUSTERS

The brighter members of clusters furnish extreme distances for given apparent luminosities and determine the range over which red shifts have been actually measured. The coefficient b in the relation

$$\log v=bm+c$$

is 0.2, within the uncertainties of the observations. Since the distances of objects with a constant absolute magnitude are

$$\log d=0.2m+C\,,$$

it follows that the relation between v and d is sensibly linear as far out into space as spectra have been recorded.

Data for ten clusters are given in Table I. The velocities are the means of all those measured in the individual clusters, the numbers (second column) ranging from 1 to 32. Dispersions within the clusters, as suggested by the two with the most numerous velocities,[7] are probably of the general order of 700 km/sec. The percentage

[7] Humason, *Mt. W. Contr.*, No. 531; *Ap. J.*, **83**, 10, 1936; Zwicky, *Helv. phys. acta.*, **6**, No. 2, 1933.

uncertainties in the distance effect, as derived from single members, are large in the case of the first four clusters in the table but are greatly reduced by the numbers of members observed. In the remaining clusters the dispersions are only a few per cent of the distance effects. The mean for the Virgo cluster, in spite of thirty-two individual velocities, is probably the most uncertain of the list.

TABLE I

MAGNITUDES AND RED SHIFTS IN CLUSTERS

CLUSTER	No.	VEL.*	β	m_{pg} OF NEBULAE†				MEAN m_{pg}		Δm_β	Δm_λ	m_{c5}‡
				1st	3d	5th	10th	1 to 3	1 to 10			
Virgo	32	1230	76°	10.2	10.3	10.5	10.7	10.23	10.48	0.00	0.01	10.49
Pegasus	5	3810	49	12.1	12.9	13.0	13.5	12.37	13.0	.08	.04	12.88
Perseus	4	5220	13	13.1	14.2	14.4	14.5	13.77	14.22	.87	.05	13.48
Coma	8	7360	87	13.5	14.0	14.3	14.4	13.77	14.17	.00	.07	14.23
U Ma I	1	15500	59	15.9	16.2	16.3	16.7	16.03	16.38	.03	.15	16.12
Leo	1	19600	54	16.4	16.5	16.6	16.9	16.47	16.68	.07	.20	16.33
Cor. Bor.	1	21200	55	16.5	16.8	16.8	17.0	16.67	16.84	.05	.21	16.54
Gem	2	23400	20	16.8	16.9	17.0	17.2	16.83	17.0	.48	.23	16.29
Boötes§	1	39200	66	17.8	18.2	18.3	18.5	18.0	18.25	.02	.39	17.89
U Ma II§	1	42100	55	18.0	18.0	18.2	18.4	18.0	18.19	0.05	0.42	17.73

* Velocities are all by Humason except nine by Sinclair Smith and five by Slipher in the Virgo cluster and two by Pease in the Coma cluster.

† All magnitudes in the Virgo cluster and certain of those in the Pegasus, the Perseus, and the Coma clusters are by Stebbins (photoelectric cell); magnitudes in the two Ursa Major clusters are by Baade, and other magnitudes are by Hubble (schraffierkassette).

‡ m_{c5} represents the magnitude of the fifth brightest nebula, corrected for local obscuration (Δm_β) and for red shifts (Δm_λ).

§ Humason states that the velocity in the Boötes cluster from three spectrograms of the brightest nebula is "the last well-established point on the velocity-distance diagram." The velocity for U Ma II is considered as "somewhat uncertain" (*Mt. W. Contr.*, No. 531; *Ap. J.*, **83**, 10, 1936).

Solar motion in the form of galactic rotation has been removed, but peculiar motions of the clusters as units are included in the tabulated velocities. The peculiar motions are evidently small, but the precise dispersion is unknown. Any considerable percentage error due to such motion, however, is probably restricted to the Virgo cluster alone.

The magnitudes of the ten brightest nebulae in each cluster have been measured, and those of the first, third, fifth, and tenth, together with the means of the first three and of all ten, are listed in Table I. The magnitudes of all ten nebulae in the Virgo cluster and of one or more in the three following clusters were measured by Stebbins and

Whitford, using a photoelectric cell directly at the Newtonian focus of the 100-inch reflector.[8] Since large apertures were employed (and frequently series of apertures), these magnitudes are the most accurate in the table. The nebulae in the two Ursa Major clusters were measured by Baade,[8] and the remaining nebulae by the writer, both using a schraffierkassette. When the diameters of built-up (or extra-focal) images are large—2.5 to 3 times the diameters of focal images as estimated by simple inspection of well-exposed photographs—the measured magnitudes do not differ systematically from those derived with a photoelectric cell. The magnitudes thus form a homogeneous group although they represent different methods and different observers.

Corrections for local obscuration are small, except in the case of the Gemini cluster ($\Delta m_\beta = 0.48$) and of the Perseus cluster ($\Delta m_\beta = 0.87$). The former cluster at latitude $+20°$ and opposite the galactic center is very probably overcorrected, but the amount is uncertain. The residual in the velocity-distance relation is consistent with this assumption. The Perseus cluster at latitude $-13°$ and about $145°$ from the galactic center shows no large residual. However, it lies very near the edge of the zone of avoidance, and partial obscuration in the fringe of the zone might compensate a small overcorrection, owing to a longitude effect in the absorbing layer.[9]

When the observed magnitudes, m_o, have been corrected for local obscuration and for red shifts, the results may be termed corrected magnitudes, m_c. Thus,

$$m_c = m_o - \Delta m_\beta - \Delta m_\lambda .$$

The velocity-magnitude relation is derived from the correlation between corrected magnitudes and logarithms of apparent velocities corrected for solar motion.

[8] Messrs. Stebbins, Whitford, and Baade have very generously permitted the writer to use their unpublished magnitudes of cluster members.

[9] In an earlier discussion (*Mt. W. Contr.*, No. 427; *Ap. J.*, **74**, 43, 1931) selective obscuration in the Perseus cluster was suggested because of the pronounced color excess and the low latitude. It is now known that color excess is a general characteristic of early-type nebulae in all latitudes and that obscuration in the absorbing layer (as distinguished from clouds in the zone of avoidance) is probably non-selective.

A significant velocity-magnitude diagram might be constructed from the m_c in any of the six columns of observed magnitudes in Table I. Actually the fifth brightest nebulae, for which the m_c are listed in the last column, have been used in Figure 1. It will be noticed that the fifth nebulae are closely comparable with the means

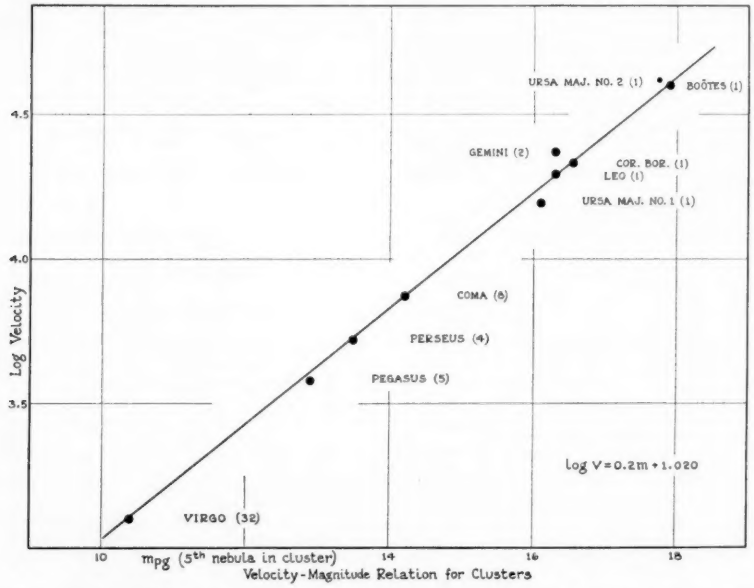

FIG. 1.—Logarithms of mean velocities of nebulae observed in each cluster, plotted against apparent magnitudes of the fifth brightest nebulae in the clusters. Velocities are corrected for solar motion; magnitudes for local obscuration and for red shifts. Figures in parentheses indicate the number of individual velocities in each cluster. The single velocity in Ursa Major II, represented by a small disk, is given half weight because it is uncertain.

of all ten. The mean difference is $5\text{th} - \overline{1 \text{ to } 10} = 0.02$; average residual, 0.06; maximum range, 0.26. The general similarity of the great clusters is so pronounced that relative distances can be discussed with some confidence on the basis of either criterion, and the fifth nebula has been selected as a matter of convenience.[10]

When the linearity of the velocity-distance relation is assumed,

[10] The differences between the first and the fifth nebulae exhibit a considerable range and are rather sensitive to the richness of the clusters. The mean difference is 0.45, but in three cases the brightest one or two nebulae are outstanding; the mean for the remaining seven clusters is 0.30.

the constant, c, is readily derived as the mean of the differences, $\log v - 0.2\, m_c 5$. The simple mean is 1.025, with a dispersion of 0.04. A closer approximation may be attempted by weighting the data according to the number of individual velocities in a cluster, the size of the mean velocity, and the freedom from local obscuration. The result,

$$\log v = 0.2 m_c + 1.020,$$

with a dispersion in the constant of 0.035, will be adopted.[11]

THE VELOCITY-MAGNITUDE RELATION FOR FIELD NEBULAE

A similar relation for field nebulae may be derived from the data in Table II. Members of the local group are excluded because of their proximity and the probability that they are not subject to the distance effect. Members of a few other conspicuous groups are also excluded because of uncertainties in the luminosity functions of such groups. Of the 109 objects that are listed, 29 are resolved nebulae which were included in Table II of Part I. They are used later to formulate the velocity-magnitude relation on the basis of apparent magnitudes of brightest stars.

The observed magnitudes, m_o, are those listed in the Harvard Survey of bright nebulae, corrected by -0.1 mag. in order to reduce them to the system established by photoelectric cell measures, except where the latter measures, or results from schraffierkassette and

[11] The largest residuals, expressed in magnitudes, are as follows: Gemini, +0.46; Ursa Major II, +0.30; Ursa Major I, −0.27; Virgo, −0.14. The first three have minimum weight; the Gemini cluster is almost certainly overcorrected for local obscuration, and the two Ursa Major clusters are represented by one velocity each, the larger velocity being described as uncertain. The residual in the Virgo cluster is readily explained by peculiar motion and by the dispersion of individual velocities. No other residual is greater than 0.07 mag.

The linearity of the velocity-distance relation, as indicated by the data for ten clusters in Table I, depends upon the corrections for red shifts, $\Delta m_\lambda = 3 d\lambda/\lambda$. If red shifts are velocity shifts, $\Delta m_\lambda = 4 d\lambda/\lambda$, and the relation may depart slightly from linearity. A least-squares solution (for the clusters) gives $\log v = 0.2064 m + 0.932$. This result suggests that the second-order term in the power series for Doppler shifts in an expanding universe—the coefficient l in the expression $d\lambda/\lambda = kr + lr^2 + \ldots$ —would probably be positive and of the general order of 0.8 km per sec per million parsecs. The significance of such a term in cosmological theory is evident. It should be stressed, however, that the departures are practically equivalent to the added corrections for recession.

TABLE II

MAGNITUDES AND RED SHIFTS OF FIELD NEBULAE

NGC	Type	v_o*	m_c†	log $v_o - 0.2m_c$	Distance‡ Unit, 10^6 par.
3031	Sb	+ 70	7.98	+0.249	0.42
253	Sc	− 130	8.20	.....	0.47
5236	Sc	+ 480	8.28	1.025	0.48
5457	Sc	480	8.96	0.889	0.66
3034	Ir	390	9.08	0.775	0.70
4736	Sb	410	9.09	0.795	0.70
4594	Sa	1130	9.12	1.221	0.72
5194	Sc	420	9.38	0.747	0.80
3115	E7	440	9.54	0.735	0.87
4826	Sb	230	9.60	0.442	0.89
3627	Sb	610	9.76	0.833	0.96
2403	Sc	175	9.85	0.273	1.00
1068	Sbc	790	10.02	0.894	1.08
4258	Sb	610	10.07	0.771	1.11
2903	Sc	260	10.09	0.397	1.12
3521	Sbc	640	10.13	0.780	1.14
4449	Ir	310	10.19	0.453	1.17
1023	SBa	310	10.20	0.451	1.17
3368	Sa	870	10.25	0.890	1.20
2841	Sb	610	10.28	0.729	1.22
3623	Sa	760	10.36	0.809	1.27
5055	Sb	590	10.38	0.695	1.28
5253	Ir	395	10.45	0.507	1.32
2683	Sc	300	10.56	0.365	1.35
4565	Sb	+ 1170	10.59	0.950	1.41
247	Sc	− 80	10.60	.....	1.41
4214	Ir	+ 380	10.60	0.460	1.41
7331	Sb	680	10.64	0.704	1.44
3379	Eo	730	10.65	0.733	1.45
4725	Sab	1180	10.69	0.934	1.47
3384	SBa	780	10.75	0.742	1.51
1407	Eo	1790	10.89	1.075	1.61
278	Sc	760	10.97	0.687	1.68
157	Sc	1780	10.97	1.056	1.68
628	Sc	580	10.98	0.567	1.69
1087	Sc	1720	11.01	1.033	1.71
1395	E	1620	11.01	1.008	1.71
4151	Sb	1040	11.08	0.801	1.76
2146	Ir	1170	11.15	0.838	1.82
3489	Sab	+ 550	11.16	+0.508	1.83

* v_o represents apparent velocities corrected for solar motion.

† m_c represents apparent magnitudes corrected for local obscuration, Δm_β, and for red shifts, Δm_λ.

‡ Distances are calculated from the formula $\log d = 0.2m_c + 4.03$.

TABLE II—*Continued*

NGC	Type	v_o*	m_c†	log $v_o - 0.2m_c$	Distance‡ Unit, 10^6 par.
5005	Sc	+ 1030	11.18	+0.777	1.85
2775	Sa	940	11.20	0.733	1.86
1332	Sa	1190	11.23	0.829	1.89
1084	Sc	1360	11.24	0.885	1.90
2681	Sa	710	11.26	0.599	1.92
3486	Sc	1250	11.27	0.843	1.92
2655	Sa	1470	11.28	0.911	1.93
5866	Sa	860	11.33	0.668	1.98
3351	SBb	605	11.34	0.514	1.99
936	SBa	1200	11.43	0.793	2.07
5322	E3	2070	11.43	1.030	2.07
3412	SBa	890	11.45	0.659	2.09
4111	E7	890	11.48	0.653	2.12
404	Eo	35	11.50	.....	2.14
7217	Sab	1250	11.51	0.795	2.15
3610	E4	1950	11.53	0.984	2.17
2985	Sb	1160	11.54	0.756	2.18
584	E3	1720	11.56	0.923	2.20
720	E6	1690	11.56	0.916	2.20
6951	SBbc	1560	11.56	0.881	2.20
3726	Sc	1230	11.57	0.776	2.21
4051	Sbc	740	11.58	0.553	2.22
5846	Eo	1850	11.59	0.949	2.23
5746	Sb	1980	11.61	0.975	2.25
5907	Sbc	620	11.62	0.468	2.26
3147	Sc	2720	11.63	1.109	2.27
3377	E5	590	11.65	0.441	2.29
772	Sb	2170	11.73	0.990	2.38
5566	SBb	1660	11.73	0.874	2.38
2344	SBc	520	11.76	0.364	2.41
2768	E6	1450	11.77	0.807	2.42
1400	E1	290	11.81	0.100	2.47
2787	SBa	790	11.84	0.530	2.50
7727	Sa	1820	11.86	0.888	2.52
2950	SBa	1560	11.88	0.817	2.55
7457	Sa	660	11.89	0.442	2.56
7177	Sbc	1390	11.94	0.755	2.62
7723	SBb	2040	11.96	0.918	2.64
5985	Sb	2820	11.98	1.054	2.67
1700	E4	580	11.99	0.365	2.68
2859	SBa	1450	12.00	0.761	2.69
3227	Sb	1090	12.04	0.629	2.74
3414	SBb	1440	12.06	0.746	2.77
6384	SBb	1690	12.10	0.808	2.82
7814	Sa	+ 1070	12.18	+0.593	2.92

TABLE II—*Continued*

NGC	Type	v_o*	m_c†	log $v_o - 0.2m_c$	Distance‡ Unit, 10^6 par.
6574	Sbc	+ 2810	12.19	+1.011	2.94
2366	Ir	190	12.24	.....	3.01
7332	E6	1470	12.27	0.713	3.05
5982	E3	3120	12.28	1.038	3.06
7741	SBb	430	12.30	0.174	3.09
6181	Sc	2740	12.31	0.976	3.10
3193	E2	1240	12.44	0.605	3.30
6340	Sa	2320	12.47	0.871	3.34
7742	Sbc	1850	12.50	0.767	3.39
7177	SBb	2700	12.59	0.913	3.53
681	Sab	2000	12.76	0.749	3.82
6703	Eo	2280	13.06	0.746	4.38
6661	Sa	4170	13.10	1.000	4.45
6824	Sb	3450	13.25	0.888	4.79
6658	Sa	4370	13.30	0.980	4.90
6359	E2	3250	13.37	0.838	5.06
6710	Sa	5380	13.39	1.053	5.11
6702	E2	2530	13.45	0.713	5.26
7343	SBb	1380	13.57	0.426	5.55
160	Scp	2660	13.82	0.661	6.22
4865	E4	5110	14.55	0.798	8.71
7242	E2	5180	14.59	0.796	8.87
Anon.	Sa	4410	15.62	0.540	14.26
Anon.	E1	+19070	17.46	+0.788	33.27

extra-focal images, are available. The observed magnitudes, as before, are reduced to corrected magnitudes, m_c, by the corrections Δm_B and Δm_λ.

The velocities include the early measures of Slipher, the later results of Humason and others, and some of the first determinations by Mayall with the new nebular spectrograph at the Lick Observatory. Solar motion has been removed, and the listed velocities are combinations of peculiar motions and distance effects.

Logarithms of velocities are plotted against corrected magnitudes in Figure 2. The influence of peculiar motions is pronounced in the lower part of the diagram, and the proper corrections are difficult to evaluate. However, the omission of three of the largest negative residuals has led to the relation

$$\log v = 0.2m_c + 0.77 ,$$

in which the constant is probably correct within 0.02. The result represents a compromise between the remaining effects of peculiar motion, which give negative residuals in the lower part of the diagram, and a tendency to select brighter members of small groups among the fainter nebulae, which introduces positive residuals in the upper part.

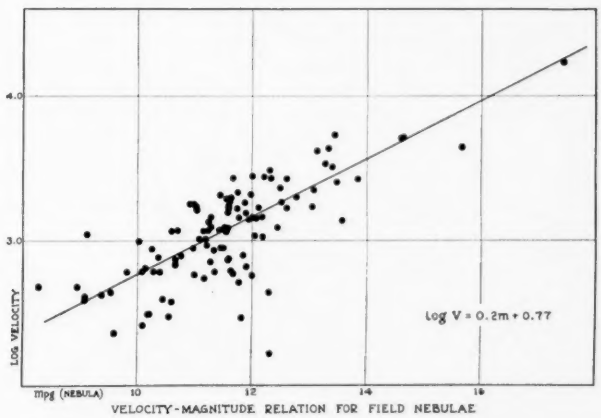

FIG. 2.—Logarithms of velocities, corrected for solar motion, are plotted against apparent magnitudes of the nebulae, corrected for local obscuration and for red shifts. Three nebulae in Table II have been omitted: NGC 247 and 253, because the velocities are negative; NGC 404, because log v falls off the diagram.

The velocity-distance relation may be written

$$\log (v_o - v_p) = \log d + c_1 ,$$

where v_o and v_p are observed velocity and peculiar motion, respectively. Since

$$\log d = 0.2(m - M) + c_2 ,$$

the velocity-magnitude relation is

$$\log (v_o - v_p) = 0.2m + c_3 - 0.2M .$$

Since v_o and m are directly observed, residuals from the relation evidently represent variations in v_p and in M. Effects of variations in v_p diminish with increasing distance, but effects of variations in M

are presumably independent of distance. Instead of neatly separating the two effects—a difficult problem—the combined residuals may be examined from the point of view of absolute magnitudes.

The frequency distribution of the residuals in the velocity-magnitude relation indicates the form of the luminosity function of the nebulae as distorted by peculiar motions and effects of selection. The frequencies are listed in Table III, and the curve is shown in

TABLE III

FREQUENCY DISTRIBUTION OF RESIDUALS IN THE VELOCITY-MAGNITUDE RELATION FOR FIELD NEBULAE

$\log v_0 - 0.2m_c$	No.	$\log v_0 - 0.2m_c$	No.
1.221	1	0.60–0.64	2
1.08–1.12	1	.56– 60	3
1.04–1.08	4	.52– 56	3
1.00–1.04	6	.48– 52	3
0.96–1.00	6	.44– 48	7
.92–0.96	4	.40– 44	1
.88– 92	11	.36– 40	4
.84– 88	3	.32– 36	0
.80– 84	9	.28– 32	0
.76– 80	13	.24– 28	2
.72– 76	12	.20– 24	0
.68– 72	4	.16–0.20	1
0.64–0.68	4	0.100	1
Total*			105

* The four cases omitted are NGC 247 and 253, which have negative velocities, and NGC 404 and 2366, for which the $\log v_0 - 0.2m_c$ are negative. The mean for the 105 nebulae is $\log v_0 - 0.2m_c = 0.752$.

Figure 3, where a normal error-curve with a dispersion of 0.18 (or 0.9 mag.) has also been included. The points in the diagram represent overlapping sums of three successive frequencies in Table II.

The dispersion of residuals, as calculated from Table III, is about 0.21 in $\log v$, corresponding to 1.05 mag. However, as the apparent magnitudes increase (distance effects increase relative to peculiar motions), the dispersion steadily diminishes: for the 29 nebulae fainter than $m = 12$, it is 0.95 mag., and for the 15 fainter than $m = 12.5$, it is 0.82 mag. The brighter branch of the frequency-curve, moreover, where effects of peculiar motions are less conspicuous, suggests a dispersion of the order of that derived in Part I for resolved

nebulae, namely, 0.85. These results, although they lack precision, indicate a general similarity in the forms of the luminosity functions for the two groups, the one containing resolved nebulae alone and the other nebulae of all types.

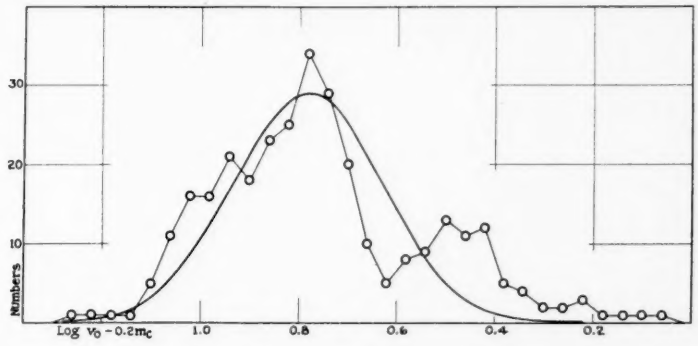

Frequency Distribution of Residuals in the Velocity-Magnitude Relation for Field-Nebulae

FIG. 3.—Ordinates are overlapping sums of three successive frequencies of $0.2m_c - \log v_0$, as listed in Table III. The frequency-curve represents the luminosity function of field nebulae as distorted by the assymetrical distribution of effects of peculiar motions. The smooth curve is a normal error-curve with the dispersion $\sigma = 0.18$, which is equivalent to 0.9 mag.

TABLE IV

VELOCITY-MAGNITUDE RELATION FOR DIFFERENT TYPES OF NEBULAE

Type	No.	$\log v_0 - 0.2m_c$
E	23	0.772 ± 0.031
Sa	23	.774 .027
Sb	28	.737 .027
Sc	26	.754 .030
Ir	5	0.607 ± 0.049

The mean residuals for the different types of nebulae are given in Table IV. Two Sc nebulae with negative velocities (NGC 247 and 253) and two other nebulae (NGC 404, E0, and NGC 2366, Ir) with negative residuals have been omitted from Table IV as well as from Table III. Differences in the residuals represent one-fifth the differences in absolute magnitudes. Elliptical nebulae and spirals are

fairly comparable, the total range being less than 0.2 mag., but the irregular nebulae are systematically fainter than the others by

TABLE V*

VELOCITIES AND DISTANCES OF RESOLVED NEBULAE IN THE GENERAL FIELD

NGC	Type	v_o	m_c	Corr.	$\log v_o - 0.2 m_c$	Distance Unit, 10^6 par.
4736	Sb	+ 410	17.39	−0.75	−0.790	0.473
5457	Sc	480	17.46	+ .13	0.824	0.598
5194	Sc	420	17.58	+ .07	0.900	0.624
2403	Sc	175	17.75	+ .01	1.308	0.665
4449	Ir	310	17.79	+ .09	1.076	0.690
5236	Sc	480	18.28	+ .43	1.018	0.935
4214	Ir	+ 380	18.30	+ .11	1.091	0.877
253	Sc	− 130	18.30	+ .45	.....	0.948
3031	Sb	+ 70	18.38	− .33	1.798	0.822
4826	Sb	230	18.50	− .63	1.275	0.811
1068	Sbc	790	18.62	+ .15	0.841	1.026
3627	Sb	610	18.66	− .63	0.884	0.873
2366	Ir	190	18.74	− .13	1.470	1.016
628	Sc	580	18.78	− .01	0.992	1.064
2903	Sc	260	18.89	+ .19	1.382	1.172
7331	Sb	680	19.04	− .73	0.903	1.016
5055	Sb	+ 590	19.18	− .65	1.000	1.104
247	Sc	(− 80)	19.20	+ .15	.....	(1.340)
4051	Sbc	+ 740	19.28	− .03	0.984	1.334
4258	Sb	610	19.47	− .03	1.056	1.297
5005	Sc	1330	19.68	+ .13	0.812	1.663
278	Sc	760	19.77	+ .19	1.092	1.758
4725	Sab	1180	19.79	− .59	0.827	1.483
3521	Sbc	640	19.93	+ .39	1.219	1.982
1084	Sc	1360	19.94	+ .17	0.872	1.892
4151	Sb	1040	19.98	− .63	0.916	1.603
3486	Sc	1250	20.17	+ .21	0.958	2.123
7177	Sbc	1390	20.34	+ .11	0.936	2.244
1087	Sc	+1720	20.51	+0.33	−0.900	2.553

* Velocities, v_o, are corrected for galactic rotation. The magnitudes of brightest stars, m_c, are corrected for local obscuration by the formula $\Delta m = -0.25$ (cosec $\beta - 1$), and for red shifts. The quantities in the fifth column, headed "Corr.," are additional corrections to m_c, depending upon nebular type and stellar contents. The quantities in the last two columns are the means of the corresponding quantities calculated from m_c alone (case *a*) and from m_c corrected by the quantities in the column headed "Corr." (case *b*).

about 0.75 mag. (half the luminosity). The latter result is consistent with the small total luminosity of irregulars derived from brightest stars.

There is some evidence that elliptical nebulae and early spirals may be very slightly brighter than the intermediate and late spirals. Although the data are not sufficient fully to establish the difference, they suggest that nebulae in general, among which the later types predominate, may average about 0.1 mag. fainter than the group whose velocities have been measured.

THE VELOCITY-MAGNITUDE RELATION FOR BRIGHTEST STARS

The third formulation of the velocity-magnitude relation is a correlation of log v with apparent magnitudes of brightest stars in resolved nebulae. The data for 29 resolved field nebulae are given in Table V. These nebulae are included in Table II and, with the exception of NGC 1087 and 7177 ($m_s > 20.5$), are also listed in Table II of Part I. The values of $m_s - m_n$ are 9.5 (1087) and 8.4 (7177).

Effects of peculiar motions are more important in the present data than in those used for the two previous formulations, because the resolved nebulae are restricted to the neighborhood of the galactic system where distance effects are relatively small. The relation actually adopted,

$$\log v = 0.2 m_c - 1.00 ,$$

is again uncertain by one- or two-hundredths in the value of the constant. The correlation is shown in Figure 4.

Effects of peculiar motions may be partially compensated by omitting the two nebulae with negative velocities and also M 81, which has the outstanding residual among the remaining objects. The simple mean of the differences, log $v - 0.2m$, is then about -1.015. When the brightest stars are corrected for types and for stellar contents of the nebulae (see Part I), the mean is -0.995. For reasons previously mentioned it is believed that the most probable value lies between these limits. The mean of the limits is -1.005, and the round number, -1.00, has been adopted. The adopted value agrees very closely with that derived later from the velocity-distance relation in which the peculiar motions are less important.

COMPARISON OF THE VELOCITY-MAGNITUDE RELATIONS

The three formulations of the velocity-magnitude relations may now be compared:

$$\log v = 0.2 m_c - 1.00 \text{ (brightest stars)}$$
$$+0.77 \text{ (field nebulae)}$$
$$+1.02 \text{ (fifth cluster nebulae)}$$

The differences in the constants are evidently one-fifth of the differences in the absolute magnitudes of the objects whose apparent mag-

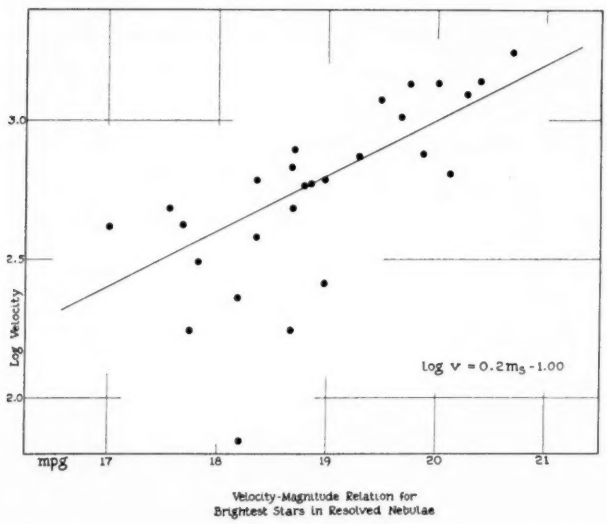

Velocity-Magnitude Relation for
Brightest Stars in Resolved Nebulae

FIG. 4.—Logarithms of velocities of resolved nebulae, corrected for solar motion, are plotted against apparent magnitudes of the brightest stars in the nebulae, corrected for local obscuration and for red shifts. The data are listed in Table V. NGC 247 and 253 have been omitted from the diagram because the velocities are negative.

nitudes are used as criteria of distances. The absolute magnitude of one criterion, namely, brightest stars, is known (Part I); therefore the absolute magnitudes of the other criteria are readily calculated:

$$\overline{M}_s = -6.35, \qquad \overline{M}_n = -15.20, \qquad \overline{M}_{c5} = -16.45.$$

The mean for the field nebulae is in excellent agreement with the value derived from brightest stars in resolved nebulae ($\overline{M}_n = -15.18$), although the two groups of 109 and 145 objects, respectively, have only 29 nebulae in common. The value for cluster nebulae furnishes a satisfactory criterion of distance and a zero point for the scale of absolute magnitudes in each cluster. The luminosity function of cluster members is very imperfectly known, but a range of 5 mag., with the mean coinciding with the median, is frequently assumed. The available evidence, restricted to the brighter branch, suggests that the function may be approximately represented by a normal error-curve, as so frequently happens in groups of celestial bodies.

The brightest cluster nebulae average about 0.45 mag. brighter than the fifth nebulae; $M_{(\max)} = -16.9$. The median, -14.4, on the assumption mentioned above, may be compared with the value $M_{on} = -14.2$, previously found for field nebulae. Cluster nebulae thus appear to be roughly comparable with field nebulae. By assuming strict comparability, the luminosity function for cluster nebulae may be provisionally described as a normal error-curve with a dispersion of 0.83 mag. and an average range of about 5.5 mag. The most frequent magnitude would then be about 2.25 mag. fainter than the fifth nebula.

THE VELOCITY-DISTANCE RELATION FROM BRIGHTEST STARS

The uncertainties in the velocity-magnitude relation are largely those introduced by peculiar motions. For this reason the velocity-distance relation, in which peculiar motions cancel out, will be derived from brightest stars and from field nebulae in the form, velocity $= k \times$ distance. The relation starts from the origin of co-ordinates and is known to be approximately linear. Therefore, the slope k is determined by the single point representing the mean distance and the mean velocity of all the nebulae considered.

The data for brightest stars in nebulae with measured velocities are found in Table V. One nebula, NGC 247, has been omitted in the derivation of k. NGC 247 and 253 form a pair of large, conspicuous spirals less than 5° apart in the sky and probably at comparable distances. The velocities, corrected for solar motion, are also com-

parable. They are the only negative velocities that have been recorded outside the local group, and the residuals from the velocity-distance relation are outstanding. In both cases the spectra refer to patches of emission nebulosity found in the outer arms. In NGC 247, which gives the larger residual, the patch is well out to one side of the nucleus and, therefore, the velocity must be regarded as a combination of rotation and motion of the nebula as a unit. Nevertheless, internal motion probably does not account for more than a fraction of the observed residual.

The two nebulae may be regarded as a pair, sharing a common, exceptionally large, peculiar motion toward the galactic system. The influence of the two outstanding residuals on the mean of the short list of available velocities is so great that some kind of weighting is desirable. For this reason NGC 247, in which the probability of internal motion is the greater, has been omitted. The result is about the same as that of combining the pair and giving half-weight to each component.

The mean velocity of the 28 nebulae is 662.5 km/sec, with a probable error, as will appear later, of the order of 4 per cent. The mean distance is less certain. By following the procedure used in calibrating the brightest stars, the distances may be calculated from the apparent magnitudes of the stars: (*a*) corrected only for local obscuration and for red shifts, (*b*) further corrected for nebular type and for stellar contents, and (*c*) using the means of the two sets of corrections.

In each case the distances are indicated by the relation

$$\log d = 0.2 m_s + (1 - 0.2 \overline{M}_s) ,$$

but the mean distance of the group must be increased by the term $\Delta \log d = 1.152\ (0.2\sigma_s)^2$, where $\overline{M}_s$ and σ_s^2 have different values, depending on the system of corrections employed. The results are given in Table VI. For reasons previously mentioned the true values of $\bar{d}$ and k probably lie between the limiting cases *a* and *b*, and the values for case *c* are adopted as reasonable approximations.

When the systematic correction for dispersion is disregarded, the

value of k is 535. Therefore, the velocity-magnitude relation, corrected for effects of peculiar motion, should be

$$\log v = 0.2 m_s - 1.002 .$$

TABLE VI

THE COEFFICIENT IN THE VELOCITY-DISTANCE RELATION FROM BRIGHTEST STARS

Corr.	$\overline{M}_s$	σ_s	$\overline{d}$ (par.)	k (per 10^6 par.)
Case a	−6.48	0.52	1.355×10^6	489
Case b	6.24	.29	1.176	563
Case c	−6.35	0.41	1.260	526

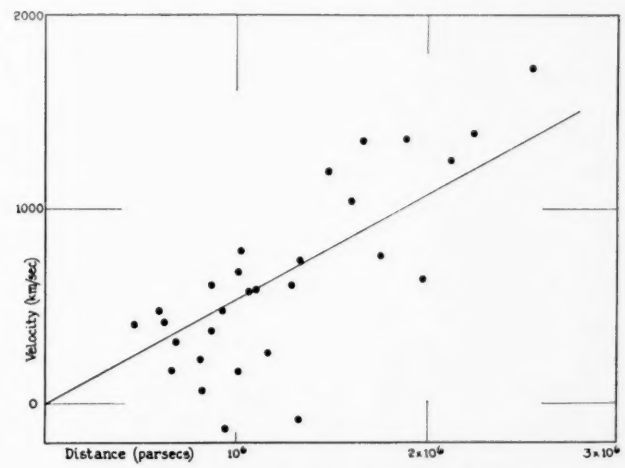

Velocity-Distance Relation from Brightest Stars

FIG. 5.—Velocities of resolved nebulae, corrected for solar motion, are plotted against distances derived from apparent magnitudes of brightest stars. The statistical correction required by the dispersion of the absolute magnitudes has not been applied; it would increase the distances by about 1.8 per cent. All the nebulae in Table V are included in the diagram but one, NGC 247, which has been omitted in calculating the slope of the velocity-distance relation.

The constant adopted in the direct formulation—namely, 1.00—is evidently of the right order.

A plot of individual distances (case c) against velocities is shown in Figure 5. When residuals from the correlation-curve are expressed

as velocities, the dispersion, which includes peculiar motions and accidental errors from all sources, is about 260 km/sec. The probable error in k is therefore of the order of 34 km/sec, or about 6 per cent. Systematic errors may be expected in the distances rather than in the velocities, and each increment of 0.1 mag. in $\overline{M}_s$ will change the value of k by approximately 5 per cent.

The dispersion among peculiar motions alone is probably of the order of 200 km/sec. This value for field nebulae may be compared with the dispersion of the order of 650 km/sec for members of the Virgo cluster.[12] Since the dispersion arising from accidental errors of measuring the velocities is of the order of 50 km/sec, the probable error in the mean velocity of the 28 nebulae is of the order of 27 km/sec, or, as previously mentioned, about 4 per cent.

TABLE VII

THE COEFFICIENT IN THE VELOCITY-DISTANCE RELATION FROM FIELD NEBULAE

Corr.	$\overline{M}_n$	σ_n	$\bar{d}$ (par.)	k_n*	k_s*
Case *a*	−15.05	0.72	2.751×10^6	564	489
Case *b*	15.3	.94	3.209	484	563
Case *c*	−15.18	0.85	2.985	520	526

* k_n and k_s, for nebulae and from brightest stars, are expressed in terms of km/sec per million parsecs.

THE VELOCITY-DISTANCE RELATION FROM FIELD NEBULAE

The 109 field nebulae in Table II furnish a mean velocity of 1552 km/sec, with a probable error of the order of 1 per cent. The mean distance depends on the values assigned to $\overline{M}_n$ and σ_n. The three cases considered in deriving the velocity-distance relation from brightest stars lead to the values of $\bar{d}$ and k which are listed in Table VII. The last row (case *c*) shows the closest agreement between the results from nebulae and from brightest stars, and when the six irregular nebulae are corrected for type (M_n reduced by 0.7 mag.), the agreement is almost exact ($k=525$ as compared with $k=526$). The comparison justifies the adoption of the system of corrections in case *c*.

[12] Humason, *loc. cit.*; Smith, *loc. cit.*

The values of k from nebulae of different types are given in Table VIII, together with the mean distances. The agreement in k confirms the earlier conclusion that, with the exception of the irregular nebulae, the absolute magnitudes are of the same order. The appreciably larger mean distances of the earlier types (E and Sa), as compared with the later types, arise from an effect of selection. The

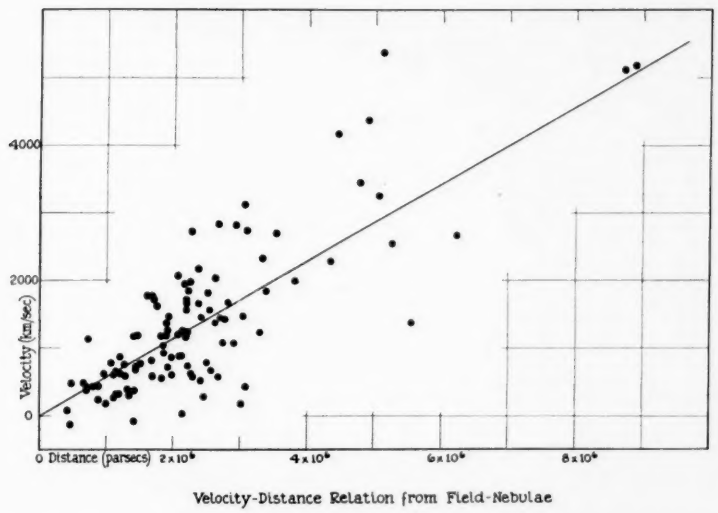

FIG. 6.—Velocities, corrected for solar motion, are plotted against distances derived from apparent magnitudes of the nebulae. The statistical correction for dispersion in M_n, which would increase all distances by about 8 per cent, has not been applied. The distances of the last two nebulae in Table II, 14.26 and 33.27 million parsecs, fall beyond the limits of the diagram. The outstanding residual (NGC 6710, top-central region) represents the brightest member of a small group of nebulae.

difficulties of recording spectra increase as the nuclear concentration of nebulae diminishes. For this reason there is a tendency to select early rather than late types among the faint, distant nebulae. This tendency also accounts for the relatively large number of early-type nebulae in Table II, as compared with that to be expected among nebulae in a given volume of space.

Since the absolute magnitudes of the various types are comparable, the predominance of early types among the distant nebulae does not appreciably influence the value of k. However, a systematic

effect is present, as previously mentioned, in the form of a marked tendency to select the brighter members of small groups. Such nebulae are intrinsically brighter than normal; hence their estimated distances are too small and lead to values of k that are too large. The outstanding residual for NGC 6710 is very probably to be explained in this way. The total effect of the tendency cannot be determined with precision, but an examination of the data suggests that a value of M_n between -15.1 and -15.15, with a dispersion of 0.85 or slightly less, would offer a reasonable compromise. Thus the prob-

TABLE VIII

COEFFICIENTS IN THE VELOCITY-DISTANCE RELATION FROM NEBULAE OF DIFFERENT TYPES

Type	No.	$\bar{d}$	k
E	24	2.56	534
Sa	23	2.93	537
Sb	28	2.22	530
Sc	28	1.92	529
Ir*	6	1.57	301
Ir	(5)	(1.28)	(412)

* The results for five Ir nebulae (omitting the exceptional case of NGC 2366) are also included. If the five nebulae are corrected for type (M_n corrected by 0.7 mag.), the value of k is 531, in good agreement with those for the other types.

able value of M_n ranges from -15.1 to -15.2, depending on the methods of estimation; and for this reason the distances listed in Table II are calculated on the assumption that $\overline{M}_n = -15.15$.

The coefficient, $k = 526$, indicates a distance for the Virgo cluster of $1230 \div 526 = 2.34$ million parsecs. The probable error, derived from the dispersion of individual velocities, is about 0.15, but uncertainties arising from the peculiar motion of the cluster are not included. If the small negative residual for the cluster is interpreted as due to a peculiar motion of approach, the distance would be about 2.5 million parsecs. This value may be regarded as a maximum. The corresponding moduli are

$$m - M = 27.0 \text{ (maximum)},$$
$$= 26.85 \text{ (observed velocity)},$$

which may be compared with the value, 26.6 or slightly larger, suggested by the incomplete data from brightest stars. Pending further investigation, the value 26.8 is adopted. The corresponding value of the mean apparent magnitude of the cluster members is about 12.7, provided the cluster members are comparable with resolved field nebulae. The brighter nebulae of both groups are known to be comparable, and the data for the fainter cluster members, although incomplete, suggest that these objects also are comparable with field nebulae.

The group of 109 field nebulae of all types and that of 125 resolved field nebulae, discussed in Part I, have 29 objects in common but are otherwise independent. The analyses indicate quite clearly that the total assemblage of more than 200 nebulae is a homogeneous collection of which the resolved nebulae form a fair sample. The inclusion of clusters enlarges the collection many fold without seriously affecting the homogeneity.

CARNEGIE INSTITUTION OF WASHINGTON
MOUNT WILSON OBSERVATORY
May 1936

VARIATIONS IN THE SPECTRUM OF P CYGNI*

O. C. WILSON

ABSTRACT

An examination of spectrograms of P Cygni taken at the Lick and Mount Wilson observatories has shown that the Balmer lines in this star consist of an emission component and two absorption components, instead of one, as formerly supposed. These two absorption components vary in intensity (and probably in position) in such a way that on some occasions both are visible, while on others only one or the other is to be seen. No period for the variation can be deduced from the available material, but it is demonstrated that significant changes have occasionally occurred within intervals of the order of one month. The helium lines also appear to pass through a similar cycle in step with those of hydrogen.

Since P Cygni (Nova 1600) is the brightest star of a class which has recently come to be known as permanent novae, its spectrum has been the subject of numerous researches. The most recent of these have been published by Beals,[1] Struve,[2] and Kharadse;[3] and all contain numerous references to earlier work. The question of changes in the spectrum has been discussed principally by Gerasimovič[4] and Elvey.[5]

From an inspection of a number of Harvard objective-prism spectra, covering the period 1887–1927, Gerasimovič concluded that at times the lines to the red of $H\delta$ had abnormal absorption components on the red side of the emission components. On other occasions all the lines seemed normal, i.e., to consist of an emission line with absorption on the violet edge; while on still others, bright $H\beta$ was devoid of any absorption on either edge. Elvey secured several spectrograms of the star in 1927 and 1928 and was unable to find any changes such as Gerasimovič had described.

On a spectrogram taken by the writer on April 15, 1933, it was noticed that several of the Balmer lines to the violet of $H\epsilon$ clearly showed two approximately equal absorption components to the vio-

* *Contributions from the Mount Wilson Observatory, Carnegie Institution of Washington*, No. 550.

[1] *Observatory*, **57**, 319, 1934.

[2] *Ap. J.*, **81**, 66, 1935.

[3] *Zs. f. Ap.*, **11**, 304, 1936.

[4] *Harv. Bull.*, No. 852, 16, 1927; No. 867, 16, 1929.

[5] *Ap. J.*, **68**, 416, 1928.

let of the corresponding emission lines. An earlier plate, obtained by Adams on June 22, 1931, seemed to show, at first glance, only single absorption components for the same lines. This was a fairly obvious variation which appeared to justify further investigation.

On looking into the literature it was found that structure in the hydrogen absorption components had previously been noted by Merrill[6] and by Adams and Dunham.[7] The latter described the hydrogen absorption lines as double, while Merrill stated that, on certain of his plates, "dark $H\gamma$ is divided by what appears as a faint bright line of wave-length 4337.67. . . . ."

In order to investigate further the spectral variations of P Cygni, the writer has secured a series of spectrograms during the past three years. In addition, he has been privileged, through the courtesy of Director R. G. Aitken and Dr. J. H. Moore, of the Lick Observatory, to examine a number of Lick spectrograms of the star, including those studied by Merrill. The plates used are listed in Table I.

An inspection of all the material indicates that the variations may be described as follows: The Balmer lines of hydrogen in P Cygni consist of three components. At approximately the normal wavelength is a fairly wide emission band to the violet of which are two absorption lines. The absorption components vary in intensity, and perhaps to some extent in position. At times the two are of approximately equal strength, while at other times one or the other is nearly, or perhaps entirely, invisible.

To illustrate these statements, microphotometer tracings of several spectrograms have been reproduced. In Figure 1 are shown portions of Mount Wilson plates V 10 and V 345. The double character of the absorption at λ 3797.9, $H10$, is clearly visible on the latter, in distinct contrast to the former, where the violet component is much weaker. These differences are not confined to $H10$, however, but are plainly visible in at least three other Balmer lines in this region. It merely happens that $H10$ is best for illustrative purposes, owing to the rapid weakening of the spectrum toward the violet and the decrease of dispersion toward the red, coupled with the fact that

[6] *Lick Obs. Bull.*, **8**, 24 (No. 246), 1913.

[7] *Annual Report, Director Mount Wilson Observatory*, p. 181, 1931.

$H7$ and $H8$ are unavailable because of blends. The dispersion has decreased so much at $H\delta$ that practically no structure is visible in the $H\delta$ absorption. The dispersions of the Mount Wilson plates are 17.6 and 24.8 A/mm at K for 15- and 10-inch camera plates, respectively.

TABLE I

SPECTROGRAMS OF P CYGNI

Plate	Date G.C.T.	$E-A_R$	$E-A_V$	H–$H\epsilon$	Camera
7978 C*	1912 Aug. 12.34	.....	2.83 A		
8033 A*	Sept. 30.23	2.28 A			
8281 H*	1913 July 16.42	2.10†	3.18†		
8283 B*	17.31				
V 10	1931 June 23.29	.....	.....	$R>V$	15-inch
337	1933 Apr. 16.47	.....	.....	$R<V$	
345	May 14.49	1.42‡	2.84‡	$R<V$	
356	June 12.47	.....	.....	$R>V$	10-inch
358	13.46	.....	.....	$R>V$	
381	July 10.41	.....	.....	$R<V$ (slightly)	15-inch
391	31.37	.....	.....	$R>V$ (slightly)	
392	Aug. 1.33	.....	.....	$R>V$	
406	31.34	.....	.....	$R=V$	10-inch
443	Oct. 6.19	.....	.....	$R\gg V$	
454	Nov. 6.19	.....	.....	$R>V$?	
507	1934 June 27.29	.....	.....	$R>V$	
511	July 27.27	.....	.....	$R>V$	
532	Aug. 23.32	.....	.....	$R>V$	
613	Oct. 1.19	.....	.....	$R=V$	
617	2.21	.....	.....	$R=V$	
662	30.17	.....	.....	$R>V$	
682	Nov. 26.15	.....	.....	$R>V$?	
902	1935 June 9.46	.....	.....	?	
1346	1936 May 12.44	.....	.....	$R>V$	

* Lick Observatory spectrograms.
† Mean of 8281 H and 8283 B, $H\gamma$.
‡ Mean of V 345 and V 337; $H9$, $H10$, $H11$.

On the Lick spectrograms, however, the dispersion at $H\gamma$, 8.6 A/mm, is sufficient to show considerable detail, even though the line is outside the region of best definition. Microphotometer tracings of $H\gamma$ on three Lick plates which cover the entire range of variation are shown in Figure 2. In this figure, (*a*) is plate 8033 A, on which the violet component is very weak; (*b*) is plate 8281 H, showing both components of approximately equal strength; while in (*c*), plate 7978 C, the red component is either absent or extremely weak.

Plate 8281 H is one of those to which the quotation from Merrill's paper, concerning the faint bright line at $H\gamma$, applies. In view of the appearance of Figure 1, it is scarcely possible, however, to doubt the present interpretation.

The differences in angstroms, emission *minus* absorption, have been measured on the Lick plates and on two of the Mount Wilson plates, with the results tabulated in the third and fourth columns of

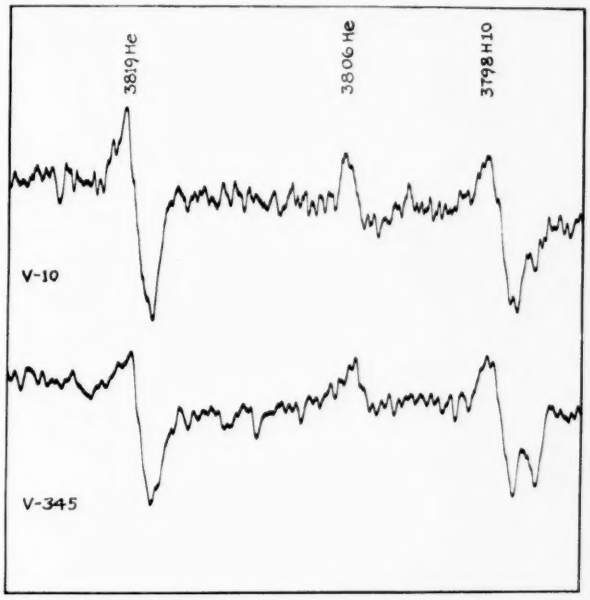

FIG. 1.—Variations in the absorption components of $H10$

Table I. A_R and A_V denote, respectively, the red and violet absorption components. Comparison of these measures indicates that the two absorption components do not always remain in precisely the same positions, but further data are needed on this point.

As noted above, both $H7$ and $H8$ are blended, the former with interstellar H and the latter with λ 3888.6 *He*. $H8$ is entirely useless for the purposes of this paper; but the situation at $H7$ is illustrated in Figure 3, where use is again made of plates V 10 and V 345. It is clear that the red absorption component of $H\epsilon$ falls almost exactly upon the interstellar H line, while the violet component lies suffi-

ciently far away to be separately visible. In fact, these variations at H–$H\epsilon$ can be distinguished even on our 10-inch camera plates, none of which shows the changes in the later Balmer lines with any

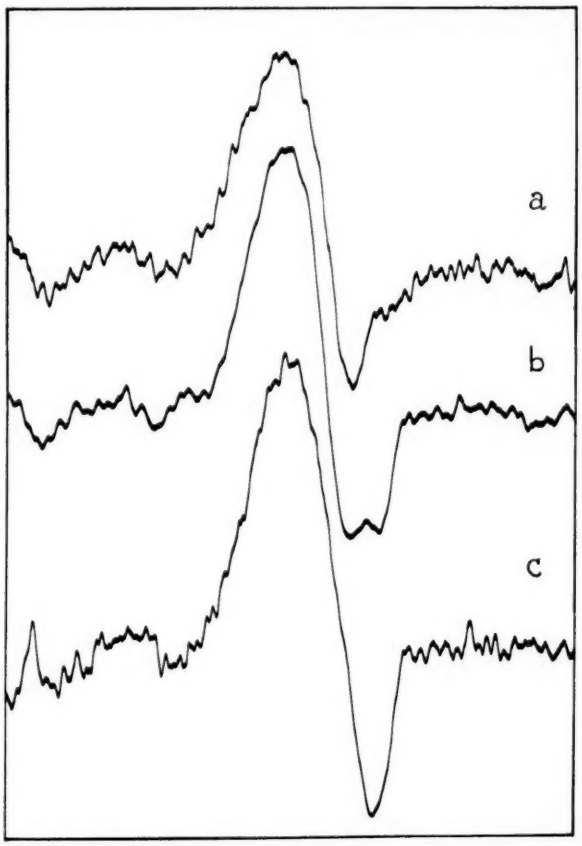

FIG. 2.—Tracings of three Lick Observatory spectrograms showing changes in absorption at $H\gamma$; a) plate 8033 A; b) 8281 H; c) 7978 C.

degree of satisfaction. Rough estimates of the relative strengths of the red and violet components of $H7$ have, in consequence, been entered in the fifth column of Table I, the purpose being merely to shed some light on the frequency with which the variations occur. While it would be useless to attempt to deduce a period from these results, it is nevertheless clear that the changes described here can

take place in the course of a month, or perhaps even less. In this connection it should be noted that Lick plates 7978 C and 8033 A, which represent fairly extreme phases, are separated by less than two months.

One further question of importance remains. Do the variations just described take place in the lines of elements other than hydrogen? This may be definitely answered in the affirmative as far as

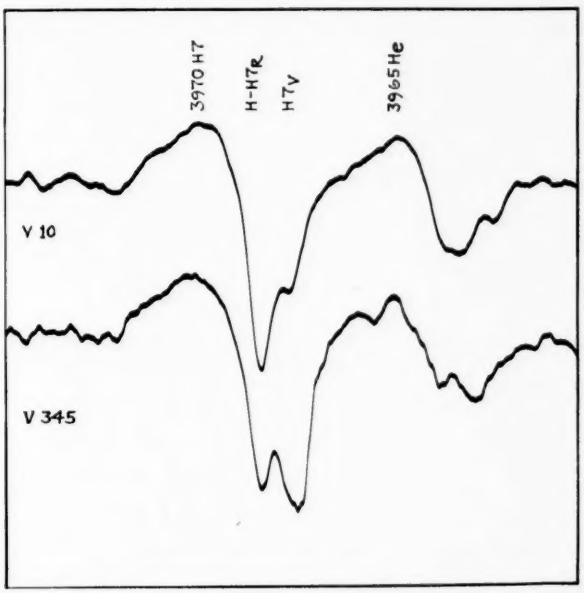

FIG. 3.—An example of the variation at H-He

helium is concerned, though the changes in this case are less readily observable. On the Lick plates, λ 4471 *He* appears to vary in much the same way as does $H\gamma$. Measures of $E-A$ for λ 4471 on plates 7978 C and 8033 A give the values 2.72 A and 1.92 A, respectively, which differ by an amount far outside any possible error of measurement. Moreover, in Figure 3, changes in λ 3965 *He* corresponding to those at H–$H7$ are apparent, although the variations in λ 3819 *He* in Figure 1 are not so obvious. In any event, there is no doubt that the lines of helium do go through a cycle very similar to, if not identical with, that of the hydrogen lines.

The bearing of the facts discussed here on the various theories concerning the origin of the spectrum of P Cygni is not altogether clear. It must be emphasized, however, that although these variations have hitherto escaped observation, they are by no means minor, but constitute one of the major features of the problem. It should be noted also, that the double absorption lines of P Cygni heighten the resemblance of this star to 17 Leporis, a point which has already been discussed by Struve. Finally, since the time intervals involved appear to be of the same order, it is very likely that these spectral variations are intimately connected with the changes of brightness recently found by Kharadse, Nikonov, and Kulikovsky.[8]

CARNEGIE INSTITUTION OF WASHINGTON
MOUNT WILSON OBSERVATORY
May 1936

[8] *Observatory*, **59**, 88, 1936.

LOW-DISPERSION SPECTRA OF RED STARS*

RUPERT WILDT[1]

ABSTRACT

Over the range from λ 3000 to λ 9000 (total dispersion 3 mm approximately) the spectra of selected late-type stars have been compared. M giants and N stars are marked by a continuous absorption of wave-lengths shorter than λ 4000, the amount being of the order 0^m5 and 2^m5, respectively. Types S and gM cannot be distinguished on low-dispersion spectrograms. Dwarfs of class M have a strong ultra-violet spectrum and R stars a fairly strong one. Various absorption bands are found in the far ultra-violet and are attributed tentatively to *CN*, *CH*, *NH*, *OH*, *CaH*. The classes R and N are possibly to be regarded as forming separate, parallel branches. The hypothetical physical processes causing the continuous ultra-violet absorption in gM and N stars are discussed.

The preparation of photographic emulsions highly sensitive to infra-red radiation has opened an enormous field to astrophysical research. Important investigations on the infra-red absorption spectra of the sun and some of the brighter stars have been completed, but little attention has been paid so far to the continuous infra-red spectrum of the stars. W. W. Morgan and B. A. Wooten[2] estimated the relative spectral intensities of five stars at λ 0.87 μ and 1.0 μ and pointed out that their results, combined with those of Jensen, indicated strong deviations from black-body radiation. At the Göttingen Observatory 22 bright stars have been under observation since last year by spectrophotometric methods on infra-red sensitive plates. Spectrophotometric observations in the visual range of these stars, in which the writer participated from 1930 until 1934, have been finished but are not yet published. Even now, before systematic knowledge of the energy distribution in normal stars can be derived from such cumbersome observations, attractive problems are open to an attack by methods of a more qualitative nature. Such is a comparison of the rare types R, N, and S with the M stars over a range of wave-lengths as wide as possible. All these red stars are well known to be radiometrically very bright, but they are very

* *Contributions from the Mount Wilson Observatory, Carnegie Institution of Washington*, No. 551.

[1] Fellow of the Rockefeller Foundation.

[2] *Ap. J.*, **80**, 229, 1934.

difficult objects to photograph to wave-lengths shorter than λ 4000 or so. Low dispersion and overexposure of the visual spectrum would aid in getting down to the ultra-violet. The reduction in scale of a prismatic spectrum as one goes to longer wave-lengths might be such that both the ultra-violet and infra-red could be recorded by the same exposure-time on the same plate, although the sensitivity of the best available plates measured in energy units is far lower to the infra-red than to the ultra-violet rays. These expectations have been confirmed; and low-dispersion spectra of red stars, covering the ultra-violet and infra-red, have yielded valuable information about their common features and individual properties.

A slit spectrograph, containing a collimating mirror, 60°-prism of the Cornu type, and a Schmidt camera $f/1$, was used at the Cassegrain focus of the 60-inch telescope. All mirrors are aluminized, and light is absorbed only by the prism and the Schmidt correcting plate, both made of quartz. The spectrograph was designed for the study of faint nebulae by S. Smith.[3] The length of the spectra is extremely small, about 1 mm between λ 3000 and λ 4000 and approximately 2 mm between λ 4000 and λ 9000. Focus plates taken with a very narrow slit revealed only a minute difference in the positions giving the best definition in the ultra-violet and infra-red, respectively. Since with this low dispersion the infra-red stellar spectra showed no absorption features at all, the ultra-violet focus was used throughout the course of the observations. With good seeing a slit width of 0.2 mm was considered appropriate. For several very faint stars and when the seeing was poor, the slit was opened, occasionally to 0.5 mm. Agfa plates "Infrarot Rapid 850" were used without having been hypersensitized and were developed 5 minutes in Rodinal 1:15 at 65° F. The infra-red sensitivity of these plates is distributed nearly symmetrically around λ 8500, and the sensitivity to radiation of the ordinary photographic range is rather low. After testing several brands of Kodak and Agfa plates, I selected this special one as a compromise with regard to the partially irreconcilable demands for high speed, fine grain, and absence of fog. With fair seeing and a narrow slit an hour was necessary for the proper expo-

[3] *Phys. Rev.*, **47**, 257, 1935; see also Th. Dunham, Jr., *ibid.*, **46**, 326, 1934.

sure of an M star of ninth visual magnitude in both the infra-red and the ultra-violet, where it could be traced easily as far as λ 3300. The spectrograms consist of the infra-red part, a short tadpole-like figure without structure, and the long range of ordinary, actinic wave-lengths, separated by a wide gap. The violet and blue regions are heavily overexposed under such conditions. The appearance of the infra-red region varies in the most conspicuous manner with the spectral type from K to late M stars, being hardly visible in the former and even stronger than the overexposed blue in the latter. This circumstance makes it feasible, under the adopted constant conditions of working, to estimate by rough steps the relative intensities of the infra-red and the blue and thereby to establish a scale of color equivalents.

It is well known that the gradation of photographic plates for infra-red rays exceeds considerably that for shorter wave-lengths. One might expect that this difference would exert a disturbing influence on the estimates of color. Actually, this effect has been found to be of minor importance and is probably well eliminated by comparing only equally exposed spectra of stars of the same apparent magnitude. The procedure was to choose from the new Mount Wilson list of spectroscopic absolute magnitudes[4] a comparison star of the required apparent visual brightness. Differences of a few tenths of a magnitude had to be admitted. Stars of medium declinations were preferred in order to make the exposures at zenith distances smaller than 30°. As several southern stars had to be exposed outside this limit near the meridian, the spectrograph was turned 90° to set the slit parallel to the direction of the atmospheric dispersion. All the stars on a plate, the maximum number being six, received equal exposures; but often two different exposure times, in the ratio 1:3 or 1:5, were used on the same plate for several stars to record the fading of intensity throughout the ultra-violet range.

Evidently the long range of wave-lengths covered by these low-dispersion spectra will facilitate the recognition of small differences of color temperature. In order to give some quantitative idea of this effect, monochromatic differences of magnitude for black-body radi-

[4] *Mt. W. Contr.*, No. 511; *Ap. J.*, **81**, 187, 1935.

ations of several temperatures have been computed and are given in Table I. The absolute intensities have been adjusted by making them equal at λ 5500 for all temperatures, while the relative intensities are referred to radiation at 3500° as zero point.

CARBON STARS

In his comprehensive study of the carbon stars C. D. Shane[5] has estimated their faintness in the more refrangible region by numbers on an arbitrary scale. These numbers increase steadily from Ro to N6, and it is evident that the relative weakening of the violet spectrum parallels the increasing redness of these stars, as in the main

TABLE I

MONOCHROMATIC INTENSITY RATIOS OF BLACK-BODY RADIATION EXPRESSED IN STELLAR MAGNITUDES

T K	λ 3500	λ 4500	λ 5500	λ 8500
4500°	−0.99	−0.39	0.00	+0.61
3500	0.00	0.00	.00	0.00
3000	+0.86	+0.34	.00	−0.53
2500	+1.94	+0.76	.00	−1.20
2000	+3.57	+1.39	0.00	−2.20

spectral sequence. Nevertheless, Shane doubts whether temperature is the essential factor controlling the spectral features of the carbon stars. In the first place, the drop in intensity at shorter wave-lengths in the N stars is too strong to be assigned to any reasonable black-body radiation. Secondly, the strength of the C_2 bands shows a puzzling behavior which is difficult to explain solely by a steady variation of temperature along the sequence R−N. The intensity of the Swan bands rises from Ro to R8 and from No to N6, being about as low in No as in Ro. Information on the temperature of carbon stars from radiometric measurements is meager. E. Pettit and S. B. Nicholson[6] observed four N stars radiometrically and from a comparison of heat indices and water-cell transmissions inferred that the N stars radiate much more like black bodies than do the M stars. The radiation temperatures of these four stars range between 2400°

[5] *Lick Obs. Bull.*, **13**, 123 (No. 396), 1928.

[6] *Mt. W. Contr.*, No. 478; *Ap. J.*, **78**, 320, 1933.

and 2000°, which places them among the long-period variables of class M at maximum.

The low-dispersion spectra of the 16 carbon stars observed revealed some unexpected features which strengthen the doubts as to whether the physical changes along the sequence R—N can really be explained by the steady variation of a single parameter, namely, the surface temperature. These doubts are based on observational evidence different from Shane's. His system of classification aims at a refinement of the Harvard system and is founded on the development of the cyanogen, Swan, and certain unidentified bands. It implies a continuous transition from R8 to No. According to Shane, the visual region of the spectra of carbon stars is not suited to purposes of classification. Shane reproduced spectra of HD 25408, R8, and HD 233075 (19 Piscium), No, which closely resemble each other between λ 4000 and λ 5000. Low-dispersion spectra show these stars differing both in the ultra-violet and the infra-red. Generally speaking, the R stars have a fairly strong ultra-violet spectrum which could be traced easily to λ 3350 in the R8 star just mentioned, while the N stars can be photographed only as far as H and K, and then only with difficulty. This fact has already been pointed out by Shane. The bright prototype 19 Piscium (visual magnitude, 5.3) has been compared with HD 4408, gM4 (visual magnitude, 5.6). The exposure-times were varied in steps from 2 minutes to 60 minutes. Over this whole range the spectra look nearly identical in the infra-red and the blue (λ 4500–λ 5000). But beyond λ 4000 the intensity of the N star drops rapidly, and the exposure-time has to be increased thirty times in order to reach the same ultra-violet limit as in the M star (λ 3200). Evidently, a strong continuous absorption must be at work in the ultra-violet of the N stars. This point will be discussed later.

As for the infra-red, Table II gives the intensity difference between infra-red and blue, estimated in steps on an arbitrary scale, the symbol $IR > B$ indicating that the infra-red image is regarded as one step brighter than the blue part of the spectrum (λ 4500–λ 5000). These rough estimates furnish a sort of color equivalent and lead to a linear arrangement of the 16 stars along what is supposed to be a temperature scale. By repeated estimates of 16 M

giants the following spectral types and symbols were found to correspond:

$$\text{Mo: } IR\langle\langle\langle B; \qquad \text{M3.5: } IR = B; \qquad \text{M6: } IR\rangle\rangle\rangle B\,.$$

The estimates of M giants give a rough calibration of the scale of color equivalents. Whatever the exact physical meaning of these

TABLE II

COLOR EQUIVALENTS OF CARBON STARS

(Decimal Classifications of Spectra according to Shane)

I.	Infra-red extremely faint, no sure estimate possible		
	HD 224959	Ro	Infra-red almost invisible, resembles HD 64092, gG6
	HD 5223	R3	
	HD 16155	R3	Infra-red very faint, approximately as in K
II.	$IR\langle\langle B$		
	*HD 30443	Nb	Infra-red little stronger than in BD+43°1332, gM1
III.	$IR\langle B$		
	HD 52432	R5	
	HD 25408	R8	
	HD 206570	N1	
IV.	$IR = B$		
	*HD 34467	Nb	
V.	$IR\langle B$		
	HD 19557	R5	
	HD 223075	No	19 Piscium, blue and infra-red resemble HD 4408, gM4
	HD 30243	Nb	ST Camelopardalis, blue and infra-red resemble HD 919A, gM4
VI.	$IR\rangle\rangle B$		
	*HD 32088	Nb	Infra-red little fainter than in BD+42°1180, gM6
VII.	$IR\rangle\rangle\rangle B$		
	HD 44687	N3	UU Aurigae
	HD 32736	N5	W Orionis
VIII.	Infra-red extremely strong, blue almost invisible		
	HD 1546	N7	VX Andromedae
	HD 208512	Nc	

color equivalents may be, one would expect to find a unique and steady relation between color equivalent and spectral classification in the R−N sequence if the physical state of the carbon stars is

governed by the same single factor as that in the oxygen stars, namely, the surface temperature, as generally assumed. The appearance of Nb stars in the upper part of Table II and of an R5 star in the same group as 19 Piscium, No, clearly contradicts the premise just made. The outstanding star, HD 19557, R5, closely resembles 19 Piscium, No, in the blue and the infra-red; but it has a rather strong ultra-violet spectrum, recorded as far as λ 3350. The three Nb stars marked by an asterisk in Table II have been compared with BD +43°1332, gM1, and BD+42°1180, gM6, the visual magnitudes of these five stars being confined to the narrow range of 9.0–9.5. HD 30443 and HD 34467 look very much like the M1 and the M6 giants, respectively, the lack of ultra-violet in the N stars being disregarded for the moment. The third Nb star occupies an intermediate position and may resemble gM4 approximately.

A possible objection ought to be forestalled at once. Shane mentions that an underexposed R5 star, showing no violet, is hard to distinguish from an N3. Now one might argue that the "hot" Nb stars, appearing in the upper part of Table II, have erroneously been classified as N because of underexposure, being really R stars. But R stars of the same apparent magnitude, as observed by the writer, do show the characteristic ultra-violet spectrum which is missing from the stars classified as N. Therefore, the overlapping of R and N stars in Table II cannot thus be disposed of. The close relation of the early R stars to classes G and K has already been pointed out by C. Rufus[7] and by Shane, and may be restated here with regard to the infra-red intensities too. The question whether there are any stars forming a transition from the "hot" N stars to the main spectral sequence deserves further examination. It may even be that the question put in this way is meaningless: L. Berman's[8] recent identification of R Coronae Borealis as a hot carbon star is highly significant. Meanwhile the results presented in Table II raise the suspicion that class N is to be distinguished from class R principally on account of an absorption process going on in the N atmospheres which reduces the ultra-violet intensity very efficiently. If the idea that the R and N stars form a continuous sequence is given up, the variation of the

[7] *Pub. Univ. Mich. Obs.*, **2**, 103, 1916. [8] *Ap. J.*, **81**, 369, 1935.

intensity of the C_2 bands loses its puzzling character and the different intensities of the *CN* bands in Ro and No may reasonably be attributed to differences in the abundance of nitrogen, as H. N. Russell has remarked.[9] The splitting up of the carbon stars into two separate, parallel branches would mean simply the introduction of a new abundance parameter into the classification of late-type stars. No special suggestion as to its chemical origin need be advanced at this moment, but its nature may be elucidated in due time by a study of the continuous ultra-violet absorption in N stars.

CLASS S STARS

This class has been set up separately because of its peculiar absorption features, and little is known about the energy distribution throughout the continuous spectrum. P. W. Merrill has stressed repeatedly the similarity of this class to class M and has stated:

> These stars are red, the color indices of the variables probably as great as that of Md variables. . . . . As compared with Md stars the continuous spectrum falls off toward the violet from about λ 4500, and with greater rapidity after λ 4430.[10]

Pettit and Nicholson[6] observed radiometrically the variables R Cygni (S3e), χ Cygni (S5e, also M6e–M8e), and T Sagittarii (S4e), which showed no characteristic peculiarities compared with other long-period variables. The minimum temperatures of the last two stars are among the lowest observed so far, namely, 1600°. The spectral classifications just given and those to be quoted later have been taken from Miss Davis,[11] who based the subclassification of S on the relative intensity of *ZrO* and *TiO* bands. The recent investigations on the dissociative equilibrium in low-temperature atmospheres strongly suggest that the relative prominence of *ZrO* and *TiO* is not caused by particular values of atmospheric temperature and pressure but by real differences in the abundance of *Zr* and *Ti*. If this assumption is right, Miss Davis' classification may be considered as extending perpendicularly to the K–M sequence, which is essentially a temperature sequence. In that case no correlation is to be expected between subclasses of S and temperature or any of its equivalents.

[9] *Mt. W. Contr.*, No. 490; *Ap. J.*, **79**, 317, 1934.

[10] *Mt. W. Contr.*, No. 252; *Ap. J.*, **56**, 457, 1922.

[11] *Pub. A.S.P.*, **46**, 267, 1934.

Anyhow, the detection of *ZrO* bands in many M spectra by N. T. Bobrovnikoff[12] has raised the delicate question as to where the borders between classes M and S are really to be drawn.

The spectra of five S stars, four non-variables and one variable near maximum, were found to be very similar in both the ultra-violet and the infra-red to M spectra. Judging from these low-dispersion spectra alone, one could not distinguish the two classes. Observational details follow:

1. **HD 22649** (Boss 826), S4, closely resembles HD 4408, gM4, and HD 2411, gM3. The S4 star is slightly weaker in the infra-red than this gM3 but extends a little farther into the ultra-violet (limits λ 3240 and λ 3270, respectively). The star has been classified as gM4 at Mount Wilson and assigned the absolute magnitude −0.8. Another plate with Boss 826 and HD 4408 shows spectra widened by an accidentally extra-focal position of the plate within the plateholder and exhibits better the ultra-violet band structure, which is identical in both stars.

2. **HD 35155,** S4. An amply exposed spectrum of this star extends as far as λ 3250. No M star is available on this plate, only a K giant, which is considerably fainter in the infra-red. The intensity ratio, blue : infra-red, is about the same as in Boss 826.

3. **HD 63733,** S4, was compared with HD 74484, gM0, and HD 85904, gM4. These three stars look identical throughout the blue and violet. As for the infra-red intensity, the S star has a medium position between these two M stars and is decidedly "hotter" than both the foregoing S stars.

4. **HD 64332,** S5, could be compared directly only with HD 85904. It is much stronger in the infra-red than this gM4 star and may be estimated as resembling M6.

5. **R Lyncis,** S3e, was observed 22 days before the predicted maximum (period 378 days). The visual magnitude was estimated as between 9.0 and 9.5. The variable was even stronger in the infra-red (relatively to the blue) than HD 64332. Its energy distribution may have resembled that of M7, as estimated from a comparison with BD+42°1180, gM6.

Miss Davis has emphasized the fact that the problem of classifying the S stars is by no means settled definitely, and has pointed out how valuable spectrophotometric observations would be. The striking similarity of M and S stars, as revealed by the low-dispersion

[12] *Ap. J.*, **79**, 483, 1934.

spectra, leaves no doubt about the position of the observed S stars on the temperature scale. Since R Lyncis, S3e, is the "coolest" star and HD 63733, S4, the "hottest" one, the other two S4 stars and one S5 having an intermediate position, it becomes obvious that Miss Davis' subclasses do not follow a temperature sequence.

GIANTS AND DWARFS OF CLASS M

The temperature differences of giant and dwarf stars of classes F, G, and K have been the subject of many observational studies and theoretical discussions. But the faintness of the M dwarfs has prevented anyone so far from obtaining empirical material of similar completeness for the stars of the lowest surface temperature. Not much more can be said than that the temperature difference of giants and dwarfs diminishes considerably as one approaches Mo from the earlier spectral types. The recent detection of dwarfs of extremely low luminosity, especially by A. van Maanen's systematic search, invites an investigation of their physical characteristics. But for most of them not even spectral types have yet been determined. A Russell diagram published by van Maanen[13] shows that the decrease in luminosity is accompanied by only a slow advance in spectral type. Unless the correlation between surface temperature and spectral type is very different among the later M giants and the dwarfs, the rapid decrease of luminosity along the dwarf branch must be caused mainly by a corresponding reduction of the radiating surface, or, if the existence of low-temperature spots can be excluded, by a shrinking of the stellar diameter.

Twelve M dwarfs with absolute magnitudes ranging from +7.5 to +12.7 have been photographed. Their spectra are marked by great strength in the ultra-violet as compared with the giants. This is very conspicuous in the following three pairs, selected because of approximately equal apparent brightness:

HD 88230	dMo	6^m8	HD 232979	dM1	8^m5	HD 95735	dM2	7^m6
HD 111862	gMo	6.5	HD 47019	gM2	8.8	HD 101585	gM3	7.8

In the dwarfs the photographic density steadily and slowly decreases throughout the violet and ultra-violet; in the giants there is

[13] *Mt. W. Contr.*, No. 507; *Ap. J.*, **81**, 152, 1935.

a sudden drop between λ 4100 and λ 4000 or so, and no further recovery at shorter wave-lengths down to λ 3300, where the spectra fade out. This drop of intensity could not be fitted to any black-body curve, and the wide extent of the absorption forbids ascribing it to ordinary bands. Moreover, the blue and infra-red intensities of each of these pairs are practically equal. It seems reasonable, therefore, to assume that these pairs have equal surface temperatures, respectively, and that a peculiar absorbing mechanism situated in the atmospheres of the giants is responsible for their low ultra-violet intensities. This conclusion is fully confirmed by a spectrophotometric comparison of HD 120933, gM2, and HD 95735, dM2, made by B. Lindblad[14] between λ 5100 and λ 3800. Lindblad noted a drop in the giant's energy-curve, approximately 0^m5, to the violet of λ 4100. Since his spectra extended only to λ 3700, he had, unfortunately, no chance to observe the fact that this region of absorption extends throughout the entire observable ultra-violet. It is not difficult to distinguish M dwarfs and giants just by looking at their low-dispersion spectra. There is a single possible contradiction: the star 490 of *Cincinnati Publication* No. 20 has been classified at Mount Wilson as dM1 (absolute magnitude 8.5), but the ultra-violet spectrum looks like that of a giant. This star of apparent visual magnitude 10.5 has been photographed only once by the writer, and because of its faintness a misidentification seems not impossible. The close resemblance of S stars and M giants, as noted above, makes it most probable that the characteristic ultra-violet depression is present in the S stars too. The same may be conjectured for the K giants (HD 88048, gK4, is a conspicuous example), although no low-dispersion spectra of K dwarfs are available for a direct comparison.

The M giants exhibit a well-marked correlation between spectral type and color equivalent estimated from the low-dispersion spectra. As for the same correlation among the M dwarfs, only one dM4 and one dM5 star were photographed successfully, most of the advanced M dwarfs being too faint. Observational details follow:

dM5e, companion of 40 Eridani, abs. mag. 12.7, has been photographed with slit 0.5 mm wide and three hours' exposure. Very faint in infra-red. $IR \ll\ll B$ estimated directly, but this does not mean very much because the conditions

[14] *Stockholms Obs. Annaler,* **12,** No. 2, 1935.

(slit width and exposure time) differ markedly from those chosen otherwise and no comparison star of the same apparent magnitude was secured. Strong ultra-violet spectrum; limit, λ 3120!

dM4e, 1244 *Cincinnati Pub.* No. 18, abs. mag. 11.0, and **dM3,** HD 36395, abs. mag. 10.1, closely resemble each other; $IR\langle\langle B$.

dM2, HD 95735, abs. mag. 10.7, has been mentioned before as compared with HD 101585, gM3. It is estimated as $IR\langle\langle B$ and its low luminosity is striking when one considers its early spectral type.

dM2, Anon. (5^h10^m0 $+45°44'$, 1900), abs. mag. 9.5; **dM1,** 1383 *Cincinnati Pub.* No. 18, abs. mag. 9.2; **dM1,** HD 232979, abs. mag. 8.8, mentioned above as compared with HD 47019, gM2. These three stars have also been estimated as $IR\langle\langle B$.

dM0, four stars with absolute magnitudes ranging from 7.5 to 8.7: HD 88230 and 233719; 837 and 3143 *Cincinnati Pub.* No. 18. They all have exceedingly low infra-red intensities, estimated as $IR\langle\langle\langle\langle B$, and therefore differ conspicuously from the foregoing group.

It is difficult to derive clear-cut conclusions from these few observations. The stars of the dM0 group look "hotter" than the M0 giants. But the temperature difference of giants and dwarfs seems to be less pronounced among M1–M4 stars. Now the Mount Wilson classification of M-type stars depends on the strength of the *TiO* bands. With very plausible assumptions as to the physical parameters, Russell[9] has shown that the asymptotic value of the strength of the *TiO* bands is reached at higher temperatures in the dwarfs than in the giants, but that the maximum intensity in giants, though found in cooler stars, should be much greater. His prediction explains the previously puzzling fact that no dwarfs later than M6, i.e., none with stronger *TiO* bands than in gM6, have been observed and that the difference of color indices of giants and dwarfs decreases from K to M. The observations of low-dispersion spectra, though too few to confirm Russell's predictions conclusively, are consistent with them.

ABSORPTION BANDS IN THE FAR ULTRA-VIOLET

Some of the low-dispersion spectra, taken with a narrow slit, reveal a great many absorption features in the far ultra-violet practically unknown hitherto in late-type stars. The positions of the stellar ab-

sorption features were estimated by using the micrometer scale of a measuring machine, the wave-lengths being derived graphically after it had been found that no accuracy was gained by measuring with the screw and computing a dispersion formula. All stellar exposures have a mercury arc for comparison. The accuracy of the wave-lengths evaluated is not greater than ± 5 A; but undoubtedly the definition of the spectrograph is such as to give better results, if widened spectra taken with a narrow slit on fine-grain plates were used.

In view of the low dispersion, we can only assume that the observed absorptions are molecular bands covering broad regions. Plausible identifications can be made for most of them, and only these are to be dealt with here, a few doubtful ones being omitted:

CN.—In classes R and K the cyanogen bands at λ 3883 and λ 3590 are very conspicuous. The first head of the next lower diagonal group is λ 3360.1 (Deslandres). It shows up well in HD 52432, R5. Shane found the cyanogen bands developed best in R5 and fading out in N3 approximately. K. Wurm[15] has criticized these statements of Shane. A long exposure of 19 Piscium, No, confirms Shane's observation that the *CN* bands λ 3883 and λ 3590 are very faint in this star and hardly comparable with those in R3 stars.

NH.—The 0–0 head of the resonance system ($^3\Pi \rightarrow {}^3\Sigma$), λ 3360, has recently been suspected in the spectrum of α Boötis by R. W. Shaw.[16] Unfortunately, it coincides with the new *CN* band just mentioned. The absorption shown by several R stars in this region may better be ascribed to *CN* since this molecule is an abundant constituent of their atmospheres. The presence of *NH* may be checked further by observation of the singlet systems $^1\Pi \rightarrow {}^1\Sigma$ (λ 4520) and $^1\Pi \rightarrow {}^1\Delta$ (λλ 3610, 3240, 3035). There is good evidence for a band at λ 3240 in several R3 and R5 stars.

CH.—The resonance system $^2\Sigma^+ \rightarrow {}^2\Pi$ has the strongest heads at λ 3143 and λ 3157. A broad band at this place is clearly indicated in HD 224959, Ro, and HD 5223, R3.

OH.—Shaw[16] has observed a strong line at λ 3428.40 in α Boötis, not identified with any atomic line. This is the position of the 0–1 band of *OH* resonance system ($^2\Sigma \rightarrow {}^2\Pi$). A broad absorption is seen at this place in low-dispersion spectra of α Orionis and a sharper one in two M dwarfs, HD 233719 and 1383 *Cincinnati Pub.* No. 18. In all checked carbon stars this absorption has not been found.

[15] *Zs. f. Ap.*, **5**, 270, 1932.

[16] *Ap. J.*, **83**, 225, 1936.

CaH.—This molecule is a characteristic feature of the M dwarfs, as shown by Y. Öhman from observations of the red system $B^2\Sigma \rightarrow X^2\Sigma$. Another resonance system $C^2\Sigma \rightarrow X^2\Sigma$ is situated in the ultra-violet. The o–o band at λ 3534 coincides with an absorption seen in low-dispersion spectra of α Orionis and of three M dwarfs (HD 233719, and 1244 and 1383 *Cincinnati Pub.* No. 18).

ATMOSPHERIC OPACITY ARISING FROM MOLECULES

The wide absorption regions observed in gM and N spectra require some further comment as to their hypothetical origin. Their appearance is distinctly different from ordinary absorption bands. The only well-known continuous absorption in stellar spectra is the Balmer continuum in early types. The observation of the Paschen continuum is interfered with by a rather dense group of terrestrial lines.[17] Of course, analogous continua are adjacent to all series limits. Although not conspicuous individually, these superposed continua of a great many constituents less abundant than hydrogen make an important contribution to the general opacity of stellar atmospheres. Several authors have pointed out that at low temperatures the opacity arising from molecular absorption cannot be disregarded, but no theory of molecular opacity has advanced thus far. Lindblad[14] observed a new type of continuous absorption in the spectra of M dwarfs and interpreted it as originating from a quasi-molecule Ca_2 bound by polarization forces. In the laboratory such spectra of quasi-molecules of many elements of the first and second column of the periodic system have been found. They extend from the resonance lines of these metals toward longer wave-lengths and have no sharp limit. Lindblad remarked that the absorption spectrum of the quasi-molecule Mg_2 should be noticeable on the red side of the Mg resonance line λ 2852. The strong ultra-violet intensity of the M dwarfs, as observed in the low-dispersion spectra, makes it improbable that the predicted Mg_2 band extends more than 500 A with perceptible strength.

The various types of continuous molecular absorption have been discussed thoroughly by W. Finkelnburg.[18] Beyond the convergence limits of the vibration series, continuous absorption spectra are to be

[17] P. W. Merrill and O. C. Wilson, *Mt. W. Contr.*, No. 494; *Ap. J.*, **80**, 361, 1934.

[18] *Phys. Zs.*, **31**, 1, 1930, and **34**, 529, 1933.

expected which are truly analogous to the continua at the limits of atomic series. Besides, certain molecules have electronic states in which there is no minimum of potential energy at any nuclear distance and are therefore forced to dissociate by repulsion. The best-known example of such repulsive terms is the $1s\sigma 2p\sigma\ ^3\Sigma_u$ term of H_2, which is the lower level of the famous ultra-violet hydrogen continuum, the upper discrete level being $1s\sigma 2s\sigma\ ^3\Sigma_g$. This repulsive state cannot be reached by absorption from the ground state since this is a $1s\sigma^2\ ^1\Sigma_g$ term, and intersystem combinations are practically forbidden for such light nuclei. In electric discharges hydrogen molecules can be excited by collisions to the $^3\Sigma_g$ state mentioned before and then, by jumping to the repulsive state, can dissociate, emitting the ultra-violet continuum. The inverse process may occur by recombination of high-speed hydrogen atoms at very low pressures and by simultaneous absorption of light; but the required velocities are far higher than those attained in thermal equilibrium at the surface temperatures of M and N stars. Helium excepted, in no other molecule have continuous spectra involving a repulsive electronic state so far been observed, but a great many such states can be predicted for theoretical reasons.

Only future observations can decide whether the continuous absorption spectra of gM and N stars have a common origin. Meanwhile it is tempting to ascribe the absorption appearing in N stars to some sort of carbon compound. This does not exclude the possibility that the gM absorption is caused by the same molecule, but this hypothesis would even account for the increased intensity as observed in N stars. The absence of the continuous absorption from class R stars may possibly be explained by a deficiency of the other constituent of the hypothetical diatomic molecule. The term systems of diatomic carbon compounds are still rather incompletely known. Professor R. S. Mulliken kindly expressed his opinion on this subject and, at the writer's request, granted permission to quote from his letter the following passage, which reveals some promising views:

> From the probable normal state of *CH* ($1s^2 2s\sigma^2\ 2p\pi$, $^2\Pi$) absorption could occur to the unknown but predicted excited state ($1s^2 2s\sigma^2\ 2p\pi^3$, $^2\Pi$), which should have a repulsive curve which should probably be not very steep, but which

would lead on dissociation to H+excited carbon atom. Because the C atom is excited, the maximum λ would correspond to over 5 eV; besides, the transition would involve a two-electron jump, so should be weak. Hence this doesn't look very promising.

A rather attractive possibility, however, is that the transition is (. . . . $2p\sigma$ $2p\pi^2$, $^4\Sigma^-$)→(. . . . $2p\sigma$ $2p\pi$ $3s\sigma$, $^4\Pi$). The $^4\Sigma^-$ is a state (not yet observed) which is predicted to lie not far above the $^2\Pi$ normal state of CH (possibly even to be the normal state), so might be sufficiently populated to give strong absorption. The $^4\Pi$ state is a predicted repulsive one which has the merit that it should dissociate into unexcited atoms. I should be inclined to expect the $^4\Pi$ repulsion-curve to be rather steep, however. On the other hand, the transition would very likely be intrinsically an intense one—i.e., of much higher transition probability than even for the known CH bands—since it apparently involves $\Delta l = 1$, $\Delta n = 1$ for one electron, like an atom: $2p\pi \rightarrow 3s\sigma$.

The writer is under deep obligation to Director W. S. Adams, who placed at his disposal the great facilities of the Mount Wilson Observatory. He also appreciates the helpful advice of various members of the staff. During the preparation of this paper he profited greatly from conversations with Professors E. U. Condon and H. N. Russell.

Carnegie Institution of Washington
Mount Wilson Observatory,
Princeton University Observatory
May 1936

THE MOTIONS OF PROMINENCES OF THE ERUPTIVE AND SUN-SPOT TYPES*

EDISON PETTIT

ABSTRACT

First law of motion of eruptive prominences.—Data given for five eruptive prominences confirm the original observation that the motion of eruptive prominences is uniform but may be suddenly increased at intervals, as if by an impulse.

Second law of motion of eruptive prominences.—Collected data for the velocities of forty eruptive prominences show that when a change takes place the new velocity is a small multiple of the old velocity.

Change of position angle of an eruptive prominence.—A case is cited where a considerable change in heliographic position angle takes place during the eruption. This angular change is proportional to the time and the velocity of the prominence.

Prominences of the sun-spot type (class 3).—These are rather rare, showing on only eighty-three of the daily routine spectroheliograms of the past twenty years. Three subdivisions of this class are described.

Motions of streamers and knots from a prominence into a sun-spot.—A case permitting detailed measurements of streamer and knot motions is discussed. The velocities obey both the first and second laws of motion applying to eruptive prominences.

Retarded eruptions.—Certain eruptive prominences which move very slowly are subject to violent attraction by centers of attraction or by sun-spots. This low velocity persists as long as large streamers at high velocity pour into the affected area.

Small eruptions of high velocity.—A number of eruptions have been observed which lasted only a few minutes but had very high velocities. Velocities exceeding 500 km/sec seem to be indicated.

Streamer characteristics.—Streamers are emitted preferably from the top of a prominence to a center of attraction or a sun-spot. As the action develops, points farther down become affected. The exponential form of the streamer-curves is illustrated. Certain exceptions show a sudden fall to the chromosphere from an otherwise normal form.

In previous work on eruptive prominences[1,2,3] it was found that the motion was uniform but increased rather abruptly at intervals of about an hour (first law of motion of eruptive prominences). No really satisfactory explanation of this behavior has yet been given, and, as the data applied to only about a dozen well-observed cases, any additional observations are still of interest. Since the completion of the investigations mentioned, data for two additional eruptive prominences have been published by others.[4,5] Numbers have

* *Contributions from the Mount Wilson Observatory, Carnegie Institution of Washington*, No. 552.

[1] *Ap. J.*, **50**, 206, 1919.

[2] *Pub. Yerkes Obs.*, **3**, Part IV, 1925.

[3] *Mt. W. Contr.*, No. 451; *Ap. J.*, **76**, 9, 1932.

[4] P. C. Keenan and P. Rudnick, *Ap. J.*, **80**, 157, 1934.

[5] J. O. Hickox, *Pub. A.S.P.*, **46**, 355, 1934.

been assigned to these prominences in continuation of the catalogue previously given. In both cases the material was presented only in the form of plots of height against time, which are reproduced in Figure 1. The corresponding numerical quantities given in Table I were obtained from these plots, except the times for which the original observing books were available. The catalogue numbers are in continuation of the lists already published.[2,3]

In No. 36 the extreme height of the prominence (o and + in Fig. 1) as measured by both authors is in excellent agreement. In addition, the plot gives the extreme height and center of gravity (Δ and θ) measured by Hynek. For extreme height he has evidently chosen a point of extraordinary faintness for setting, as the plot is much higher than that of Keenan and Rudnick and shows greater scattering, although in great measure it runs parallel to the latter. For the purpose of Table I the means of Keenan's and Rudnick's measures are given.

In No. 37, *A* is a bright knot which finally became the top of the prominence, *B* is a faint knot, and *C* is the bottom of the rising column.

These two prominences illustrate several features common to the eruptive class. In both cases the motion of ascent is evidently uniform. No. 37 typifies a rapidly moving prominence of short life in which no break occurs in the time-height diagram for the crest, while lower down such a break occurs. Numbers 16, 18, 19, 20, 24, and 33 of previous papers are also illustrations of this type, in which the duration is less than one hour. Of slowly moving prominences of long duration, Nos. 38 and 39 are examples. Number 38 was observed by J. O. Hickox on November 14, 1934, and measured by the author. It has been the author's habit to make but one set of measurements of an eruptive prominence in order to insure an unbiased plot of the results. This prominence appeared at Lat. 20° S. on the west limb. No marking was visible at this point on the sun, but the heliographic position angle of the prominence increased during the eruption in the direction of a disappearing spot-group on the limb at Lat. 23° N.

This change of heliographic position angle during an eruption has been noted in several cases, e.g., Nos. 3, 5, 7, and 9. Of course, the

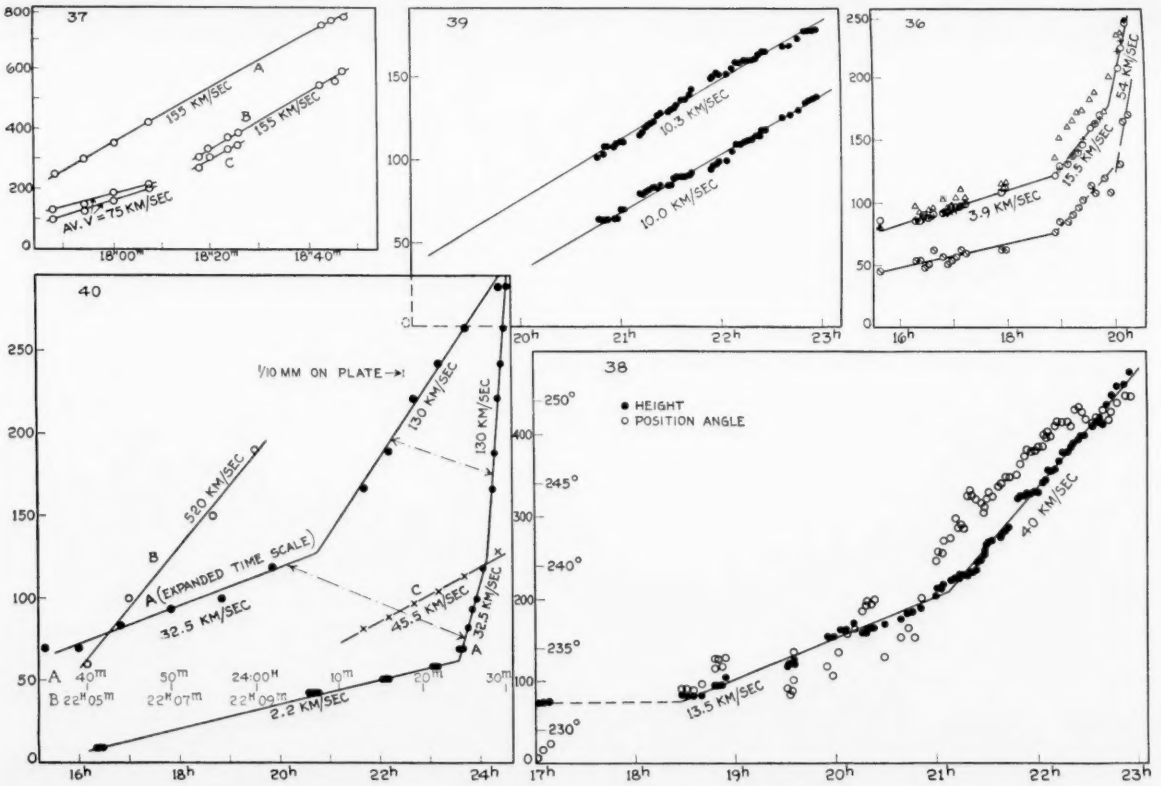

FIG. 1.—Motions of eruptive prominences: No. 36, September 21, 1932; No. 37, October 21, 1934; No. 38, November 14, 1934; No. 39, July 27, 1920; No. 40, September 22, 1935. Abscissae are G.C.T. of observation; ordinates, heights of prominence; unit = 1000 km.

TABLE I

COLLECTED DATA ON ERUPTIVE PROMINENCES MEASURED SINCE 1931

Identity and Remarks	G.C.T. of Observation	Height in Thousand Kilometers
36. September 21, 1932. Observed by P. C. Keenan with the Rumford spectroheliograph at the Yerkes Observatory. H line of Ca^+. Lat. 20° S. on the east limb. No spot. The values given here are the averages of the measures of the top by Keenan and Rudnick, as shown on the plot. Times from observing book. *Ap. J.*, **80**, 157, 1934. No velocities were given by the authors. Velocities read from plot of average measures are $V = 3.9$, 15.5, and 54.2 km/sec.	$15^h38^m.7$	80
	16 18.4	86
	23.4	87
	28.3	88
	33.3	89
	38.3	90
	49.2	92
	54.0	91
	59.0	94
	17 04.0	94
	09.0	96
	14.0	98
	53.5	110
	58.2	111
	18 53.5	121
	58.7	128
	19 07.8	132
	12.8	137
	19.1	141
	24.1	148
	33.9	160
	38.7	163
	44.0	168
	48.9	.....
	55.2	.....
	20 06	215
	10	227
	16	247

Identity and Remarks	G.C.T. of Observation	Height in Thousand Kilometers		
		Bottom	Lower Knot	Upper Knot
37. October 21, 1934. Observed by J. O. Hickox. 13-foot spectroheliograph at Mount Wilson. K line of Ca^+. Lat. 0° on the east limb. No spot within 40° of the limb when this prominence was first observed. Times taken from the observing book; heights read from the plot. *Pub. A.S.P.*, **46**, 355, 1934. $V = 75$ and 155 km/sec.	17^h48^m	100	134	253
	54	124	149	301
	18 00	161	189	354
	07	200	214	422
	17	269	308	.....
	19	307	334	.....
	23	333	372	.....
	25	360	386	.....
	42	.....	546	760
	44	.....	562	778
	47	.....	596	793

TABLE I—*Continued*

Identity and Remarks	G.C.T. of Observation	Height in Thousand Kilometers	Position Angle
38. November 14, 1934. Observed by J. O. Hickox, measured by the author. 13-foot spectroheliograph at Mount Wilson. Middle of prominence, Lat. 20° S. on the west limb. Faint disappearing spot-group 43° N. of this position on the limb. Prominence moved 18° in position angle toward this group during the eruption. $V = 13.5$ and 40 km/sec.	17^h02^m	67	228°.3
	05	67	8.9
	08	67	229.2
	18 27	84	232.5
	31	84	2.5
	35	81	2.4
	38	81	2.9
	47	95	3.7
	49	95	4.4
	50	95	4.4
	52	95	3.9
	54	105	4.5
	19 31	119	2.5
	32	121	2.1
	33	121	2.2
	34	121	3.1
	35	127	4.7
	55	154	3.9
	59	154	3.4
	20 03	162	4.7
	07	162	6.0
	11	170	6.1
	16	159	7.2
	18	159	7.6
	19	162	7.8
	21	162	7.7
	23	162	7.9
	29	170	4.5
	38	175	5.6
	42	181	6.1
	46	184	5.6
	51	189	8.0
	21 00	202	240.2
	01	211	0.8
	03	211	0.7
	04	216	1.5
	08	221	1.6
	11	224	2.9
	13	224	2.3
	14	229	2.4
	16	229	2.3
	18	229	4.1
	20	232	4.5
	21	232	4.1
	23	235	4.0
	24	243	3.7
	26	246	3.2
	28	254	3.5
	29	259	4.0
	30	265	4.3
	32	267	4.1

TABLE I—*Continued*

Identity and Remarks	G.C.T. of Observation	Height in Thousand Kilometers	Position Angle
38—*Continued*	21^h34^m	270	244°.7
	39	273	4.9
	40	278	5.2
	42	281	5.2
	44	286	5.5
	48	321	6.1
	50	324	6.7
	53	324	7.0
	54	327	6.8
	56	327	6.9
	59	329	7.1
	22 01	329	7.1
	03	340	7.8
	05	343	7.7
	07	354	8.0
	09	354	7.7
	11	356	8.4
	13	364	8.7
	15	378	8.6
	18	378	8.7
	20	381	8.4
	22	386	9.4
	24	391	9.5
	26	397	9.2
	28	397	8.7
	33	408	8.5
	35	413	8.8
	37	418	8.5
	39	410	9.3
	41	432	8.7
	44	445	9.2
	47	456	9.7
	51	459*	250.1
	54	472*	0.1

* Measured twice on account of faintness.

TABLE I—*Continued*

Identity and Remarks	G.C.T. of Observation	Height in Thousand Kilometers	
		Bottom	Top
39. July 27, 1920. Observed by the author at Yerkes Observatory. H line of Ca^+. Not published. Plates measured in 1936. Prominence rose from the east limb at solar Lat. 17° S., pouring into a pair of small spots in solar Lat. 7° S. First nine measures given at approximately 15-minute intervals to show uniformity of height, although measures were made at 3-minute intervals. $V = 10$ km/sec.	15^h25^m	20	70
	45	20	70
	16 01	19	71
	16	20	75
	30	20	75
	45	20	75
	17 03	19	70
	14	20	72
	24	20	72
	20 46	64	102
	49	63	104
	50	63	108
	52	63	108
	56	64	108
	57	65	110
	21 00	70	111
	01	70	111
	12	80	115
	13	80	117
	15	81	120
	16	82	121
	19	84	122
	20	84	123
	23	84	127
	24	85	128
	28	85	129
	30	85	131
	32	89	132
	33	90	134
	36	90	137
	38	90	137
	40	91	140
	42	92	143
	54	95	150
	55	97	151
	57	98	153
	59	100	152
	22 04	100	152
	06	107	156
	08	110	160
	12	110	160
	14	111	161
	16	112	161
	18	113	161
	21	115	162
	23	115	165
	25	118	162
	27	118	162

TABLE I—*Continued*

Identity and Remarks	G.C.T. of Observation	Height in Thousand Kilometers	
		Bottom	Top
39—*Continued*	22^h37^m	126	170
	41	127	170
	46	130	175
	50	135	175
	52	136	175
	55	137	180
	57	138	180

Identity and Remarks	G.C.T. of Observation	Height in Thousand Kilometers	
		A	*B* *C*
40. September 22, 1935. Observed by J. O. Hickox. 13-foot spectroheliograph at Mount Wilson. Measured by the author. K line of Ca^+. The principal eruption, A, took place in solar Lat. 33° N. on the west limb, pouring into a center of attraction 41° N. Another eruption, *B*, of another part of the same prominence took place in Lat. 12° N. No spot near.	16^h22^m	8	.....
	25	8	.....
	28	8	.....
	20 38	43	.....
	39	43	.....
	41	43	.....
	42	43	.....
	22 05	51	60
Velocities of *A* are 2.2, 32.5, and 130 km/sec; *B*, 520 km/sec; *C*, 45.5 km/sec.	06	51	100
	08	51	150
	09	51	190
	23 04	59	.....
	05	59	.....
	06	59	.....
	35	70	.....
	39	70	.....
	44	83	.....
	50	94	.....
	56	100	.....
	24 02	118	.....
	13	167	81
	16	189	89
	19	221	97
	22	242	105
	25	264	113
	29	288	129

position angle is greatly affected by changes in form of the prominence, but in this instance the form was fairly constant during the last two hours of the eruption. The measurements were made on a

position-circle measuring-machine having a glass-covered aperture. This glass was ruled with two lines intersecting at right angles in the center of the circle and with a small circle, the size of the solar image, circumscribed about this center. Another glass plate mounted close above the ruled plate carried the spectroheliogram to be measured, and a bridge across the ways carrying the circle on a cross-slide operated by a screw served for orienting and centering the successive images of the chromosphere upon the circle and cross-lines. The position circle was read to $0^{\circ}.01$ by microscope, successive settings agreeing within $0^{\circ}.2$ or $0^{\circ}.3$. In view of the considerable amount of material it was therefore decided to make single settings.

The open circles in Figure 1 (No. 38) show the plot of heliographic position angle against time. It will be noted that during the last two hours, and probably during the first two, the change of angle was nearly proportional to the time and to the speed of ascent. If these measurements in polar co-ordinates are plotted to scale, it is found that the prominence was actually moving in a slightly curved line concave to the chromosphere and at an angle of approximately 50° to the vertical. Since only the vertical component was measured for the plot (No. 38), the actual velocities are 40 per cent greater than appear there and in Table I.

Number 39 was a very slow-moving eruptive prominence of long duration. Its low velocity (10 km/sec) makes it a borderline case, and it will be discussed under "Retarded Eruptions."

Number 40, observed by J. O. Hickox on September 22, 1935, began as an extremely slow-moving prominence, which maintained a vertical velocity of 2.2 km/sec for seven hours while pouring into a center of attraction at Lat. 41° N. on the west limb of the sun. This phenomenon was not a growth velocity but the motion of a distinct detached portion which could be identified throughout the eruption. Its velocity then suddenly increased to 32.5 km/sec and after a half-hour became 130 km/sec. About an hour and a half before the end of the low velocity a small eruption from the chromosphere occurred (plot *B*), rising to a height of 190,000 km at a velocity of 520 km/sec, not quite touching the erupting portion of the large prominence. This extraordinary velocity is the first greater than 400 km/sec for which a definite time-height plot is available. It will be discussed

along with small eruptions of short life. During the last twenty minutes of the great eruption the other end of this prominence began to erupt (plot *C*) at a velocity of 45.5 km/sec. Thus, two independent eruptions took place at different times in the same area and simultaneously with the major eruption. All heights less than 162,000 km were measured with a microscope provided with a field scale reading to 0.1 mm. The value of this unit is shown in the figure. In these last cases also, the first law of motion of eruptive prominences is well established.

More recently it was found[6] that, when the velocity of an eruptive prominence changes, the new velocity is a small multiple of the old, and consequently that the accelerations (this term here expresses simply the *change* in the velocity, since the time required for the change is unknown, although it must be small) are simple multiples of the initial velocity. The basis of this second law of motion of eruptive prominences is Table II. Here are collected the velocities V_0 observed in all eruptive prominences for which four or more measurements have been made. They are identified by the catalogue number. A value of the initial velocity V was computed by a simple least-squares solution, and the next velocity was then found by applying to V the factor in the fourth column opposite that velocity, and so on. By this means the residuals (O−C) were found for the various velocities of the prominence. An inspection of the original plots gave the quality Q of the velocity V_0 as excellent, "E"; good, "G"; fair, "F"; poor, "P"; and not dependable, "NG." The initial acceleration is V_0 or more probably V, if there is no smaller velocity. The succeeding accelerations, which are the changes in computed velocity found in the sixth column, are all multiples of V, the respective factors being denoted by F_a. The column of residuals (O−C) shows how closely the second law of the motion of eruptive prominences is verified by observation.

The usual development of an eruptive prominence proceeds about as follows: A great eruption always begins with a prominence already in existence; and, so far as I am aware, no case has been observed among the great eruptions where the prominence rises out of the chromosphere and continues to ascend, eventually detaching

[6] *Mt. W. Comm.*, No. 118; *Proc. Nat. Acad. Sci.*, **22**, 249, 1936.

TABLE II

VELOCITIES V_0 AND ACCELERATIONS A_c IN ERUPTIVE PROMINENCES

No.	V_0	O−C	F	Q	A_c	F_a
1	5.5	+0.6	1	F	4.93	1
	14.7	−0.1	3	E	9.9	2
	27.9	−1.7	2	G	14.8	3
	60.0	+0.8	2	F	29.6	6
2	37.0	−3.7	1	F	40.74	1
	163.9	+0.9	4	E	122.1	3
3	4.0	−1.2	1	F	5.15	1
	26.0	+0.2	5*	G	20.6	4
4	11	+0.6	1	F	10.32	1
	19	−0.6	2	G	10.3	1
	42	+0.7	2	P	20.6	2
5	7	−0.2	1	F	7.20	1
	22	+0.4	3	G	14.4	2
	43	−0.2	2	G	21.6	3
6	6	−0.2	1	F	6.19	1
	31	0.0	5*	F	24.8	4
	54	.....	.....	NG	.....	.....
7	7	+0.4	1	NG	6.60	1
	37	+4.0	5*	F	26.4	4
	64	−2.0	2	F	33.0	5
8	3	+0.1	1	F	2.90	1
	29	0.0	10*	G	26.1	9
9	64	+0.3	1	F	63.7	1
	191	−0.1	3	G	127.4	2
	317	.....	.....	NG	.....	.....
10	14	+0.5	1	NG	13.5	1
	54	0.0	4	F	40.5	3
11	.....	.....	.....	.....	.....	.....
12	53	+6.8	1	P	46.2	1
	89	−3.4	2	G	46.2	1
13	2.2	.....	.....	NG	.....	.....
	83.3	−3.4	1	F	86.86	1
	175.5	+1.8	2	P	86.9	1
14	70	−3.9	1	G	73.9	1
	223	+1.6	3	G	147.8	2
15	82	+6.9	1	NG	75.1	1
	223	−2.3	3	F	150.2	2

*Uncertain because an error of 1 unit in V_0 would change F by 1 unit.

TABLE II—*Continued*

No	V_o	O−C	F	Q	A_c	F_a
16	400	.....	1	G	400	1
17	119	−5.4	1	F	124.4	1
	375	+1.8	3	G	248.8	2
18	15	+0.6	1	NG	14.4	1
	144	0.0	10*	E	129.6	9
19	400	.....	.....	G	400	1
20	357	.....	.....	G	357	1
21	23	.....	.....	P	23	1
22	4.4	+0.8	1	F	3.58	1
	6.6	−0.6	2	F	3.6	1
	28.3	−0.3	4	P	21.5	6
	57.2	−0.1	2	F	28.6	8
	115.0	+0.4	2	P	57.3	16
23	8	0.0	1	F	8	1
	136	0.0	17*	G	128	16
	59	.....	.....	G	.....	.....
24	71	.....	.....	P	71	1
25	2	+0.06	1	G	1.94	1
	20	+0.6	10*	G	17.5	9
	155	−0.1	8	G	135.8	70
	13	−0.6	1	G	13.65	1
	82	+0.1	6	F	68.2	5
26	.....	.....	.....	NG	.....	.....
27	.....	.....	.....	NG	.....	.....
28	81 top	.....	.....	G	.....	.....
	200 top	.....	.....	G	.....	.....
	103 bottom	.....	.....	G	.....	.....
	176 bottom	.....	.....	G	.....	.....
	av. 92	−1.6	1	G	93.6	1
	av. 188	+0.8	2	G	93.6	1
29	4	.....	1	P	4	1
30	45	+6.0	1	P	39.0	1
	75	−3.0	2	P	39.0	1

TABLE II—*Continued*

No.	V_0	O−C	F	Q	A_c	F_a
31	3	−0.1	1	G	3.1	1
	19	+0.4	6*	G	15.5	5
	37	−0.2	2	G	18.6	6
32	21	.....	.....	F	21	1
33	86	.....	.....	F	86	1
34	4	−0.8	1	G	4.16	1
	25	0.0	6*	G	20.8	5
35	5	+0.4	1	G	4.63	1
	19	+0.5	4*	E	13.9	3
	74	−0.1	4	G	55.6	12
	126	.....	.....	E	.....	.....
	105	.....	.....	G	.....	.....
36	3.9	+0.5	1	G	3.42	1
	15.5	+1.8	4*	G	10.3	3
	54.2	−0.5	4	P	41.0	12
37	155	.....	.....	G	155	1
	75	−2.0	1	F	77.0	1
	155	+1.0	2	G	77	1
38	13.5	+0.2	1	G	13.35	1
	40	0.0	3	G	26.7	2
39	10.0	.....	.....	G	10.0	.....
40	2.2	+0.03	1	G	2.17	1
	32.5	−0.1	15	G	30.4	14
	130	−0.2	4	G	96.7	45
	45.5	.....	.....	G	45.5	.....

itself. A case of direct emission from the chromosphere will be noted among the small eruptions of short life, however. A center of attraction, possibly electrified, develops near an ordinary quiescent prominence, or the contrary. The prominence at once becomes active and pours into the center of attraction, the matter moving in curved streamers. If the center is weak, this process may proceed for hours or days. Other centers develop and subside until the prominence material is entirely returned to the chromosphere by this means. If, however, the intensity of the attraction at the center increases rapidly, the streamers form arches which, moving toward

the center of attraction, begin to overshoot the mark and thus bend back into it. The prominence is then torn apart and may be rapidly pulled into the center of attraction along the continually rising arched streamers. The "Sigma" prominence,[2] already described, illustrates such an instance. If the attraction increases still more rapidly, the arches along which the streamers form rise, and the whole prominence may leave the chromosphere in a more or less vertical direction.

The presence of a sun-spot near by has occasionally been observed to produce similar results; but of the forty cases now on record, only eight (Nos. 1, 2, 13, 19, 20, 27, 31, and 39) were connected with sun-spots. Number 27 is a typical sun-spot prominence and probably should not be called "eruptive." In nine cases the observers have noted that no marking appeared on the disk which might be associated with the prominence.

PROMINENCES OF THE SUN-SPOT TYPE (CLASS 3)

This action of sun-spots on prominences which accidentally occur near by is, in some respects, very similar to that of centers of attraction. The associated prominences, which consist of broken filaments moving radially into the spot-area (class 3*a*), or which rise and fall like a fountain in closed loops within the spot-area (class 3*b*), are of a different kind, however, and are distinctive of sun-spots alone. Plate XI illustrates these three subdivisions of the sun-spot type (class 3) prominences. Class 3*a* is perhaps the most common, and class 3*b* almost equally so. Class 3*c*, in which accidental prominences occur near one of class 3*a*, or less frequently near class 3*b*, is of still rarer occurrence.

Not every spot is accompanied by a prominence as it passes over the limb. Indeed, the phenomenon of a prominence of the sun-spot type is a rare one. An examination of all the prominence plates (6151) taken with the 13-foot spectroheliograph every clear day from August 4, 1915, to January 1, 1936, revealed only eighty-three (or 1.3 per cent) having prominences of the sun-spot type.[7] In three cases more than one prominence of class 3 was found. Of the fore-

[7] O. J. Lee (*Ap. J.*, **45**, 206, 1917) found from a study of 4068 prominences chosen at random that 236 (5.1 per cent) were "in the immediate vicinity of sun-spots."

PLATE XI

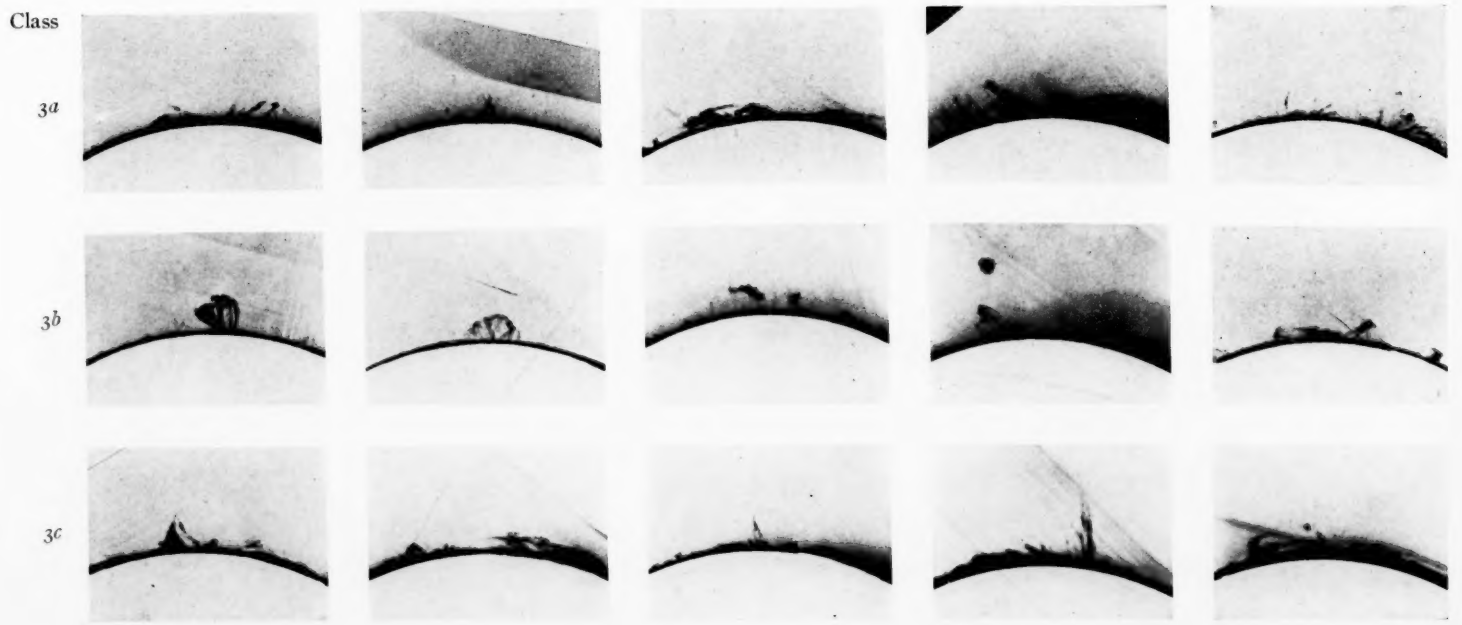

SUBDIVISIONS OF THE SUN-SPOT TYPE PROMINENCES (CLASS 3)

Five illustrations of individual prominences (Ca^+), in sequence from left to right, are given for each subdivision

UNIV. OF MICH.

going, thirty-four belong to class *3a*, thirty-one to class *3b*, and eighteen to class *3c*. In every case save one, the prominence appeared over areas associated with very complicated spot-groups in the early or late stages of development, seeming to prefer the very earliest or latest stages. In fact, for several cases the prominence appeared just after the spot-group had died out, and in at least one or two cases it appeared just before the spot-group developed.

Of class *3a* the prominence of September 20, 1917, appeared on the west limb of the sun in the position of spot-group Mt. W. 809 two days after the latter disappeared; that of September 22, 1935, over the position of a new group, Mt. W. 4622, three days before the group came over the east limb, and was then visible only as a speck. Of class *3b* the prominence of July 12, 1924, appeared on the east limb in Lat. 5° S. No spot was observed on this or succeeding days, and no important marking showed on the calcium disk plates. This circumstance may be accounted for by the supposition that the spot disappeared just previous to reaching the east limb and that the prominence (a weak one) appeared in the position of the spot. The highest loop observed in class *3b* prominences was 216,000 km, and the lowest was 27,000 km. Of class *3c*, the prominence of May 14, 1918, appeared over the position of spot-group Mt. W. 1099 on the west limb about one day after the group had died out. This class seems to form most commonly during the disappearing stage of spots, since of the eighteen cases only four were associated with developing groups. Of the eighty-three plates showing prominences of class 3, only one prominence, that of December 4, 1932, class *3a*, appeared over a simple spot. This exception was very weak but unmistakable.

In class *3a*, in so far as appearances go, the material which forms the broken filaments seems to come from the surrounding chromosphere. Indeed, it can be assigned to no other source, since the filaments seem to be continually moving into the spot. In class *3b* the material moves along loops which rise from and return to the spot.

In addition to the broken filaments which usually occur in *3a*, class *3c* shows one or more streamers from a nearby prominence along which matter moves into the spot, sometimes in the form of knots or new projecting streamers. These lateral prominences are often

low objects, less than 25,000 km high; but occasionally they are raised high above the chromosphere as detached clouds, and sometimes are very large (Pl. XII).

ATTRACTION OF SUN-SPOTS FOR PROMINENCES

Prominences which appear near spots (class 3*c*) and are torn apart by them have several characteristics very much like those of ordinary active prominences (class 1) which are torn apart by centers of attraction: (*a*) both send streamers and knots into the center of attraction or spot; (*b*) both may become eruptive; and (*c*) it now appears that the character of the motion of the moving knots and streamers as they pour back into the sun is the same and like that of the eruptive prominences. The evidence for (*a*) is illustrated by comparing the examples of active prominences already given[8,9] with Plate XII. The evidence for (*b*) is that eruptive prominences, Nos. 1, 2, 31, and 39, for example, were associated with spots; while Nos. 30, 32, 33, and 34, previously given,[10] were affected by centers of attraction.

It has already been pointed out[11] that the motions of knots along the curved streamers of the active prominences "Sigma," September 23, 1919, and "Rocket," October 6, 1919, like those of the vertical motions of eruptive prominences, were uniform, with sudden increases at intervals, as if by an impulse. These are the only prominences of this kind which were large enough, on the scale of the 40-inch refractor, for these details to be measured. It was therefore interesting to find one of class 3*c* connected with a sun-spot in which similar measurements could be made. This opportunity occurred with the class 3*c* prominence which was torn apart by a sun-spot group on August 27, 1935.

The life-history of this spot group and the prominence is briefly as follows: A pair of very faint spots surrounded by an area of bright hydrogen and calcium flocculi appeared in Long. 41° E. of the central meridian, Lat. 29° N., on August 16. The floccular area in-

[8] *Pub. Yerkes Obs.*, **3**, Part IV, Pl. XXVIII, 1925.

[9] *Mt. W. Contr.*, No. 451, Pl. III; *Ap. J.*, **76**, Pl. II, 1932.

[10] *Ibid.*, Pls. VI and V, respectively.

[11] *Pub. Yerkes Obs.*, **3**, Part IV, Fig. 6, Nos. 2 and 3.

PLATE XII

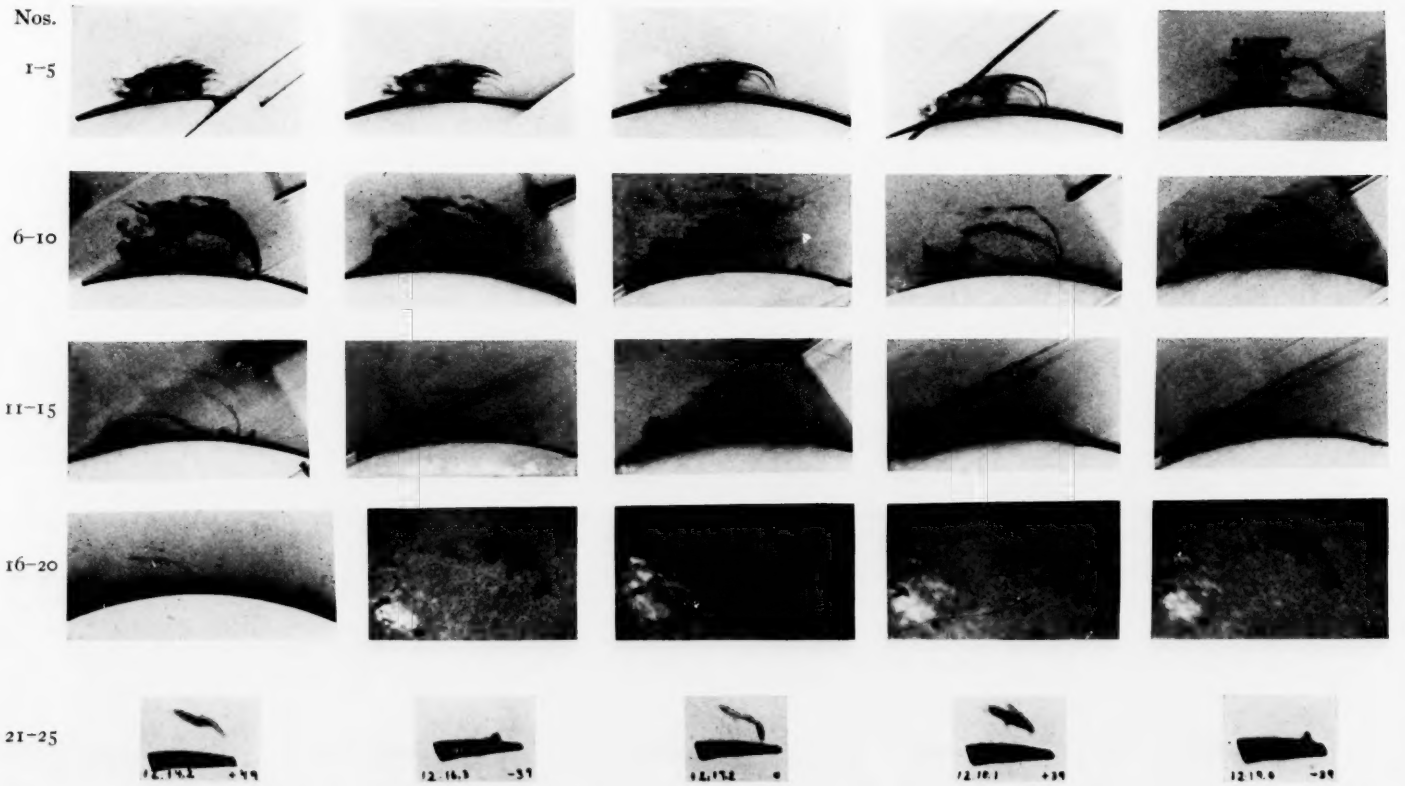

CLASS 3*c* PROMINENCE (Ca^+) OF AUGUST 27, 1935

Nos. 1–4, at 6-minute intervals, August 26. No. 5, early on August 27; Nos. 6–10, sun-spot pulls prominence apart; Nos. 11–16, at 10-minute intervals during final destruction. Nos. 17–20, August 22, *Hα*, disk, at hourly intervals. Nos. 21–25 in *Hα*, August 27; instrument set for various radial velocities.

UNIV. OF MICH.

creased in brightness daily and was always followed by a small prominence 5°–10° to the east and in Lat. 43°–50° N. The faint spots disappeared, however, on August 18. A bipolar sun-spot group, Mt. W. 4596, appeared in the position of the bright floccular area and developed to its full size, such that it was just visible to the naked eye,[12] in twenty-four hours, August 19–20. On August 22 an active prominence of considerable size with eruptive characteristics developed in the usual position. Four exposures on the disk in *Hα* at intervals of about an hour (Pl. XII, Nos. 17, 18, 19, and 20) show a part of the top of the prominence torn away by what was probably a partial eruption.

On August 26 it had reached the western limb and was photographed at Yerkes Observatory, the first exposure being made through clouds at 17^h6^m G.C.T. At this time it was pouring into the spot-group then on the limb of the sun 100,000 km to the south. Its dimensions, height 60,000 km and length 160,000 km, and the presence of the spot-group indicated that it would not last long. Exposures at five-minute intervals were begun and continued throughout the day. The prominence rose slowly to a height of 75,000 km, although at times a vortical section on the northern end reached 100,000 km. It then became broken and poured into the spot with velocities reaching 180 km/sec. In Plate XII, Nos. 1, 2, 3, and 4 are exposures at intervals of about six minutes taken at this phase of the action. On August 27, a clear day, the observations began at 14^h18^m G.C.T. and continued to the end of the action at 21^h. In Plate XII, exposure No. 5 at 16^h25^m shows the state of the prominence during the early morning hours, sending streamers into the sun-spot located at the right. Toward 17^h these streamers became very strong, forming a close bundle. Numbers 6 and 7 show the condition at 18^h20^m and 18^h40^m. Numbers 8, 9, and 10 at twenty-minute intervals after 19^h25^m show the head parted from the stem and the entire mass being drawn into the spot. Numbers 11–16 taken at about ten-minute intervals after 20^h15^m show the final disappearance of the prominence into the spot, the last exposure being taken at Mount Wilson at 21^h8^m. Sixty-three exposures at five- to ten-minute intervals made by the author at Yerkes and ten by Hickox and R. S. Richardson at

[12] J. O. Hickox, *Pub. A.S.P.*, **47**, 272, 1935.

Mount Wilson during this day furnish abundant material for a study of the motions of knots and streamers into the spot-group.

Measurements of the motions of knots along streamers and of the projections of streamers into the sun-spot were made with a divided scale photographed upon film with divisions equal to 10,000 km on the scale of the pictures. This was bent along the streamers for purposes of measurement, the origin being the brilliant column in the north central portion of the prominence, which remained quite stationary in solar latitude during the action.

Figure 2, Nos. 1–22, are time-distance diagrams of twenty-two streamer and knot motions from their origin in the brilliant column to the spot-area measured along their trajectories, the streamers. Here again it will be noted that the particles move with uniform motion, increased at intervals as if by a rather abrupt impulse. The last four cases, for each of which a greater number of observations was obtained, are especially convincing. The relatively small space over which the action takes place makes the percentage accuracy of such measurements considerably less than for the great eruptive prominences.

Thus it is seen that the motions of knots and streamers from prominences into sun-spots, like the similar motions of matter from active prominences into centers of attraction, obey the first law of motion of eruptive prominences. We will now inquire if the second law is also applicable. Table III gives the data for the spot-type prominence of August 27, 1935, arranged as in Table II for the eruptive prominences. Here it is seen that the values of O−C, while somewhat larger than those in Table II, are of the same order. The knots and streamers in this class *3c* prominence therefore obey the second law of motion of eruptive prominences, as well as the first.

Unfortunately, we have no adequate data for a similar examination of active prominences, class 1—only one plot each for the "Sigma" and "Rocket" prominences[13] cited above. The former shows a well-defined case of uniform motion with one break depending on two points only, while the latter has too few points to be certain about most of the breaks. Another case, however, will be cited in the section entitled "Streamer Characteristics."

[13] *Pub. Yerkes Obs.*, **3**, Part IV, 219, 1925.

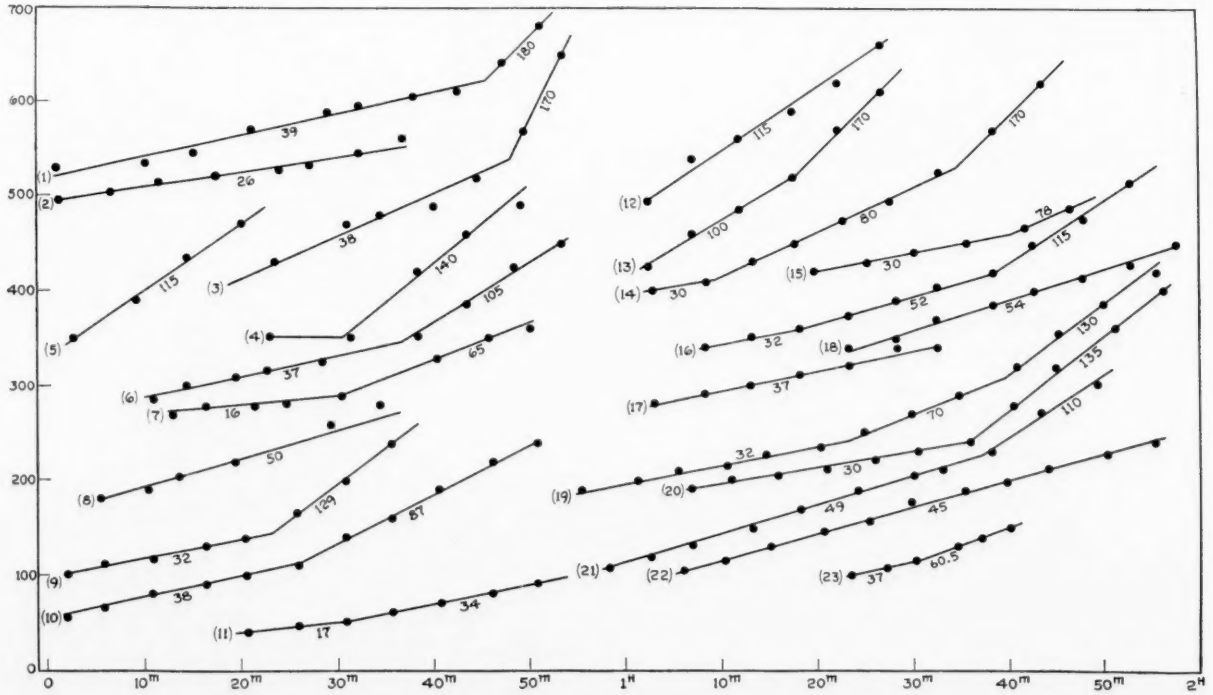

FIG. 2.—Numbers 1–22, motions of streamers and knots in the class *3c* prominence of August 27, 1935, measured along their curved paths. Number 23, similar motions for the active prominence of June 8, 1920.

TABLE III

VELOCITIES V_0 AND ACCELERATIONS A_c OF KNOTS AND STREAMER ENDS IN THE CLASS 3*c* PROMINENCE OF AUGUST 27, 1935

No.	V_0	O−C	F	Q	A_c	Fa
1	39	+ 2.9	1	G	36.1	1
	180	− 0.5	5	F	144.4	4
2	26	.....	.....	G	26	.....
3	38	+ 3.8	1	F	34.2	1
	170	− 1.0	5	F	136.8	4
4	140	.....	.....	F	140	.....
5	115	.....	.....	G	115	.....
6	37	+ 1.8	1	G	35.2	1
	105	− 0.6	3	F	70.4	2
7	16	− 0.2	1	G	16.2	1
	65	+ 0.2	3	G	48.6	3
8	50	.....	.....	F	50	.....
9	32	− 0.2	1	G	32.2	1
	129	+ 0.2	4	G	96.6	3
10	38	− 2.2	1	G	40.2	1
	87	+ 6.6	2	G	40.2	1
11	17	0.0	1	G	17	1
	34	0.0	2	G	17	1
12	115	.....	.....	F	115	.....
13	100	+12.0	1	G	88	1
	170	− 6.0	2	G	88	1
14	30	+ 2.0	1	G	28.0	1
	80	− 4.0	3	G	56	2
	170	+ 2.0	6	G	84	3
15	30	+ 3.6	1	G	26.4	1
	78	− 1.2	3	P	52.8	2
16	32	+ 3.6	1	G	28.4	1
	52	− 4.8	2	G	28.4	1
	115	+ 1.4	4	G	56.8	2
17	37	.....	.....	G	37	.....
18	54	.....	.....	G	54	.....

TABLE III—*Continued*

No.	V_0	O−C	F	Q	A_c	F_a
19.....	32	− 1.0	1	G	33.0	1
	70	+ 4.0	2	G	33.0	1
	130	− 2.0	4	G	66.0	2
20.....	30	+ 2.9	1	G	27.1	1
	135	− 0.5	5	G	108.4	4
21.....	49	− 4.8	1	G	53.8	1
	110	+ 2.4	2	G	53.8	1
22.....	45	.....	.....	G	45	.....
*23.....	37.0	+ 5.4	1	F	31.6	1
	60.5	− 2.7	2	F	31.6	1

* Streamer from active prominence of June 8, 1920.

A criticism of the data in Table III which does not apply to any serious extent to the eruptive prominences in Table II is that the radial component of the motion may be partially, or even mostly, in the line of sight. With the Rumford spectroheliograph, however, any part of a prominence whose radial velocity exceeds ± 30 km/sec is not recorded. There is also other evidence that the component in line of sight did not greatly affect the measurements. The prominence appeared in the usual position in latitude, the brilliant column rising in apparent solar Lat. 49° N. on the west limb, the streamers pouring into the spot in apparent solar Lat. 30° N. If it were also in the customary longitude, a little east of the spot, the inclination of the pole of the sun would conspire to make it nearly due north of the spot on the limb.

It is well known that prominences drawn into a spot enter in a somewhat spiral path,[14] probably a consequence of the relation of the magnetic field of the spot and the electrical field of the streaming atoms of the prominence. If the spot is small (magnetic field small), the spiraling effect is greatly diminished. In a motion-picture film of a prominence entering a small spot, obtained at the McMath-Hulbert Observatory,[15] no spiraling is apparent. The sun-spot group as-

[14] G. E. Hale, *Mt. W. Contr.*, No. 26, Pls. XXXVIII and XXXIX; *Ap. J.*, **28**, 100. Pls. XI and XII, 1908.

[15] R. M. Petrie and R. R. McMath, *Pub. A.A.S.*, **8**, 49, 1934.

sociated with the prominence of August 27, 1935, was of considerable size when first observed on August 20; but when last seen on August 24, it was greatly diminished and was probably rather small at the time the velocities were measured.

Additional data on the motions of this prominence were obtained by P. C. Keenan at the Yerkes Observatory, photographing in *Hα* with an adaptation of the spectrohelioscope.[16] The exposures, some of which are shown in Plate XII, Nos. 21–25, were made with the line-shifter set for velocities of +49, −39, 0, +39, and −39, km/sec. The most obvious interpretation of these exposures is that the inclined streamer arch (No. 24) was moving away from the observer with a velocity of something like 20 or 30 km/sec. The exposure at +49 km/sec is much fainter; but the streamer also shows at zero velocity, and is entirely absent at −39 km/sec. For +39 km/sec the streamer is much the brightest, but probably the real velocity was less than this amount. If we adopt +25 km/sec at 12^h15^m, the observing interval will be covered by plot No. 18 in Figure 2, giving a velocity across the line of sight of 54 km/sec. Inclusion of the radial component would then make the real velocity 60 km/sec. Likewise it would increase the second velocity of No. 16 in Figure 2 from 52 to 58 km/sec, and somewhat improve the values of O−C for this plot in Table III.

The character of the motions of knots and streamers into sun-spots and centers of attraction thus appears to be like that of the eruptive prominences. The evidence is not so complete as could be wished, but it certainly suggests that the force and its manner of action are alike in the two cases and that it is probably, at least in part, electrical and not entirely radiation pressure. Some additional evidence on the nature of this force and its action is found in cases of retarded eruptions.

RETARDED ERUPTIONS

A rather unusual phenomenon is an eruption which begins apparently in every way like an ordinary eruptive prominence, but very slowly, the prominence feeding streamers of relatively large proportions into the center of attraction or the sun-spot.

Plate XIII illustrates an example, a normal eruptive prominence,

[16] *Ap. J.*, **83**, 55, 1936.

PLATE XIII

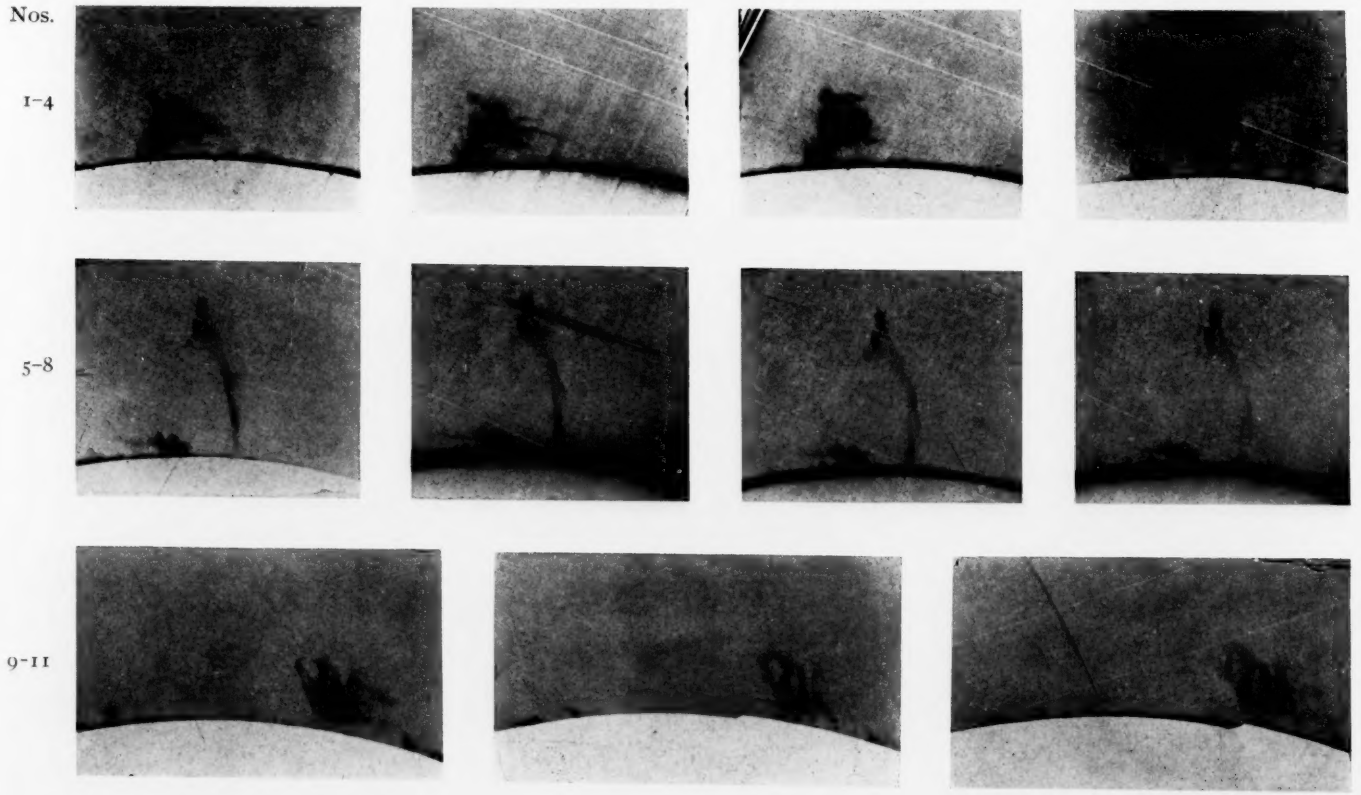

RETARDED ERUPTION OF JULY 27, 1920

Nos. 1–3, stationary stage; No. 4, early stage of eruption; Nos. 5–8, intervals of 5 minutes, showing streamer moving into sun-spot. Nos. 9–11, active prominence of June 8, 1920, 10-minute intervals (Ca^{+}).

UNIV. OF MICH.

No. 39, save that the speed was very slow. It appeared as a class 3*c* prominence on the east limb of the sun on July 27, 1920, rising from a point in solar Lat. 17° S., with streamers pouring into a pair of small spots on the limb in Lat. 7° S. The first exposures were made at Yerkes at 15^h25^m G.C.T. The elevation of the under side of the head was 20,000 and of the top 70,000 km above the chromosphere, and remained at nearly these values for two hours, until 17^h24^m G.C.T. (Pl. XIII, Nos. 1, 2, 3), with no very sensible change in form. The streamers poured into the spots with velocities of 30 km/sec. At this time clouds intervened. The sky clearing 3^h22^m later, the next exposure showed the head of the prominence already detached (Pl. XIII, No. 4), the under side being now 64,000 and the top 102,000 km above the chromosphere. As the plot (Fig. 1, No. 39) shows, this ascent continued with a uniform motion of 10 km/sec until the phenomenon became lost in the haze of the low evening sun. The downward velocities of the streamers and knots had increased to 100 km/sec when the eruptive stage was first observed and stayed at this value as long as the observations continued. Plate XIII, Nos. 5, 6, 7, and 8, gives four exposures at intervals of about five minutes during the later eruptive phase, showing a streamer condensation moving from the prominence into the spot.

Another case appeared on the east limb of the sun on November 11, 1934, like a suspended cloud, in solar Lat. 40° N., pouring into a center of attraction in Lat. 50° N. Continuous observations over a period of seven hours showed a total rise on the plate (Mt. Wilson) of only 1.9 mm (50,000 km), which corresponds to a velocity of 2 km/sec.

These examples suggest that the attractive force (which is measured by the velocities of the knots and streamers) may nearly or completely neutralize the repelling impulse which causes the eruption. That this neutralization may not take place until near the end of an eruption is seen in the plots of Nos. 14, 23, and 35 of the great eruptions, where a decrease in velocity was observed at this phase of the action.

SMALL ERUPTIONS OF SHORT LIFE

The highest velocities observed in eruptive prominences were those (Nos. 16, 17, 19, and 20) observed by J. Fenyi, which were 357–

400 km/sec. All four of these eruptions were of very short duration, five to eight minutes, the motions being uniform without increases. It was hoped that by taking three exposures at successive intervals of about five minutes during the routine solar program with the 13-foot spectroheliograph some of these brief eruptions would be observed. This program began in 1924 and has, to the present, yielded only a small amount of material. In several instances a prominence appears on one plate of the three, but is either absent from the others or shows only as a slight irregularity in the chromosphere. Most of these are faint objects which appear above the chromosphere in an interval of five minutes, and hence presumably rise directly out of it. They seem to have the form of a slender pole or column about 10,000–15,000 km in diameter and reach heights of about 100,000 km. In general dimensions they are much like tornadoes but are not of helical structure.

Plate XIV shows three illustrations of this kind. The first prominence (*a*) appeared October 31, 1931, in the region of spot group Mt. W. 4284, which disappeared one day before reaching the west limb in Lat. 15° S. The first exposure shows an elevation in the chromosphere 10,400 km high and 5400 km wide in the region of the eruption. Several other prominences on the chromosphere are the same as in succeeding exposures. Five minutes later this eruptive prominence had grown to a height of 112,400 km, measured along the direction of projection which is inclined 40° to the vertical, and was 15,000 km wide. This implies a minimum velocity of 375 km/sec. On the third exposure, six minutes later, it was still higher, about 7000 km wider and much fainter. It is possible that this is a case of close-loop formation, of class 3*b*, over a sun-spot, for certainly it has a double structure; if so, the velocity was much higher. Another case which appeared on the west limb December 1, 1930, in Lat. 33° S. was not connected with a visible spot-group or with one that had faded out. It shows on the second plate only, 108,000 km high and 15,000 km wide; and no trace is seen five minutes earlier or later, thus implying a minimum velocity of 360 km/sec. I think this case shows no evidence of looping, and it was probably an eruptive prominence of ordinary characteristics and high speed. Indeed, there is so far no certain evidence that looping of streamers occurs

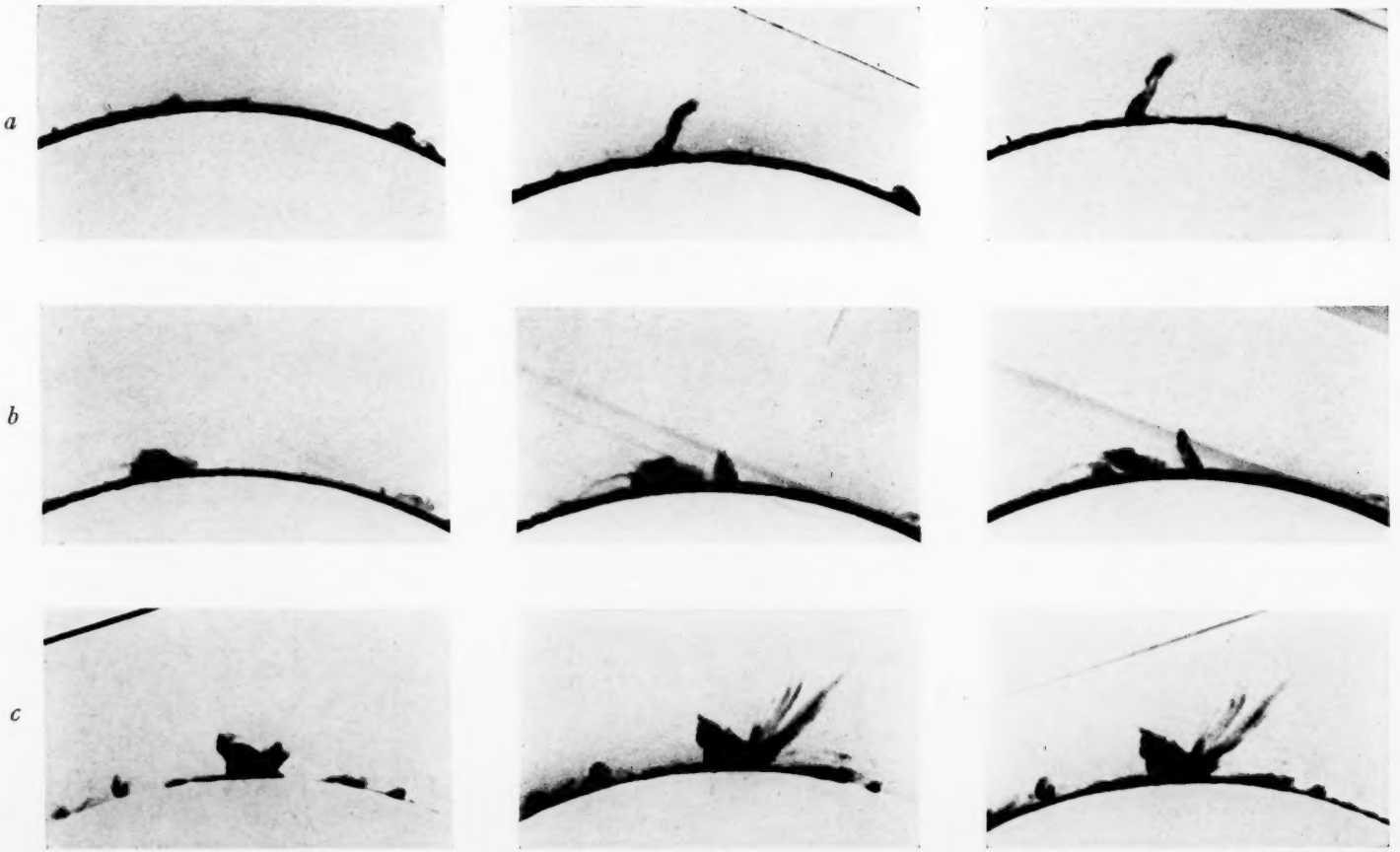

SMALL ERUPTIONS OF SHORT LIFE

Exposures at intervals of about 5 minutes (Ca^+): (*a*) October 31, 1931; (*b*) December 13, 1929; (*c*) January 12, 1926

UNIV. OF MICH.

outside the areas of sun-spot groups or of their positions within one or two days before or after appearance—possibly a consequence of the absence of magnetic fields.

These examples are included in Table IV, which includes all the short-lived prominences observed on the 13-foot spectroheliograph plates. The positions on the limb are given in the second and third columns; δt is the interval between the exposure which shows the prominence and the one immediately preceding which does not show it. V_m is the minimum velocity indicated by the data.

TABLE IV

MINIMUM VELOCITIES (V_m) OF SMALL ERUPTIVE PROMINENCES OF SHORT LIFE

Date	Limb	Lat.	δt	V_m	Spot?
				km/sec	
Sept. 7, 1920	W.	20° S.	14^m	225	Spot
Jan. 12, 1926	W.	25 S.	6	525	Spot
Mar. 20, 1926	E.	18 N.	7	225	No spot
June 27, 1926	E.	25 N.	5	324	No spot
Dec. 13, 1929	E.	7 S.	6	114	No spot
Dec. 1, 1930	W.	33 S.	5	360	No spot
Oct. 31, 1931	W.	15 S.	5	375	Spot
Sept. 22, 1935	W.	41 N.	1	520	No spot

In the case of the prominence of January 13, 1929 (Pl. XIV*b*), the first exposure shows as a bump in the chromosphere, 2700 km high; six minutes later it was a prominence 45,900 km high; and four minutes later still, 70,200 km high. A plot of these data gives a straight line, like the great eruptive prominences.

The high velocity for the prominence of January 12, 1926 (Pl. XIV*c*), must be accepted with some reservation, as the photography was somewhat defective, the first exposure being underdeveloped. However, by comparing fainter portions of the same prominence in the three exposures, this defect could be allowed for, and the observation seems to be reliable. This was a class *3c* prominence, over a complicated group of spots, Mt. W. 2432. It took the form of a spray shot out at an angle of 45° to the vertical and is the first in the author's experience for which a velocity greater than 400 km/sec has been observed. Several of these sprays are on record, but the data

are insufficient to establish velocities. The form, however, strongly suggests an extraordinary velocity.

The small eruption connected with No. 40 (Fig. 1) is another instance where the velocity exceeded 400 km/sec, and in this case the observations are sufficient to establish definitely the velocity and its uniform character. No break occurred in the time-height diagram, but this is probably due to its short life. It seems, then, that these prominences, like the retarded eruptions, also have the motion characteristics of the great eruptions.

STREAMER CHARACTERISTICS

The disappearance of a prominence into a center of attraction or a sun-spot always takes place through the formation of streamers, or of elongated knots moving in curved lines of the same form as the streamers, which are projected into the spot or the center. It is noteworthy that these streamers or knots are commonly given off by the top of the prominence at the beginning of the action; but, as the attractive force continues, other points farther down the prominence begin to emit them. An example of the first stage of this action is the active prominence which appeared on the west limb of the sun on June 8, 1920 (Pl. XIII, Nos. 9, 10, 11). This prominence rose to a height of 80,000 km in solar Lat. 17° S. A single section of a streamer was emitted from the top and, moving in a curved line, entered a center of attraction in Lat. 2° S.

The forward end of this streamer section was fairly well defined and was therefore submitted to measurement. The distance from the dense central core of the prominence to this end of the streamer was measured along its curved path with the flexible scale as previously described for the class *3c* prominence of August 27, 1935. The plotted results for six exposures are shown in Figure 2, No. 23. Here again it will be seen that the motions of streamers into centers of attraction obey the two laws of motion of eruptive prominences.

The forms of the streamers emitted by prominences and entering centers of attraction are strongly suggestive of exponential curves or of the lines of force about a magnetic pole. Figure 3 shows tracings of streamer forms from typical active prominences found on plates taken with the Rumford spectroheliograph at the Yerkes Ob-

servatory. In every case the direction of motion along the arc is from left to right. The first case is that of June 8, 1920; and the last two, deformed streamers.

This peculiar deformation of streamers has been noted on several occasions. The material in the streamer moves along in the customary manner toward the center of attraction or spot, then turns ver-

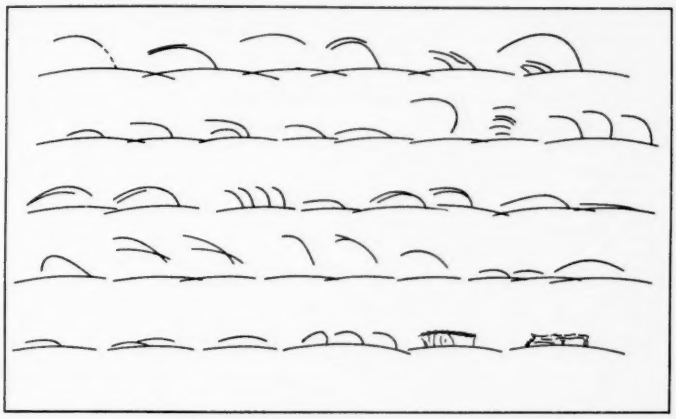

FIG. 3.—Typical streamer forms from active prominences. Tracings made from plates taken with the Rumford spectroheliograph of the Yerkes Observatory (H line of *Ca*+).

tically downward to the chromosphere. This may be due, in part at least, to a large angle of projection and possibly to the development of a strong center of attraction nearer the prominence.

I am indebted to Dr. O. Struve for the use of the 40-inch refractor and Rumford spectroheliograph of the Yerkes Observatory over a period of several years; to Dr. Keenan for much assistance with this equipment; and to members of the Solar Department at Mount Wilson for collaboration in various ways.

CARNEGIE INSTITUTION OF WASHINGTON
MOUNT WILSON OBSERVATORY
May 1936

THE CHANGE OF THE SOLAR VELOCITY WITH INCREASING DISTANCES OF THE STARS FROM THE GALACTIC PLANE

EMMA T. R. WILLIAMS

ABSTRACT

The analysis of the proper motions of 18,000 stars, made at the McCormick Observatory, together with several previous investigations of proper motions, of radial velocities, and of space motions, indicates that the solar velocity decreases with respect to stars of a given spectral class, at increasing distances from the galactic plane. The investigations in which no stars were excluded on account of high velocity or stream membership, such as the McCormick analysis, show the effect more clearly than those in which such stars were excluded.

In the study of the proper motions of faint stars, just completed at the McCormick Observatory,[1] the mean parallaxes of stars in various galactic zones were derived by two essentially independent methods: first, from secular parallaxes, and second, from τ-components. It was immediately obvious that there were pronounced systematic differences between the two sets of parallaxes, depending on galactic latitude. The probable source of the discrepancy seems to be that the solar velocity with respect to any given spectral class of stars, such as gK stars, has been assumed to be independent of galactic latitude. A decrease of the solar velocity with increasing distance in parsecs from the galactic plane is clearly indicated in many previously published investigations. This would explain the observed discrepancy satisfactorily, and suggests that with the present knowledge of solar motion the mean parallaxes of faint stars derived from τ-components are at least as reliable as those obtained from secular parallaxes.

First, we shall examine the McCormick methods and results. The secular parallaxes were reduced to mean parallaxes by means of the relation:

$$\bar{\pi}_v = \frac{4 \cdot 74}{V_o} \times \text{secular parallax} ,$$

[1] Van de Kamp and Vyssotsky, *Pub. Leander McCormick Obs.*, **7**, in press; also *A.J.*, 1936.

where $\overline{\pi}_v$ denotes the mean parallax obtained from v-components and V_0 denotes the solar velocity. The values adopted for V_0 varied with spectral class according to the best available material from bright stars.[2] When adopting V_0 for a mixed group, such as all twelfth-magnitude stars, for example, due allowance was made for the relative numbers of different spectral types and of giants and dwarfs. Except for the change in composition, however, the adopted value of V_0 was independent of latitude.

To obtain mean parallaxes from the observed τ-components, it was first necessary to correct the observed τ-components for the systematic effects of the accidental errors. Then the following relation was used:

$$\overline{\pi}_\tau = \frac{4.74}{\overline{V}_\tau} \times \overline{\tau}_{\text{corr.}}$$

Here $\overline{\pi}_\tau$ denotes the mean parallax obtained from the τ-components; $\overline{\tau}_{\text{corr.}}$ denotes the mean τ-component corrected as just explained; and $\overline{V}_\tau$ denotes the mean peculiar velocity of the stars, in kilometers per second and without regard to sign, *in the τ direction*. Since various regions of the sky were considered separately, it was necessary to allow for the changes in $\overline{V}_\tau$ in different parts of the sky due to the ellipsoidal distribution of peculiar velocities (thus making unnecessary any corrections of the type suggested by Fletcher[3]). Also, as with V_0, the adopted values of $\overline{V}_\tau$ varied with spectral class in accordance with the best available material from bright stars, and the same kind of allowance was made for the spectral and giant-dwarf composition of mixed groups.

Now, comparing the values of $\overline{\pi}_v$ with $\overline{\pi}_\tau$ derived by van de Kamp and Vyssotsky, we find in every case more than 10° from the galactic plane that the values of $\overline{\pi}_\tau$ are larger than the corresponding values of $\overline{\pi}_v$, whereas in the lowest galactic zone the situation is reversed, as is shown in Table I. The same effect is also conspicuous in the subdivisions by spectral classes; but the scatter is considerably larger, owing to the smaller number of stars in each group.

[2] Wilson and Raymond, *A.J.*, **40**, 121, 1930.

[3] *M.N.*, **92**, 780, 1932; **95**, 737, 1935.

Now, since

$$\frac{\overline{\pi}_\tau}{\overline{\pi}_v} = \frac{\text{Adopted } V_0}{\text{Adopted } \overline{V}_\tau} \times \frac{\overline{\tau}_{\text{corr.}}}{\text{Secular parallax}},$$

we may look for the cause of this systematic difference in any one of the four factors involved. Thus, one might doubt the assumption that the values of V_0 and $\overline{V}_\tau$ of a given spectral subclass, say gK, are the same for stars of tenth apparent magnitude as for stars of fifth apparent magnitude. But even if it were incorrect, we should still expect the ratio $V_0/\overline{V}_\tau$ to remain practically unchanged on account of the Strömberg relation between relative solar velocity and mean

TABLE I

$\overline{\pi}_\tau/\overline{\pi}_v$

Gal. Lat.	Apparent Magnitudes				
	12.5—	11.5–12.4	10.5–11.4	9.5–10.4	7.5–9.4
±41° to ±90°	1.84	1.29	1.61	1.37	1.52
21 40	2.00	1.75	1.13	1.54	1.43
11 20	1.57	1.09	1.17	1.28	1.04
0 10	0.84	0.89	0.90	0.82	0.86

peculiar velocities. Hence the systematic differences may not be accounted for in this manner. Neither do van de Kamp and Vyssotsky feel that systematic errors in the secular parallaxes or in the values of $\overline{\tau}_{\text{corr.}}$ could account for it. Therefore, we are led to examine the two possibilities: (*a*) that for a given type of star, V_0 varies with latitude; and (*b*) that there is a systematic variation with latitude in the lengths of the axes of the velocity ellipsoid, so that $\overline{V}_\tau$ varies in a manner that differs from the variation already allowed for.

Now, there is practically no evidence that the lengths of the axes of the velocity ellipsoid vary with latitude, but several investigators have found evidence of the variation of V_0 with latitude. Thus, from an investigation of proper motions and radial velocities of more than 2,000 stars brighter than sixth magnitude by Gyllenberg and Malmquist,[4] we find the data in Table II, where ξ, η, and ζ are the components of the solar motion.

[4] *Medd. Lund Astr. Obs.*, Ser. I, No. 108, 1925.

TABLE II*

VALUES OF V_0 FOUND FROM RADIAL VELOCITIES

GAL. LAT.	Ao–A5		Fo–F8		gGo–gG5		Ko–K5	
	No.	V_0	No.	V_0	No.	V_0	No.	V_0
0° to ±30°	328	21.4	182	17.5	126	19.1	372	27.1
±30 ±90	260	13.1	132	21.2	109	11.5	292	21.7

VALUES FOUND FROM RADIAL VELOCITIES AND PROPER MOTIONS OF B–M STARS, EXCEPTING dGo–dG5

Gal. Lat.	No.	ξ	η	ζ	V_0 p.e.
+30 to +90	525	14.3	8.0	7.9	18.2±1.1
0 +30	594	17.3	9.5	8.0	21.3 1.0
0 −30	683	18.2	8.7	9.0	22.1 0.9
−30 −90	399	13.4	7.2	6.0	16.3 1.2

* No stars were excluded because of membership in streams, and few because of high velocities.

Again, from a discussion by Robb[5] of 577 B8–A5 stars with known parallaxes, proper motions, and radial velocities, we find the information in Table III. Here,

$$U=\frac{\sigma_1+\sigma_2+\sigma_3}{3}$$

has been adopted as a measure of the peculiar velocities of the stars, σ_1, σ_2, and σ_3 being standard deviations which measure the dispersion of the peculiar velocities along the three axes of the velocity ellipsoid.

TABLE III*

Gal. Lat.	No.	V_0 p.e.	U p.e.
0° to ±30°	324	15.6±.6	11.3±.3
±30 ±90	253	12.9 .6	11.8 .4

* No stars were excluded because of membership in streams; three stars with velocities of more than 100 km/sec were excluded.

Similarly, from an analysis by Jones[6] of the proper motions of the Boss stars, by the two-stream hypothesis, we find the results in

[5] *M.N.*, **94**, 406, 1934.

[6] *Ibid.*, **91**, 563, 1931.

Table IV. This table by itself is, of course, no evidence in favor of the change of V_0 with latitude, for the unit $1/h$ is proportional to the peculiar velocities of the stars, so that the dependence on latitude might be ascribed to a variation in the peculiar velocities. Again, it might be due to the variation in spectral composition, since it is known that the ratio V_0/U is about 1.2 for A stars and about 0.8 for G, K, and M giants.[2] However, as will be seen from Tables III and VI, any appreciable variation in U seems to be unlikely. In this connection, Smart's recent investigation[7] of the variation of mean peculiar velocities with latitude indicates an increase of 7 ± 3 per cent in the peculiar velocities between 0° and 43° galactic latitude. Smart has grouped together stars of all spectral types from A to M. This treatment would be expected to show a slight increase with

TABLE IV*

Gal. Lat.	Speed of Solar Motion in Terms of Unit $1/h$
0° to ±10°	1.110
±10 ±30	1.152
±30 to ±60	0.792

* B stars, members of moving clusters, and faint components of multiple stars were excluded.

latitude, since the A stars are of higher galactic concentration and have considerably smaller peculiar motions than the others.

Finally, in a recent study based on radial velocities, with terms for the galactic rotation included in the solution, Nordström[8] finds the values for the relative solar motion given in Table V. Thus, Nordström's data show a much smaller effect. His exclusion of stars of large radial velocity, however, tends to obscure the effect, since relatively more large-velocity stars have been excluded in low latitudes than in high latitudes, while in the McCormick material the exclusions were essentially[9] limited to faint components of double stars.

It seems more probable that any variation of V_0 and U would depend more on the distance from the galactic plane than on the galactic latitude. Accordingly, the space motions of 627 giants pub-

[7] *Ibid.*, **96**, 165, 1936. [8] *Medd. Lund Astr. Obs.*, Ser. II, No. 79, 1936.

[9] Three stars out of the 18,000 were excluded from the $\bar{\pi}_7$ because of very large proper motions.

lished by Balanovsky[10] have been analyzed to determine their variation with $|Z|$, the distance in parsecs from the galactic plane. The A stars were omitted since there were relatively few of them and

TABLE V*

V_0 FROM STARS OF PARALLAX $\leq 0''.015$

GAL. LAT.	A		F-G		K0-K2		M	
	No.	V_0	No.	V_0	No.	V_0	No.	V_0
	Stars Brighter Than Apparent Magnitude 6							
0° to ±30°	231	15.9	175	17.3	332	18.6	154	21.8
All latitudes	416	15.7	270	15.9	567	18.3	299	21.7
	All Apparent Magnitudes							
0° to ±30°	308	17.1	289	17.8	453	18.3	218	21.9
All latitudes	573	16.9	477	17.0	829	17.7	425	21.2

* Faint components of multiple systems, high-velocity stars and a number of members of the Ursa Major and Taurus streams were excluded.

TABLE VI*

A5-M STARS OF ABSOLUTE MAGNITUDE −1.0 TO +1.9

$\|Z\|$	No.	V_0	U
0–30 parsecs	256	20.6±0.9	20.1±0.6
31–60 parsecs	196	20.4 1.1	22.1 0.8
61–90 parsecs	104	18.0 1.4	20.6 1.1
Over 90 parsecs	71	15.7±1.5	19.2±1.2

* No stars were excluded.

since the values of V_0 and U for A stars are systematically smaller than for the late-type giants. The results are given in Table VI.

To summarize, then, the values of the solar velocity, V_0, and of the peculiar velocities, U, collected in Tables II, III, IV, V, and VI indicate that the variation of the ratio V_0/U with galactic latitude (or

[10] *Bull. Astr. Inst. Leningrad*, No. 11, 1925.

more probably with the distance $|Z|$ from the galactic plane) is due to a progressive decrease of V_0 with increasing distance from the plane of the Milky Way, and not to any progressive change in U. The investigations with relatively few excluded stars show the change in V_0 most clearly.

Figure 1 shows approximately the variation in V_0 with $|Z|$, as indicated by various investigations, as well as the variation in V_0, which would be sufficient to reconcile the $\bar{\pi}_v$ and $\bar{\pi}_r$ values of the McCormick material.

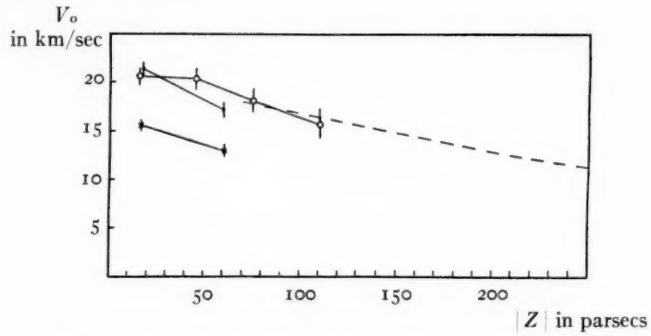

FIG. 1.—Relation between the solar velocity, V_0, and the perpendicular distance from the galactic plane, $|Z|$.

• B to M giants, Table II. × A stars, Table III. o A_5 to M giants, Table VI. --- variation in V_0 sufficient to reconcile McCormick $\bar{\pi}_v$ with $\bar{\pi}_r$.

NOTE ON THE VARIATION OF THE POSITION OF THE APEX WITH LATITUDE

From the point of view of galactic rotation, the decrease of V_0 with $|Z|$ corresponds to a higher velocity of rotation for the stars at a distance from the galactic plane than for the stars of the same spectral subtype in the plane. If this is correct, we should expect that the apex derived from stars of high latitude would be at a smaller longitude than that derived from the low-latitude material of the same spectral subclass. Now, it is fairly clear from numerous studies that the longitude of the apex is probably somewhat smaller for stars of low galactic latitude than for stars of high galactic latitude, *when all spectral classes are combined together.* This results from the fact that the apex of the B and A stars is at a smaller longitude than

the apices of the late-type giants. The data are too meager to tell much about the variation of its position with latitude in the separate spectral classes.

Mention should also be made of the possibility of a progressive variation in the position of the apex with Z, which was reported first by Mineur[11] and independently by Rosenhagen[12] from radial velocities. They found that the η-components of the sun's velocity range from about 13 km/sec relative to stars 150 parsecs south of the sun to 2 km/sec relative to stars 150 parsecs north of the sun. This results in a shift in the longitude of the apex from about 60° in the first case to about 5° in the second. It is found also in Nordström's investigation of radial velocities.[8] On the other hand, it is not found in Mohr's study of space velocities[13] nor in the work of Gyllenberg and Malmquist (see the values of η in the second part of Table II). Finally, there is practically no trace of it in the proper-motion work of van de Kamp and Vyssotsky;[1] for all stars in latitude zone +40° to +90°, which are about 500 parsecs north of the sun, they find 34°.3 for the longitude of the apex, which is to be compared with 36°.6 for the corresponding zone in the south.

I wish to thank Professor Vyssotsky for many helpful suggestions.

LEANDER MCCORMICK OBSERVATORY
UNIVERSITY OF VIRGINIA
June 8, 1936

[11] A series of articles by Mineur and collaborators: *M.N.*, **90**, 789, 1930; *B.A.*, (2) I Mem. et Var., **6**, 355, 1931; *C.R.*, **195**, 208, 1932.

[12] *A.N.*, **242**, 401, 1931.

[13] *M.N.*, **92**, 562, 1932.

FRAUNHOFER'S SPECTRUM IN THE INTERVAL FROM 77,000 TO 110,000 A

ARTHUR ADEL AND V. M. SLIPHER

ABSTRACT

Recent observations of one hundred fine structure lines in the solar grating spectrum, lying in the interval from 77,000 to 110,000 A, are described in connection with previous measurements of the solar prismatic spectrum.

During the winter of 1934–1935 and the summer of 1935, the infra-red solar spectrum was examined with low[1] and with high resolving power. This report is an account of the analysis made with high resolving power, but is preceded by a brief review of the earlier work in order to reveal the relative significance of the Sun's prismatic curve and the fine structure of its spectrum.

The prismatic spectrum, shown in Plate XV, was secured on January 2, 1935—a particularly clear day—within an hour on each side of apparent solar noon, at Ann Arbor (lat. 42°17′). A potassium bromide prism served as the dispersing element and a vacuum thermocouple as the detecting element of the Wadsworth-Littrow self-recording spectrometer used in the experiment. The telluric spectrum was examined over the range from 50,000 to 210,000 A. Reference to Plate XV immediately discloses the excellent atmospheric window defined on the short-wave side by the extensive absorption by water vapor stretching from 50,000 to 77,000 A, and on the long-wave side by the comparatively narrow ozone band extending from 90,000 to 100,000 A. Beginning at 100,000 A, the energy of transmitted sunlight decreases in an approximately uniform manner until the atmospheric curtain at 135,000 A is abruptly begun. Several small, but relatively unimportant, absorption bands occur between.

For reasons given elsewhere,[1] there are but three atmospheric molecules possessing pure rotation and rotation-vibration spectra; these molecules are therefore responsible for the spectra discussed in

[1] Arthur Adel, V. M. Slipher, E. F. Barker, *Phys. Rev.*, **47**, 580, 1935.

PLATE XV

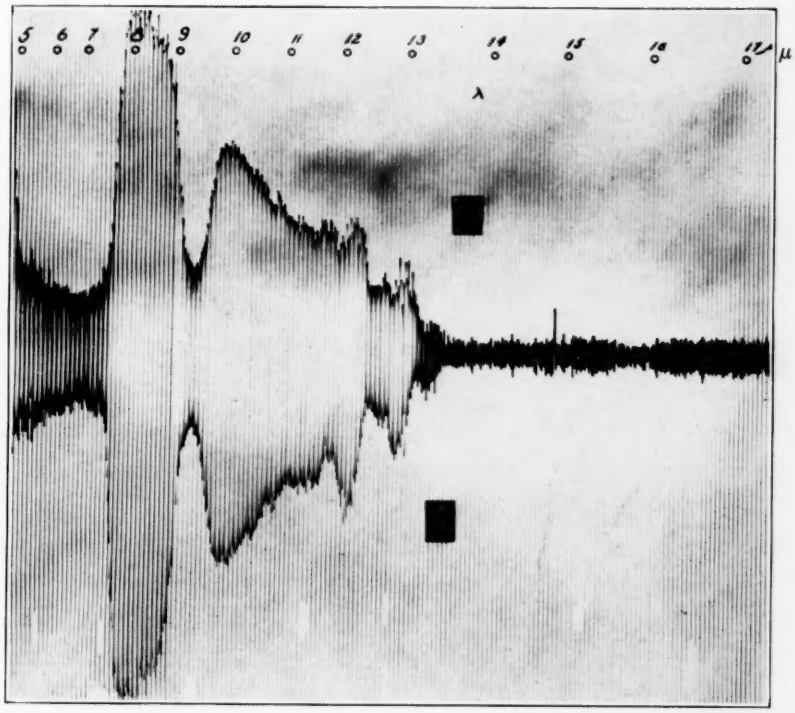

FRAUNHOFER'S SPECTRUM

UNIV. OF MICH.

this paper. They are water vapor, ozone, and carbon dioxide. Absorption bands of the first two have already been mentioned while the most intense absorption band in the infra-red spectrum of the carbon dioxide molecule is responsible for the atmospheric curtain which begins at 135,000 A. Its influence extends to approximately 170,000 A, and within this region it is aided by the comparatively weak ozone band whose center lies in the neighborhood of 150,000 A. Beyond 170,000 A the curtain is maintained by absorption due to transitions between rotational states of the water-vapor molecules.

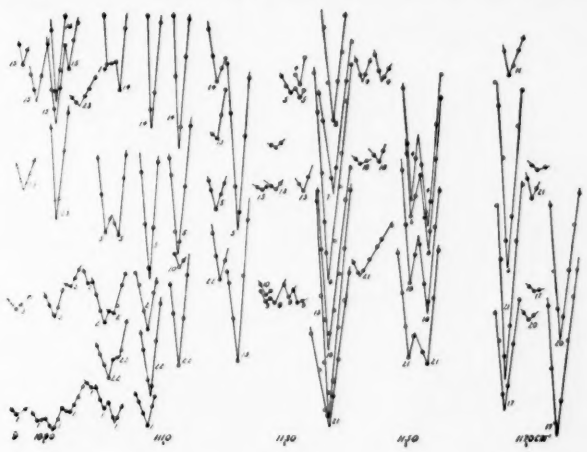

FIG. 1

The study of the solar spectrum made with the grating concentrates on the region from 77,000 to 110,000 A. This phase of the experiment was also carried out at the Physics Laboratory of the University of Michigan, approximately six months later, and consequently with a correspondingly shorter air path traversed by sunlight. The grating spectrometer, the thermocouple, and the amplifying system have been described in detail elsewhere.[2] A twelve-hundred-line grating, ruled by Barker, was used and the slit width equivalent was maintained at approximately 1.5 cm^{-1} throughout the spectral region in question. Numerous runs were made, and one hundred and one lines were recorded. Each of these lines was

[2] J. D. Hardy, *ibid.*, **38**, 2162, 1931.

TABLE I

No. of Line	Average Position	No. of Times Observed	Comparative Strengths	No. of Line	Average Position	No. of Times Observed	Comparative Strengths
1.....	909.6 cm^{-1}	2	S*	52....	1072.8 cm^{-1}	3	W
2.....	914.4	2	W	53....	1075.2	6	S
3.....	920.4	2	W	54....	1078.3	3	M
4.....	922.3	2	W	55....	1082.0	4	W
5.....	925.4	2	W	56....	1086.0	5	M
6.....	929.3	2	W	57....	1088.4	3	M
7.....	934.8	2	W	58....	1091.9	5	S
8.....	941.5	2	S	59....	1094.3	3	W
9.....	943.4	2	S	60....	1095.8	2	W
10.....	945.3	2	W	61....	1097.7	3	W
11.....	949.0	3	S	62....	1100.3	5	S
12.....	954.3	2	M	63....	1102.3	5	S
13.....	956.0	3	M	64....	1107.6	5	S
14.....	960.2	2	M	65....	1112.4	4	S
15.....	962.8	2	W	66....	1118.5	4	S
16.....	967.8	3	M	67....	1122.2	3	SS
17.....	969.4	2	M	68....	1126.3	3	W
18.....	972.0	2	S	69....	1128.3	3	W
19.....	974.4	2	M	70....	1130.4	3	W
20.....	976.8	3	M	71....	1132.4	4	W
21.....	980.2	3	W	72....	1137.3	7	SS
22.....	984.3	3	W	73....	1142.0	3	W
23.....	988.4	3	W	74....	1145.1	2	W
24.....	990.8	3	W	75....	1150.3	4	S
25.....	993.3	2	W	76....	1153.3	4	S
26.....	995.7	3	M	77....	1166.3	4	S
27.....	997.6	2	W	78....	1170.4	4	W
28.....	1001.4	3	M	79....	1175.3	2	S
29.....	1005.0	3	M	80....	1182.3	2	W
30.....	1006.8	2	M	81....	1183.7	2	W
31.....	1008.8	3	W	82....	1188.4	2	S
32.....	1111.1	3	M	83....	1192.6	2	W
33.....	1015.6	3	M	84....	1199.6	3	S
34.....	1018.5	3	M	85....	1206.6	2	W
35.....	1021.3	2	W	86....	1213.3	2	S
36.....	1022.8	3	W	87....	1219.8	2	S
37.....	1026.5	2	W	88....	1225.8	2	S
38.....	1029.5	3	M	89....	1230.4	2	W
39.....	1033.8	3	W	90....	1238.2	2	M
40.....	1037.6	2	W	91....	1240.8	4	M
41.....	1040.3	2	M	92....	1244.7	3	M
42.....	1041.6	2	W	93....	1249.5	2	W
43.....	1043.7	3	†	94....	1255.1	3	S
44.....	1051.9	3	W	95....	1261.9	2	W
45.....	1054.1	2	M	96....	1276.7	2	W
46.....	1056.2	3	M	97....	1281.5	2	W
47.....	1058.1	2	W	98....	1285.0	2	W
48.....	1060.8	4	W	99....	1288.9	2	W
49.....	1062.5	3	W	100....	1291.0	2	W
50.....	1067.0	5	S	101....	1297.8	2	W
51.....	1071.0	2	M				

* S = strong; W = weak; M = intermediate; SS = very strong.
† Ozone band center.

measured two or more times. Table I lists their positions and relative strengths, as well as the number of times each was measured.

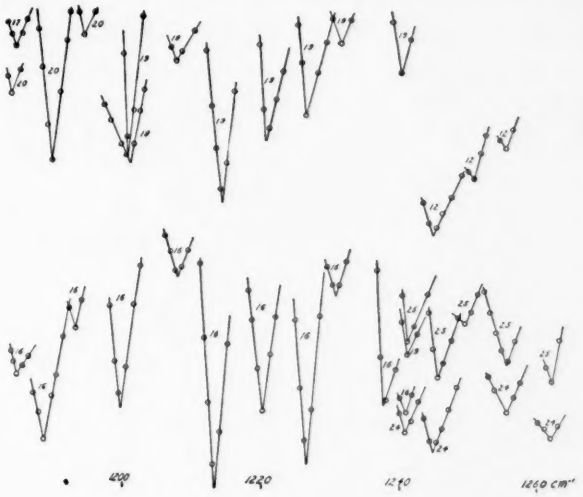

FIG. 2

TABLE II

No. Associated with Line in Fig. 2	Time of Observation (Day and Hour)	No. Associated with Line in Fig. 2	Time of Observation (Day and Hour)
1	July 17 3:15– 4:00	14	July 29 8:30– 8:55
2	18 10:40–11:15	15	29 10:10–10:30
3	18 11:20–11:50	16	29 11:40–12:20
4	20 1:10– 1:45	17	29 1:00– 1:25
5	20 1:50– 2:30	18	29 1:30– 2:00
6	26 10:10–10:20	19	29 3:10– 3:35
7	26 10:25–10:45	20	29 3:40– 4:10
8	26 10:45–11:00	21	29 4:15– 4:45
9	26 3:30– 3:40	22	30 8:00– 8:25
10	26 3:45– 3:55	23	30 8:30– 8:55
11	26 4:00– 4:15	24	Aug. 11 10:20–10:55
12	26 4:20– 5:00	25	12 10:20–10:40
13	29 8:00– 8:30		

The fine structure in the region of ozone absorption between 90,000 and 100,000 A has already been published and applied to a discussion of the form of the ozone molecule.[3] The majority of the

[3] Arthur Adel, V. M. Slipher, Omer Fouts, *ibid.*, **49**, 288, 1936.

remainder of the one hundred and one lines are shown in Figures 1 and 2, and belong to the atmospheric window lying between the strong water vapor and the ozone bands. They are most probably due to absorption by the water-vapor molecule. The numbers associated with the lines refer to the times of observation as recorded in Table II.

The authors wish to express their appreciation of grants-in-aid by the American Academy of Arts and Sciences and by the Faculty Research Council of the University of Michigan. We are indebted to Mr. Omer Fouts for his valuable aid with the spectroheliometer.

UNIVERSITY OF MICHIGAN
ANN ARBOR, MICH.
LOWELL OBSERVATORY
FLAGSTAFF, ARIZ.
July 1936

NOTES

CONFIRMATION OF THE DUPLICITY OF CAPELLA H

In the *Astronomical Journal* **45,** 120, 1936, Carl L. Stearns describes the photographic images of Capella H as having a disturbance in position angle 117°: "The most probable explanation of this appearance seems to be the presence of a faint companion of about the twelfth magnitude at a distance of about 1″.8 from H."

This interpretation was fully confirmed, on an excellent night, with the 40-inch telescope. The measures are:

1936.72 123°.0 2″.37; $\Delta m = 3^{M}.5$(est); 40,700 seeing 4.

The magnitude of H was determined visually at Leiden on three nights, and was found to be 10.20 mag. on the international photovisual scale.[1] The two components are then 10.24 and 13.7 mag.

The duplicity of the Furuhjelm companion makes Capella a quadruple system of the ϵ Lyrae type.

G. P. KUIPER

YERKES OBSERVATORY
September 19, 1936

NOTES ON VISUAL BINARIES OF LARGE PARALLAX

ABSTRACT

Some of the recently discovered visual binaries in the vicinity of the sun are discussed, together with some other pairs.

In these notes the writer will, from time to time, give results concerning the motion in binary systems in the solar neighborhood. Many new companions were found to stars of large parallax, 30″ being generally considered the upper distance limit for micrometer work. When second epochs become available after a sufficient lapse of time, the physical companions in our material will become known. The measures were made with the 36-inch telescope of the Lick Ob-

[1] The residuals for the three nights are: $+^{M}.07$, $-^{M}.04$, and $-^{M}.03$.

servatory and the 40-inch telescope of the Yerkes Observatory. The magnifying power and the seeing (5 being perfect) are added.

1. BD+45°2505 (17^h09^m2), 9^M43 M4; $\Delta m = 0^M4$; $\pi = 0''.144$; $pm = 1''.56$.—Found with 36-inch telescope. Since the separation in 1929 was[1] about $\frac{1}{2}''$, and in 1927–1928 less than that, the maximum separation probably occurs in the third quadrant, amounting to slightly over 1″. The period is probably between 10 and 20 years.

1934.39	228°.9	1″.10	$\Delta m = 0^M1$	36,540	seeing 4
1935.46	219.5	0.99	.4	36,1040	4
1935.63	219.2	1.01	.45	36,1040	3+
1936.43	209.8	0.97	.4	40,950	3+
1936.73	204.2	0.80	0.5	40,700	3

The nearest field star is optical:

1934.39	315°.9	36″.76	$C = 13^M9$	36,540	seeing 4
1935.63	317.4	38.38	13.3	36,360	3
1936.73	319.4	39.81	14.5	40,350	2+

2. Ross 165 (19^h41^m7), 12^M4 M4; $\Delta m = 0^M9$; $\pi = 0''.116$; $pm = 1''.34$.—The duplicity of Ross 165 was suspected on his plates by van Maanen[2] and was confirmed visually by the writer. The pair is rather difficult but is of great interest because the total mass of the system may be smaller than that of any other short-period visual binary known. (The absolute visual magnitudes are about 13.1 and 14.0.) Orbital motion is indicated.

1934.54	145°.2	0″.45 (est.)	$\Delta m = 0^M7$	36,540	seeing 4
1935.63	148.2	.55	0.8	36,540	4
1936.73	152.7	0.62	1.0	40,700	4

3. BD + 4°4510 (20^h34^m6), 7^M89 K6; $\Delta m = 1^M1$; $\pi = 0''.057$; $pm = 0''.85$.—Found with the 36-inch telescope. Slow orbital motion.

1934.68	312°.5	0″.66	$\Delta m = 1^M0$	36,1040	seeing 3+
1935.65	313.9	.68	1.2	36,1040	3
1936.73	315.1	0.53	1.2	40,950	3+

[1] *Pub. A.S.P.*, **46**, 236, 1934.

[2] Letter of July 7, 1934.

4. Furuhjelm 54 (20^h56^m2), 10^M10 M3e; $\Delta m = 1^M9$; $\pi = 0''.097$; $pm = 0''.66$.—Found with the 36-inch telescope. Marked orbital motion in two years.

1934.56	82°.5	0″.93	$\Delta m = 1^M6$	36,540	seeing 4+
1935.63	86.0	0.95	1.9	36,540	4
1936.73	88.6	1.12	2.2	40,700	3+

5. BD + 45°3371 (20^h59^m1), 7^M83 K3; $\Delta m = 5^M1$; $\pi = 0''.047$; $pm = 0''.40$.—Found with the 36-inch telescope. The measures show the pair to be physical.

1934.64	104°.0	2″.84	$B = 13^M0$	36,540	seeing 4+
1935.63	103.9	2.89	13.0	36,540	3+
1936.73	100.6	2.84	13.3	40,460	2+

6. Wolf 1328 (22^h04^m0), 12^M9 red; $\Delta m = 2^M0$; $\pi = 0''.043$; $pm = 0''.71$.—The duplicity was found by van Maanen[3] on his parallax plates; he gives the distance as 1″.9. The following are the first complete measures for this pair:

1935.63	236°.6	1″.83	13^M2, 15^M2	36,540	seeing 3+*
1936.73	233.5	2″.06	12.7, 15.0	40,350	3

* Approximate, B faint.

7. Of other binaries with large parallax we mention four with faint companions:

θ UMaj	1934.22	91°.3	4″.81	$B = 13^M5$	36,540	seeing 3+
11 LMin	1934.22	26.6	2.50	13.0	36,540	3+
α Leon BC	1935.03	84.7	2.03	....	36,540	2+, 3+(2n)
θ Cygn	1934.56	53.2	4.19	12.5	36,540	4+

Measures of θ UMaj were available only for the interval 1889–1899. In 1898 Aitken found the position to be 78°.4; 5″.06. 11 LMin is rapidly closing in and will soon be a difficult pair. The same is true for the double companion of Regulus. The 1923 position of θ Cygni, quoted in *ADS*, must be erroneous. The pair has become slightly wider since Burnham and Aitken measured it (1889–1898).

G. P. KUIPER

YERKES OBSERVATORY
September 28, 1936

[3] *Mt. W. Contr.*, **19**, 259, 1931.

REVIEWS

Molekülspektren. By H. SPONER. Berlin: Julius Springer, 1935 and 1936. Vol. I: *Tabellen*, pp. vi+154; Vol. II: *Text*, pp. xii+506+Figs. 87.

This book on molecular spectra by H. Sponer is a very complete and lucid compilation of the experimental data and of the theories which interpret the structure of molecules by means of their spectra. The work is divided into two volumes, the first of which consists entirely of tables giving the spectroscopic and molecular constants. The material is presented in four sections dealing, respectively, with diatomic molecules, the vibrational and rotational constants of polyatomic molecules, the electronic spectra of polyatomic molecules and electron collision processes. The tables are conveniently planned and are supplemented with detailed references to the literature. In the case of the polyatomic molecules, diagrams of the normal vibrations are included which preclude the possibility of ambiguity in identifying any particular frequency.

The second volume is an exposition of the theories which give a meaning to the observational data. It opens with two short chapters on the older and on the current quantum mechanics with applications to atomic spectra. Then follows a long and well-written chapter on diatomic and polyatomic molecules and their spectra. The next section, a shorter one, is devoted to examples of the spectroscopic methods of the determination of the structural constants of molecules, such as heats of dissociation, moments of inertia, etc. This is followed by an exposition of the theories of molecular binding, starting, of course, with the Heitler-London theory and presenting the subsequent developments. The volume closes with two further chapters, one on the excitation of molecules and the other on various applications of spectroscopy to chemical problems.

Dr. Sponer has done a great service to physicists and chemists in producing these volumes on molecular spectra. There is no doubt that the experimental data have been most carefully collected. Apparently the determinations of many of the structural constants have been rechecked, with the result that a number of errors have been found and corrected.

The past few years have constituted a period of rapid development in our knowledge of polyatomic molecules, and this is illustrated by the em-

phasis Dr. Sponer has placed upon them. It is interesting to recall that six years ago there was no single instance of a polyatomic molecule whose spectrum was completely understood, while at the present time ten or more such spectra are entirely deciphered and many others are in the process of being analyzed. The great amount of work which has been done has made it impossible for Dr. Sponer to present any of it in great detail. However, in all cases the references are so complete that it will be an easy matter to consult the original papers. This book can be enthusiastically recommended to all those interested in the problems of molecular structure.

DAVID M. DENNISON

University of Michigan

Consider the Heavens. By F. R. MOULTON. New York: Doubleday, Doran & Co., 1935. Pp. ix+332. Figs. 15, Pls. XLII. $3.50.

It is difficult to say whether the many recent books have fanned to a glow the popular interest in astronomy or whether popular interest has aroused many authors to break a lance in the lists of astronomical literature. Of popular books on astronomy there now seems a plethora.

> "Another book!" the indignant public cries,
> As piles on piles the unwelcome volumes rise!
> "Another tax on patience, purse, and brain
> For fame just printed, or for greed of gain!"

This stricture applies full force to many recent volumes. Some are trivial, some just shelf-fillers—twice-told tales without a spark of originality. A few, like the present volume, are earnest, sincere, valuable contributions for which one might justly quote further:

> Cease, gentle Public! spare the censor's tasks!
> No fame the author seeks—no ducats asks!

To the preparation of *Consider the Heavens* Dr. Moulton has brought profound scholarship, literary power, searching mathematical analysis, poetic fancy, philosophical poise, scientific imagination, which, while clearly recognizing logical restrictions, does not permit itself to be bound or shackled by tradition, by precedent, or by dogma—"creeds and schools in abeyance."

In the pages the whole range of astronomy is considered, from the superstitions from which it emerged to the indeterminacy of Heisenberg, from the naïve conceit of a small geocentric universe to the mighty con-

ception of an infinite and eternal cosmos. He finds it futile to attempt to get a conception of chaos or of infinite empty space or infinite eventless time or an abrupt discontinuity—a jump from nothing to the something of creation. He "sees no morning for the stars back of which there was eternal night, and no sunset beyond which no new day will dawn." The viewpoint is not simply observational and descriptive, not vaguely conjectural, but critical, examining with dynamical outlook. He finds that a mathematical formula to which a scientific theory may have been reduced may serve as a guide with which to venture into unknown regions, to probe into the past or future, in a sense thereby acquiring immortality.

Few matters essential to a comprehensive understanding of astronomy are omitted. The volume does not, however, follow the methodical and detailed presentation of a textbook. It is full of facts, description of the tools and methods for obtaining data, discussion of inferences from observations, and analyses of theories. Let me mention particularly the author's review of the planetesimal hypothesis; his discussion of spectral classification and related characteristics of the stars, of the various types of double stars and the theories of their origin, of the variables, especially the novae. Toward the end of his interesting consideration of novae he states: "Naturally, we follow many false clues; indeed, we may be following one when we suspect that there is possibly a relationship between the novae and the planetary nebulae." I think most astronomers will consider that the association of novae with Wolf-Rayet stars and with planetary nebulae is closer than their relation to the other variables. Dr. Moulton does not mention the appearance of separate nuclei in the novae, as in Nova Pictoris and Nova Herculis. There is an excellent discussion of star clusters, with the results from much careful computation condensed into a few pages. The exterior galaxies, the indications of an expanding universe, and supergalaxies engage his attention in closing chapters.

Always he holds to the supreme discovery of the orderliness of the universe, abjuring the idea that "chaos umpire sits, and by decision more embroils the fray." Always he holds a curb on enthusiasm lest it build a structure on unsubstantial foundations, and he gives a warning lest the "marvelous machinery of the Arabic method of writing numbers enable us to make condensed descriptions at the expense of reality."

In the final pages the author, considering the sequence upward and downward of cosmic units, permits himself a bold imaginative flight assuming the existence of intelligent beings, the cells of whose bodies or

blood corpuscles are galaxies or supergalaxies of stars with life-cycles of millions of billions of years. "When they breathe there are exhaled from their nostrils torrents of supergalaxies; when their hearts beat, the galaxies of a billion light-years are in convulsions."

A few inaccuracies have been noted. On page 26 Tycho Brahe is called a "predecessor" of Copernicus; on that same page also appears "the revolution of the Earth produces, therefore, slight variations in the *color* of the star." Photography reaches less than two octaves beyond the violet end of the visual spectrum and even less distance into the infra-red instead of the many or several octaves noted on page 58. On page 83 Eros is noted as approaching nearer the Earth "than any other celestial body except the Moon." The Delporte object 1932 EA and the Reinmuth object 1932 HA transgress the limit set by Eros, approaching to within 10,000,000 and 2,000,000 miles, respectively. The more recent Delporte object, approaching within 1,200,000 miles, was discovered subsequent to the publication of this book. On page 125 Professor George E. Hale's initials are printed erroneously "E. E." On page 169 at the end of the second paragraph "Class B" should read "Class O." On page 188 it is not necessary to "*suppose*" that "the plane of the orbit of an eclipsing variable star passes through the observer. . . . ." It is not a supposition but a requisite. Though Aitken first saw Mira as a double star (p. 211), the discovery must be credited to Joy. If one were a little cautious, he might inquire as to the nature of the evidence to justify the statement (p. 212): "We find in this binary system [Mira] two stars which have been closely associated for thousands of millions of years." On page 220 is the statement: "No optical means can make an extended surface, such as a nebula, appear brighter than it does to the unaided eye." If this were literally true, very few nebulae discovered visually would ever have been seen. On page 224, *moonlight* in the next to the last line should read *sunlight*. On page 226, in computing the size of the nebula associated with the Pleiades, complete data are not given, but the derived diameter of thirty light-years would be approximately 2,000,000 times the Earth's distance from the Sun, not "200,000." With a diameter of 200,000 AU and centered on the Sun, no neighboring star would be within its borders. On page 230 Hartmann's discovery of interstellar calcium lines is incorrectly stated to have been made in the spectrum of "the red star Betelgeuse." These lines were found in the B-type star δ Orionis,[1] they cannot be observed in Betelgeuse because of the great strength of the stellar calcium lines. An inconsistency appears in statements on pages 10 and 25;

[1] *Astrophysical Journal*, **19**, 273, 1904.

the first gives the velocity of the solar system toward Vega as 250,000,000 miles a year, the second toward Hercules as 400,000,000 miles a year. The latter is the correct value.

To read and understand this book the reader must lay aside intellectual inertia against which the author insistently inveighs, and yet it is exciting reading. Every book this author has written gives much new material and new views on old—much of his own research is involved. The volume is in an unusual measure his own. He states that it is not a picture of the physical universe alone, but partly a reflection, as every book must be, of the author himself. Every author has a heritage from the past, from his direct antecedents and the great minds of other days, but he is partly molded by immediate environment and contacts. We find the author pausing not infrequently for penetrating glimpses into many other fields of learning. Let me cite only "History was created, a more terrible warning against possible follies than any imagination could construct." This quotation might be followed by another where, after speaking of precession, he writes: "What perils may threaten civilization before Vega is again the pole star, and what levels of achievement and human happiness may be attained!" Flashes reflect the vital glow of great scholars of the past and of his colleagues in the universities and academies. He turns not infrequently from cool logical exposition to the warmth and spirituality of poetry.

We may hope that many readers will credit the latter part of his comment: "Astronomers have often been regarded as impractical dreamers, as men who muse aimlessly about the stars. We have found them, however, in their explorations of the celestial spaces, ingenious in their methods, masters of reasoning, and tireless in their labors." The volume itself bears evidence enough and in vivid form of "man's insatiable curiosity, his dauntless imagination, and the godlike reasoning powers of the human mind."

PHILIP FOX

ADLER PLANETARIUM
CHICAGO, ILLINOIS

Stars and Telescopes. By JAMES STOKLEY. New York and London: Harper & Bros., 1936. Pp. 319. 49 illustrations and numerous diagrams. $3.00.

This book is written for the layman and will serve as an excellent introduction to astronomy. It may be recommended to one who wants, in a

single volume, an account of the historical background of the science together with an adequate treatment of its most recent developments.

The author is associate director of the astronomical section of the Fels Planetarium of the Franklin Institute at Philadelphia. His acquaintance with the public mind in its relation to astronomical matters has enabled him to write succinctly and yet to guard his reader from some common misunderstandings.

In the opening chapters the apparent celestial motions are described and interpreted and the constellations are pointed out with the aid of diagrams showing the northern and southern aspects of the evening sky at four seasons. The third and fourth chapters trace the changes in ideas of the universe from ancient days to the time of Newton. The next six chapters are devoted to the telescope, its discovery and gradual improvement, the use of auxiliary apparatus, and the developments which have made possible the great instruments of our day. One of these chapters describes some of the principal observatories of the world. Another is given over to the work of amateur telescope-makers and a plea is made that a larger proportion of these become also amateur observers.

The important practical use of astronomy in determining time is then well explained and an account is given of the gradual approach to accuracy in time-keeping devices. Little reference, however, is found to the application of astronomy in navigation.

The remaining half of the book takes up the detailed consideration of the different types of celestial objects. Four chapters are given to the Moon, the Sun, the planets, comets and meteors; four more to stars and their analysis, the types of variable and double stars, star clusters and nebulae.

Two chapters deal with the structure of the galaxy, the existence of other galaxies, and the question of their recession. There is a final chapter on "Life in the Universe."

The treatment throughout appears well balanced and comprehensive. The illustrations are aquatones—reproductions chiefly of well-known astronomical photographs. There are a bibliography and an index.

O. C. COLLINS

L'origine des mondes. By PAUL LABÉRENNE. Paris: Editions Sociales Internationales, 1936. Pp. 320.

This book contains an elementary and somewhat superficial account of various cosmogonical theories, beginning with the ideas of the Egyptians

and Babylonians and ending with the theory of the expanding universe. The author has collected in book form a course of lectures given by him at the Université Ouvrière of Paris, and has included a series of articles published by him since 1932 in *La lutte antireligieuse et prolétarienne: Organe des travailleurs sans-dieu de France*. The political interests of the author have left their impression upon the form of exposition, and readers who are interested in the effect of the "dialectic materialism" upon astronomy will welcome this account, which, although admittedly prejudiced, is an honest attempt "to show in the study of a well-defined problem what new information is brought to us by the dialectic materialism of Marx and of Engels, and of what help it may be in science." The reader will have to form his own judgment of the value (or lack of it) of radicalism in astronomy.

OTTO STRUVE